THE *a* SUBUNIT OF *ESCHERICHIA COLI* F_1F_0 ATP SYNTHASE AS A MODEL FOR INVESTIGATING PROTON TRANSLOCATION

By

PHILLIP EDWIN HARTZOG

A DISSERTATION PRESENTED TO THE GRADUATE SCHOOL
OF THE UNIVERSITY OF FLORIDA IN PARTIAL FULFILLMENT
OF THE REQUIREMENTS FOR THE DEGREE OF
DOCTOR OF PHILOSOPHY

UNIVERSITY OF FLORIDA

1994

ACKNOWLEDGEMENTS

I would like to thank all the members of my supervisory committee, Dr. Michael Kilberg, Dr. Charles Allen, Dr. Sheldon Schuster, Dr. Paul Hargrave, and Dr. Lonnie Ingram, for their help and advice, no matter how far my project strayed from the original proposal. Additionally, I would like to thank Dr. Donald Allison for his expert advice and help with data interpretation. I would also like to thank Dr. Richard Boyce, because he always knew how to fix any problem I might have with the University.

I would like to express my gratitude to my mentor, Dr. Brian Cain, who has taught me how to start becoming a scientist. Hopefully, one day I will get the chance to pass on some of the knowledge he has taught me to an unsuspecting graduate student.

And last, but not least, I would like to thank all my friends and family, here and back in North Carolina; without their friendship and support I would never have made it through this process. Additional thanks goes to my long time friend Bob Whitener, for without his financial support when I needed it most, I would not have made it to Gainesville.

TABLE OF CONTENTS

ACKNOWLEDGEMENTS ii

LIST OF TABLES v

LIST OF FIGURES vi

ABSTRACT ix

CHAPTER 1
BACKGROUND AND SIGNIFICANCE 1
Introduction 1
Similarity Among F_1F_0 ATPases 3
Binding Change Mechanism 17
E. coli as a Model for Other ATP Synthases . . . 20
E. coli F_1F_0 ATP Synthase 26
The *a* Subunit of *E. coli* F_1F_0 ATP Synthase 40

CHAPTER 2
EXPERIMENTAL PROCEDURES 51
Molecular Techniques 51
Membrane Preparations 67
Assays 71

CHAPTER 3
CONSTRUCTION OF DELETION STRAIN PH105 78
Introduction 78
Results 80
Discussion 92

CHAPTER 4
MUTAGENIC ANALYSIS OF CONSERVED AMINO ACIDS a_{Q252} THROUGH a_{Y263} IN THE *a* SUBUNIT 94
Introduction 94
Results 98
Discussion 110

CHAPTER 5
BACTERIAL MODEL FOR HUMAN MITOCHONDRIAL DISEASE 116
Introduction 116
Results 119
Discussion 134

CHAPTER 6
SECOND SITE SUPPRESSOR MUTATIONS 137
Introduction 137
Results 138
Discussion 156

CHAPTER 7
CONCLUSIONS AND FUTURE DIRECTIONS 160
Overview of the *a* Subunit Missense Mutations . . . 160
Modeling Mitochondrial Mutations 169
Coupling Proton Transport to ATP Catalysis 172

REFERENCES 180

BIOGRAPHICAL SKETCH 197

LIST OF TABLES

Table 2-1. List of Strains and Plasmids 53

Table 3-1. Complementation Analysis 82

Table 3-2. Membrane Associated ATPase Activities . . . 85

Table 4-1. Mutations Generated in the *uncB* (*a*) Gene . 100

Table 4-2. Growth Properties of *a* Subunit Mutants . . 102

Table 4-3. Properties of *a* Subunit Mutations at a_{Q252} . 111

Table 5-1. Properties of the $a_{L207 \rightarrow R}$ Mutation 123

Table 5-2. Properties of the $a_{L207 \rightarrow P}$ Mutation 128

Table 6-1. Mutations Generated in the *uncB* (*a*) Gene . 140

Table 6-2. Growth Properties of Mutant Strains 141

Table 6-3. Biochemical Properties of Mutant Strains . 145

LIST OF FIGURES

Figure 1-2. Diagram of the *E. coli* F_1F_o ATP synthase. 18

Figure 1-2. Model of the binding change mechanism and its relationship to energy supplied by proton translocation. 21

Figure 1-3. Alignment of *a*-like subunits. 41

Figure 1-4. Proposed topology model of the *a* subunit. 48

Figure 2-1. Plasmid pPH12 (*a*) that was used to construct site-directed mutations in the *uncB* (*a*) gene by cassette mutagenesis. 62

Figure 3-1. Southern analysis of strain PH105 (a_{del}) and its parent strain 1100. 84

Figure 3-2. Energization of membrane vesicles determined by fluorescence quenching of ACMA. . . 87

Figure 3-3. Western analysis of strain RH305 ($a_{uncB205}$) and strain PH105 (a_{del}). 89

Figure 4-1. Alignment of amino acid sequence in the last proposed membrane spanning segment. 95

Figure 4-2. Oligonucleotides used for cassette mutagenesis and the sequence from plasmid pPH12 (*a*). 99

Figure 4-3. Energization of membrane vesicles determined by fluorescence quenching of ACMA. . . 106

Figure. 4-4. Proton impermeability of stripped membranes from *a* subunit mutant strains. 108

Figure 5-1. Alignment of *a*-like (*ATPase 6*-like) subunits. 120

Figure 5-2. Plasmid pBDC26 ($a_{L207\rightarrow W,\ E219\rightarrow K}$) and the oligonucleotide cassettes used to make the mutant plasmid pUNCB4.70 ($a_{L207\rightarrow R}$) and plasmid pUNCB4.71 ($a_{L207\rightarrow P}$) 121

Figure 5-3. F_1F_O ATP synthase mediated ATP-driven vesicle acidification for $a_{leu207\rightarrow arg}$ 124

Figure 5-4. NADH driven ACMA fluorescence quenching of $a_{leu207\rightarrow arg}$ stripped vesicles 126

Figure 5-5. F_1F_O ATP synthase mediated ATP-driven vesicle acidification for $a_{leu207\rightarrow pro}$ 130

Figure 5-6. NADH driven ACMA fluorescence quenching of $a_{leu207\rightarrow pro}$ stripped vesicles 131

Figure 5-7. Western Analysis of $a_{L207\rightarrow P}$ comparing intact verses stripped vesicles 133

Figure 6-1. Alignment of the sequence variations seen at a_{G218}, a_{E219}, and a_{H245}. 139

Figure 6-2. Western analysis of mutant strains. Stripped membranes prepared from mutant strains were used for immunoblotting with anti-*b* antibody. 147

Figure 6-3. ATP driven energization of membrane vesicles determined by ACMA. 149
Figure 6-4. NADH driven energization of stripped membrane vesicles determined by ACMA 151
Figure 6-5. ATP driven energization of membrane vesicles under different pH conditions. 153
Figure 6-6. ATP driven energization of membrane vesicles under different ATP concentrations. . . . 154
Figure 7-1. Compilation of missense mutations in the *a* subunit 161

Abstract of Dissertation Presented to the Graduate School of the University of Florida in Partial Fulfillment of the Requirements for the Degree Doctor of Philosophy

THE *a* SUBUNIT OF *ESCHERICHIA COLI* F_1F_0 ATP SYNTHASE AS A MODEL FOR INVESTIGATING PROTON TRANSLOCATION

By

Phillip Edwin Hartzog

April 1994

Chairperson: Dr. Brian D. Cain
Major Department: Biochemistry and Molecular Biology

F_1F_0 adenosine triphosphate (ATP) synthases use an electrochemical gradient of protons across energy transducing membranes to synthesize ATP. The enzyme complex consists of a F_1 sector containing the catalytic activity, and a F_0 sector capable of proton conductance. All F_1F_0 ATP synthases contain an essential *a*-like subunit in the F_0 sector. Primary structural homology with other *a*-like subunits indicates conservation of amino acid positions a_{Q252}, a_{F256}, a_{L259}, and a_{Y263}. These amino acid positions were investigated using site-directed mutagenesis techniques, and analysis of the mutant strains indicated these amino acids have an important structural role in proton translocation.

The validity of comparing studies in *E. coli* to all F_1F_0 ATP synthases was demonstrated by the modeling of the

mutation proposed to cause the human mitochondrial genetic disease neurogenic muscle weakness, ataxia and retinitis pigmentosa. The biochemical effects of two mutations occurring in the human *ATPase 6* subunit were determined by constructing the comparable mutations in the *a* subunit of *E. coli*. Both mutations greatly decreased F_1F_O ATP synthase activity by destabilizing the enzyme complex.

E. coli was also used to model the *a*-like subunits from chloroplast and alkaliphilic bacteria F_1F_O ATP synthases. The *a*-like subunits from both types of ATP synthases contain variations from the *E. coli* amino acid sequence at positions a_{G218} and a_{H245}. The double mutations $a_{G218\rightarrow D,H245\rightarrow G}$ and $a_{G218\rightarrow K,H245\rightarrow G}$ introduce substitutions which mimic the amino acids present in chloroplast and alkaliphilic bacteria, respectively. The enzymes carrying the double substitutions were functional at near wild-type levels, while those with the single substitutions $a_{H245\rightarrow G}$, $a_{G218\rightarrow D}$ and $a_{G218\rightarrow K}$ had greatly reduced enzyme function. The phenotypes exhibited by these mutants also indicated an involvement in the coupling of proton translocation to ATP synthesis.

The *a* subunit from *E. coli* was shown to be a good model for studying changes in *a*-like subunits from different F_1F_O ATP synthases. The study of these changes has led to a new understanding of how the translocation of protons is coupled to the synthesis of ATP.

CHAPTER 1
BACKGROUND AND SIGNIFICANCE

Introduction

Oxidative phosphorylation (OXPHOS) is the primary bioenergetic pathway for adenosine triphosphate (ATP) synthesis in aerobic organisms. The electron transport chain generates an electrochemical gradient of protons which is used to drive ATP production by F_1F_o ATP synthase. F_1F_o ATP synthase harnesses the energy of the proton electromotive force and uses it to synthesize ATP from ADP and P_i. The coupling of an electrochemical gradient with the synthesis of high energy chemical bonds connects the two major forms of stored energy in living organisms. In this capacity F_1F_o ATP synthase plays a central role in bioenergetics.

The chemiosmotic hypothesis presented by Peter Mitchell (Mitchell, 1961) proposed a mechanism of ATP production from an electrochemical gradient of protons. F_1F_o ATP synthase was clearly demonstrated to couple proton translocation to ATP synthesis by Racker and Stoeckenius (1974). Intense study of F_1F_o ATP synthase for more than four decades has

revealed a great deal of structural and functional information about the enzyme. Current reviews on this topic have been presented by Boyer (1987, 1993), Fillingame (1990a, b), Futai *et al.* (1989), Hatefi and Matsuno-Yagi (1992), Penefsky and Cross (1991), Schneider and Altendorf (1987), and Senior (1990). The structural and functional analysis remains incomplete. F_1F_O ATP synthase is composed of two sectors, F_1 and F_O, with defined functional activities. F_1 is easily dissociated from the membrane and retains the ATP hydrolysis activity. The mechanism of ATP hydrolysis in the F_1 sector of the enzyme has been studied in great detail (reviewed in Cross, 1992; Senior, 1990), and considerable structural data exist for this sector (Abrahams *et al.*, 1993; Akey *et al.*, 1983; Tsuprun *et al.*, 1984; Tiedge *et al.*, 1985; Boekema *et al.*, 1986, 1988; Gogol *et al.*, 1989a, b; Ishii *et al.*, 1993). However, much less is known about the mechanism of proton translocation through the F_O sector, and how the energy of proton translocation is coupled to ATP synthesis. The structural information for the F_O sector is also limited. The F_1 and F_O sectors are connected by a stalk that has been proposed to couple proton translocation to ATP synthesis. This work focuses on the mechanism of proton translocation, and indirectly, its coupling to the catalytic activities.

The facultative bacterium *E. coli* offers many advantages in the study of F_1F_O ATP synthase. The ability

of *E. coli* to grow via glycolysis allows the construction of strains defective in F_1F_0 ATP synthase. Molecular techniques can be employed to alter genes on the chromosome, as well as, express F_1F_0 ATP synthase subunits from plasmids. *E. coli* is amendable to growth analysis under a wide variety of conditions including different carbon sources and temperatures, as well as both, anaerobic and aerobic environments.

Similarity Among F_1F_0 ATPases

Biological Similarities

F_1F_0 ATP synthase is used by all aerobic organisms to produce ATP from the electrochemical gradient of protons produced by an electron transport chain (Redox) or photoreaction center (Photo-redox). F_1F_0 ATP synthases are localized to the inner mitochondrial membranes of eucaryotes, chloroplast thylakoid membranes of plants, and the cytoplasmic membranes of procaryotic organisms. F_1F_0 ATP synthases from procaryotes to eucaryotes bear a general structural resemblance and apparently have comparable mechanisms for ATP catalysis and proton translocation (Senior, 1990).

Vacuolar ATPases. Under anaerobic conditions facultative organisms can use F_1F_0 ATP synthase in reverse to produce a proton gradient by hydrolysis of ATP. This

allows the maintenance of the membrane potential important for many biological membrane functions. Similarly, anaerobic organisms are believed to use an enzyme akin to F_1F_o ATP synthases for maintaining membrane potential. Vacuolar ATPases (V-type ATPases) of eucaryotic organisms are believed to be derived from anaerobic F-type ATPases, and consequently share homology with F_1F_o ATP synthases at the amino acid sequence, structural, and functional levels (Südhof *et al.*, 1989; Stone *et al.*, 1990; Senior, 1990).

Propionigenium modestum. An example of the distant evolutionary relationship among the F-type ATPases is demonstrated by the strict anaerobic bacterium *Propionigenium modestum* which uses an enzyme related to F_1F_o ATP synthase to produce ATP by the translocation of Na^+ ions (for review see Dimroth, 1987, 1992). Laubinger and Dimroth (1989) found that *P. modestum* F_1F_o ATP synthase would pump protons under conditions of low Na^+ concentrations. Laubinger *et al.* (1990) reported that *E. coli* F_1 sector would bind to *P. modestum* F_o sector and function in a reconstituted system. Additionally Kaim *et al.* (1992) reported the expression of *P. modestum* F_o subunits in a *E. coli* strain deleted of F_o subunits, mimicking the earlier *in vitro* experiment. This demonstrated that functional and structural interactions in F_1F_o ATP synthases have been conserved between widely divergent organisms. As the above study suggests, F_1F_o ATP synthase subunits of *P. modestum*

were found to exhibit evolutionary conservation at the primary amino acid sequence level with other F_1F_O ATP synthases (Amann *et al.*, 1988; Ludwig *et al.*, 1990; Esser *et al.*, 1990; Woese *et al.*, 1990; Kaim *et al.*, 1992).

The similarities between both *E. coli* and *P. modestum* in coupling of ATP synthesis with ion translocation reveals a relationship between the translocation of protons and the translocation of other ions. The implication is that studies of *P. modestum* enzyme are applicable to the *E. coli* enzyme, as well as all other F_1F_O ATP synthases. If the mechanism of ion translocation is conserved between *P. modestum* and *E. coli*, then it is reasonable to propose that *E. coli* F_1F_O ATP synthase transports hydronium ions (H_3O^+) instead of protons (H^+). Hydronium ions are similar to hydrated Na^+ ions at the chemical level, and therefore will exhibit similar binding characteristics (Boyer, 1988; Laubinger *et al.*, 1990). The ability of the *P. modestum* F_1F_O ATP synthase to transport protons as well as Na^+ ions is conducive to a hypothetical ion binding site that could have a specificity for H_3O^+ or hydrated Na^+ ions. This proposed ion binding site of *P. modestum* F_1F_O ATP synthase has a higher affinity for hydrated Na^+ ions, but binds H_3O^+ ions in the absence of Na^+ (<1 mM). However, the *E. coli* F_1F_O ATP synthase ion binding site appears specific for H_3O^+ ions (> 10^6 affinity for H_3O^+ ion) since it exhibits no ability to transport Na^+ (Laubinger & Dimroth, 1989). A

proposed mechanism of ion transport in F_1F_O ATP synthase is discussed below.

Chloroplast and cyanobacteria. Another example of structural and functional conservation was reported by Lill *et al.* (1993). The genes encoding F_1 subunits from spinach chloroplast and the cyanobacterium *Synechocystis* sp. PCC 6803 were expressed in *E. coli* strains that carried mutations in the corresponding F_1 subunits. The strains expressing chloroplast and cyanobacteria F_1 subunits were then grown on a succinate minimal medium to determine if the chloroplast-like subunits would complement the corresponding defective *E. coli* F_1 subunits. The δ and ϵ subunits from both chloroplast and cyanobacteria proved capable of partially substituting for the *E. coli* δ and ϵ subunits. The α subunit defective *E. coli* strain was also complemented with both the chloroplast and cyanobacteria α subunits, but to a lesser extent than the δ and ϵ subunits. The cyanobacterial β subunit partially substituted for *E. coli* β subunit, but the β subunit from chloroplast failed to complement. The γ subunit defective *E. coli* strain was not complemented by either chloroplast or cyanobacteria γ subunits. The ability of F_1 subunits from chloroplast or cyanobacteria to substitute for the *E. coli* F_1 subunits demonstrated the remarkable conservation of structure and function between F_1F_O ATP synthases.

Biochemical Similarities

F_1 and F_o sectors can be dissociated with low ionic buffers freeing the F_1 sector to become a soluble ATPase, and leaving the F_o sector in the lipid bilayer as a functional proton pore. This has facilitated much of the biochemical analysis of the F_1F_o ATP synthase.

F_1 ATPase is composed of a catalytic core of $\alpha_3\beta_3\gamma$ subunits that are found in all F-type ATPases. The catalytic core is sufficient for ATP hydrolysis activity. ATP synthases contain at least two other subunits, which are necessary for coupling proton translocation to ATP production. The ϵ subunit appears to have an inhibitory action on F_1 ATPase activity (Klionsky *et al.*, 1984; Dunn *et al.*, 1987). The inhibition resulting from the ϵ subunit is apparently reversed by addition of the detergent lauryldimethylamine oxide (LDAO) (Lötscher *et al.*, 1984). The δ subunit (or the OSCP subunit in mitochondria) is required for the binding of the F_1 sector to the F_o sector (Bragg *et al.*, 1973; Sternweis & Smith, 1977).

The kinetics of nucleotide binding and catalysis have been extensively investigated (for reviews see Futai, *et al.*, 1989; Senoir, 1990; Cross, 1992; Boyer, 1993). F_1 has multiple nucleotide binding sites three of which are thought to be catalytic and three other binding sites serving in a non-catalytic capacity. The catalytic sites undergo uni-site and multi-site catalysis depending on the nucleotide

concentration. Uni-site catalysis requires that ATP be present in nM concentrations, or less than the concentration of enzyme. Multi-site catalysis occurs at μM concentrations of nucleotide and displays cooperativity (Boyer, 1993). Since cellular levels of ATP are in the 2-4 mM range in *E. coli* (Kashket, 1982) multi-site catalysis probably reflects enzyme function *in vivo*. The proposed catalytic nucleotide binding site in the β subunit contains a highly conserved amino acid sequence found in other nucleotide binding proteins such as adenylate kinase and p21 ras (Duncan & Cross, 1992).

Non-hydrolyzable ATP analogs, high concentrations of Mg^{2+}, and ADP inhibit F_1 ATPase activity. F_1 ATPase activity is also inhibited by its binding to F_O at pH 7, and this observation has been attributed to the coupling mechanism of ATP catalysis and proton translocation. The inhibition caused by coupling can be reversed by raising the pH to 9.1 (Cain & Simoni, 1989). However, the increased F_1 ATPase activity is still sensitive to dicyclohexylcarbodiimide (DCCD) (see below). This indicates that pH 9.1 and DCCD affect the ATPase activity of the F_1 sector bound to the F_O sector by different mechanisms.

The F_O sector in F_1F_O ATP synthase invariably contains a small proteolipid *c*-like subunit that binds DCCD. DCCD covalently modifies a carboxyl acid in the *c*-like subunit (c_{D61} in *E. coli*) and inhibits proton translocation. DCCD

will also inhibit the activity of F_1 ATPase when it is bound to the F_O sector. The *c*-like subunit is found in 10±1 copies in the F_O sector of *E. coli* (Hermolin & Fillingame, 1989), and believed to exist in multiple copies in other F_1F_O ATP synthases. ATP synthases also contain a single copy of an *a*-like subunit in the F_O sector. Both subunits have regions of amino acids that are highly conserved throughout F_1F_O ATP synthases. Bacterial enzymes contain a *b* subunit with the stoichiometry of 2 subunits per F_O sector which probably form a dimer (Aris & Simoni, 1983; Hermolin *et al.*, 1983; Dunn, 1992). Comparable *b*-like subunits have been found in chloroplast systems, as well as a *b*-like subunit in yeast (Velours *et al.*, 1988). No clear *b*-like analogs have been identified in mammalian mitochondrial systems; however, an analogous subunit has been proposed (Montecucco *et al.*, 1983; Torok & Joshi, 1985; Walker *et al.*, 1987, 1991; Papa *et al.*, 1992). In *E. coli* the *b* subunit has been demonstrated to be involved in F_1 binding to F_O (Hoppe *et al.*, 1983; Perlin *et al.*, 1983) as well as potentially make up part of the stalk structure (see below).

The F_O sector functions to transport protons across the membrane. Active proton translocation requires the F_1 sector. Proton conductance occurs passively when the F_1 sector has been stripped from the membrane using low ionic strength conditions. The mechanism of proton transport is unknown, though models have been proposed involving a proton

wire (Cox *et al.*, 1986, Schneider & Altendorf, 1987), a proton channel (Deckers-Hebestreit & Altendorf, 1992b) and a proton binding site (Fillingame *et al.*, 1993). The work of Dimroth and colleagues in *P. modestum* (see above) has elicited the most detailed picture of proton conductance so far and is outlined below.

An advantage of the *P. modestum* F_1F_0 ATP synthase is that the translocation of sodium ions can be measured directly with $^{22}Na^+$. This was used to look at the action of *P. modestum* F_0 mediated Na^+ conductance (Kluge & Dimroth, 1992). The kinetics of the reconstituted system supports a transporter mechanism involving at least four steps. The first proposed step of Na^+ conductance was binding of a hydrated Na^+ ion to a defined site on the membrane assumed to be the F_0 sector. In the second step, the Na^+/binding-site complex would 'translocate' to the other surface of the membrane. Presumably this is through a conformational change upon the binding of the hydrated Na^+ ion. The third step would be the release of the hydrated Na^+ ion from the binding-site. The last step would be the return of the ion binding-site back to the original side of the membrane. If a membrane potential was present then the binding site returned unloaded. However, if the membrane potential was absent the ion binding site could return to the original surface loaded. The flow of Na^+ in this experiment was the equivalent of periplasmic to cytoplasmic, or in the

direction of ATP synthesis. A voltage dependent step was not found for *P. modestum* F_1F_O ATP synthase (Dmitriev *et al.*, 1993) suggesting a membrane potential is not essential for the function of the intact complex.

The presence of Na^+ in *P. modestum* F_1F_O ATP synthase blocks the translocation of H^+/H_3O^+, apparently by competitive inhibition (Laubinger & Dimroth, 1989; Laubinger *et al.*, 1990). Kluge and Dimroth (1992) reported that the presence of Na^+ also blocks the binding of dicyclohexylcarbodiimide (DCCD), the covalent inhibitor of F_O mediated ion translocation. DCCD inhibits F_1F_O ATP synthase activity by modifying conserved carboxylic acid in the proteolipid *c* subunit, (c_{E65} in *P. modestum*, c_{D61} in *E. coli*). The kinetics of DCCD inactivation revealed a pK(Na^+) of 2.5 to 3.3, depending on the pH. The pH dependence on Na^+ binding was consistent with a competition for a ion binding site. Positive cooperativity (n_H=2.6) was also reported with respect to Na^+ transport and Na^+-activated ATPase activity at pH 9.0 (Kluge & Dimroth, 1993). The data strongly suggest the existence of a ion binding site(s) that effects the binding of DCCD to the essential amino acid c_{E65} (c_{D61} in *E. coli*). A mechanism involving an essential arginine was proposed, in which either the amino acid a_{R210} or c_{R41} is necessary for deprotonating c_{E65} so that it can bind a Na^+ ion (Kluge & Dimroth, 1993). This mechanism can

be applied to other F_1F_O ATP synthases using H_3O^+ instead of a hydrated Na^+ ion.

Structural Similarities

The F_1 sector has been extensively studied at the structural level as well. The structure of the F_1-ATPases from many sources appears to be conserved as assessed by the resolution obtainable with electron microscopy. Electron micrographs of several purified F_1-ATPases revealed a roughly spherical shape with a diameter of 90-100 Å (Akey *et al.*, 1983; Tsuprun *et al.*, 1984; Tiedge *et al.*, 1985; Boekema *et al.*, 1986, 1988; Gogol *et al.*, 1989a, b; Ishii *et al.*, 1993). The most revealing work so far has been accomplished by Capaldi and colleagues, and reviewed in greater detail below. Greater resolution has been obtained with an X-ray crystal structure of the rat and bovine heart mitochondria, and is reviewed in greater detail below (Bianchet et al., 1991; Abrahams *et al.*, 1993).

Cryoelectron microscopy of the F_1 sector. The most convincing structural data on *E. coli* F_1F_O ATP synthase comes from Capaldi and colleagues (Gogol *et al.*, 1987, 1989a, 1989b). Cryoelectron microscopy methods have been used to deduce the structure of the F_1F_O ATP synthase complex. The technique involves use of quick freezing of F_1F_O ATP synthase to suspend complexes containing liposomes in a layer of amorphous ice. The data support an alternating arrangement of α/β subunits arranged in a

hexagonal circle with a diameter ca. 90 Å (Gogol *et al.*, 1989b). An asymmetrical central mass was also observed in the middle of the α/β ring structure. Immuno-electron microscopy with anti-α, anti-γ, anti-δ, and anti-ϵ Fab antibody fragments was used to investigate the central mass (Gogol *et al.*, 1989b; Capaldi *et al.*, 1992). The anti-α Fab fragments were found to bind asymmetrically, allowing the alignment of each image. The central mass was apparently composed of the γ, δ and ϵ subunits, and found to associate with the β subunits. The positions of the γ and ϵ subunits in relationship to each other were found to be dependent on ligand binding (Gogol *et al.*, 1990), and correlated with other ligand dependent studies (see below). The work of Capaldi and colleagues supports an asymmetrical model with an alternating hexagon of α/β subunits that produces a central cavity partially obstructed with the other F_1 subunits.

Electron crystallography has also been used on F_1-ATPase crystals from the thermophilic bacteria strain PS3 (Ishii *et al.*, 1993). The molecular dimensions and structure observed in the F_1 sector from strain PS3 were similar to those reported for the *E. coli* F_1 sector (see above). The central mass was localized to the lower half of the central cavity.

X-ray crystallography of the F_1 sector. The X-ray crystal structure of bovine heart mitochondria F_1 ATPase has

been reported by Abrahams *et al.* (1993) at 6.5 Å resolution. F_1 appeared to be roughly spherical, 110 Å in diameter, and this correlated with electron microscopy data (see above). However, additional novel new features were also reported. A 40 Å stem composed of two α-helices in a coiled-coil conformation extended from the globular sphere. One of the α-helices in the stem extends 90 Å into the center of the enzyme and emerges into a 15 Å dimple on the other side of the globule. The stem is proposed to be part of the stalk domain that connects F_1 to F_0, but may also be part of the central mass observed in cryoelectron microscopy (see above) since one of the α-helices extends through the center of the α/β hexagonal ring. A pit that extends 35 Å into the F_1 particle was observed next to the stem region and proposed to be occupied by either OSCP or the *b* subunit. The asymmetry demonstrated by the crystal of the bovine F_1-ATPase is in marked contrast to the symmetry reported for the rat F_1-ATPase by Amzel *et al.* (1992). The cryoelectron microscopy data supports the asymmetrical structure, calling the symmetrical rat structure into considerable dispute.

The stalk structure. Side views of the intact membrane-bound *E. coli* F_1F_0 ATP synthase complex by cryoelectron microscopy revealed a stalk structure connecting the F_1 sector to the membrane (Lücken *et al.*, 1990). The hexagonal F_1 complex appeared elongated in profile images (110 Å by 90 Å). Equal numbers of two images

appeared in these experiments, a bi-lobed image and a tri-lobed image. This data also revealed the presence of a stalk region connecting F_1 and F_O. The stalk was observed to be approximately 40 Å in length and 25-30 Å in diameter. F_O appeared to have a small protrusion from the cytoplasmic (F_1) side of the membrane, but seemed relatively flat on the periplasmic facing (60 Å in the transmembrane direction).

A 40 Å long stem, reported to be in a left-handed coiled-coil conformation, is also observed in the X-ray crystal structure (Abrahams *et al.*, 1993). The existence of a stem, and the corresponding pit, indicates a potential conformation for the stalk structure. However, the crystal structure was composed solely of F_1 subunits, so it is uncertain whether the stem is an artifact due to the absence of OSCP or F_O.

The stalk is proposed to be composed of one or more subunits from F_1 and in the case of bacterial and chloroplast systems one or more subunits from F_O. Subunits forming a proposed stalk region are hypothesized to play a primary role in coupling proton translocation to ATP synthesis. Therefore, mutations in stalk subunits might be expected to alter the coupling mechanism. Mutations affecting the coupling mechanism have been reported in two stalk subunits, γ (Shin *et al.*, 1992) and *b* (McCormick *et al.*, 1993).

However, the existence of an extended stalk remains controversial. The β subunit of F_1 has been reported to form a disulfide bond with the *b* subunit of F_0 (Aris & Simoni, 1983), in which b_{C21} is the only cysteine in the *b* subunit and is almost certainly located near the membrane (Schneider & Altendorf, 1985). Evidence against the stalk structure also includes the observation that binding of the F_1 sector to the F_0 sector protects the *b* subunit from proteolysis and antibody binding (Hermolin *et al.*, 1983; Hoppe *et al.*, 1983; Perlin *et al.*, 1983; Perlin & Senior, 1985; Deckers-Hebestreit & Altendorf, 1986; Deckers-Hebestreit *et al.*, 1992). Additional evidence against an extended stalk structure was reported by Aggeler *et al.* (1987). The protein reactive reagents 4-[^{3}H] formylphenyl phosphate (HFPP) and 1,2-[^{3}H] dipalmitoyl-*sn*-glycerol 3-[[[(4-azido-2-nitrophenyl)amino]ethyl]-phosphate] (arylazidePE) are amphipathic and associate with the lipid bilayer like phospholipids. HFPP and arylazidePE react with proteins that come in close proximity to the phospholipid head groups of the membrane bilayer. The δ subunit was protected from labeling by HFPP and arylazidePE only when the F_1 sector was bound to the F_0 sector. The work on the *b* and δ subunits suggests that they may be buried in the interface of the F_1 and F_0 sectors, and not exposed as would be predicted in the extended stalk hypothesis. Mutations in the *c* subunit gene from *E. coli* subunit gene have been

reported to affect the binding of the F_1 sector to the F_o sector (Mosher *et al.*, 1985; Miller *et al.*, 1989; Fraga & Fillingame, 1989, 1991; Deckers-Hebestreit & Altendorf, 1992a; Fillingame 1992a, b, 1993). However, the possibility that the *c* subunit mutants effect a potential stalk protein like the *b* or *δ* subunits can not be excluded.

A model of *E. coli* F_1F_o ATP synthase is presented in Figure 1-1. The model is adapted from Papa *et al.* (1992). Proposed positions in the complex for each of the subunits is based on various sources of data discussed throughout this Chapter.

Binding Change Mechanism

The binding change mechanism was developed to explain unique features of ATP catalysis in F_1F_o ATP synthase. Unlike all other ATPases that have been studied, F_1-ATPases (and similarly V-type ATPases) do not go through a phosphorylated-enzyme intermediate. Kinetic studies have shown that the formation and hydrolysis of the phosphodiester bond is almost at energetic equilibrium. Therefore, the energy requiring steps for ATP synthesis is not bond formation, but binding of P_i and release of ATP from the catalytic site (reviewed in Senior, 1990).

The binding change mechanism proposed that synthesis of ATP is accomplished through changing ligand affinities in

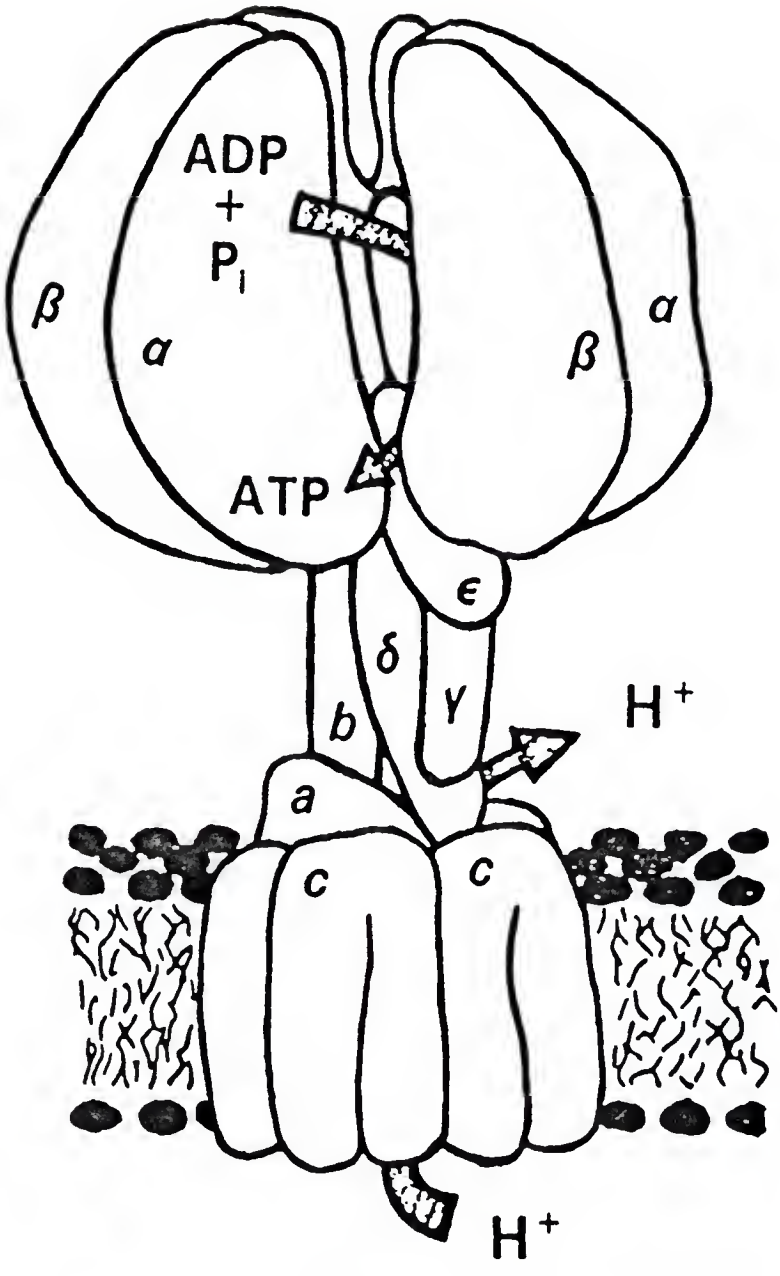

Figure 1-1. Diagram of the *E. coli* F_1F_o ATP synthase. Model is adapted from Papa *et al.* (1992).

the catalytic site of F_1F_0 ATP synthase. Ligand affinities are altered through changes in protein conformation. Conformational changes are induced by the proton motive force, and the translocation of protons. Cooperativity also plays a role in the necessary conformational changes for ATP synthesis, in which binding of ADP + P_i at a second catalytic-site appears to be required. The translocation of protons by ATP hydrolysis is thought to occur via a reversal of this mechanism.

Evidence for the binding change mechanism has been reviewed in great detail by Boyer (1993). The evidence for the binding change mechanism can be divided into three categories; nucleotide cooperativity, conformational changes, and asymmetrical features. Nucleotide cooperativity has been seen with both hydrolysis and synthesis of ATP (Matsuno-Yagi & Hatefi, 1985; Stroop & Boyer, 1985; Cunnigham & Cross, 1988). Conformational changes due to membrane energization have been seen indirectly with changes in binding affinities (Chernyak & Kozlov, 1979; Penefsky, 1985; Matsuno-Yagi *et al.*, 1985; Lunardi *et al.*, 1988; Zhou & Boyer, 1993), and conformational changes have been seen directly by exchange of hydrogens during catalysis (Ryrie & Jagendorf, 1972; Du & Boyer, 1989). Conformational changes due to ligand binding have been reported for differential cross-linking (Mendel-Hartvig & Capaldi, 1991a, b; Aggeler *et al.*, 1992) and

electron microscopy (Gogol *et al.*, 1990). Asymmetrical features have also been observed indirectly (Grubmeyer & Penefsky, 1981; Nalin *et al.*, 1985) and directly (Capaldi *et al.*, 1992, Abrahams *et al.*, 1993). A model of the binding change mechanism is presented in Figure 1-2 (Boyer, 1993).

E. coli as a Model for Other ATP Synthases

Attention has recently focused on a type of genetic disease which is maternally inherited and localized to the mitochondrial genome (mtDNA) (Wallace, 1992a, b). These abnormalities produce defects in OXPHOS, and are often referred to as mitochondrial myopathies. The severity of this type of genetic disease will depend on the ratio of defective to functional mitochondria inherited from the mother. Maternal inheritance of mtDNA is greater than 99% (Gyllensten *et al.*, 1991) and a chief indicator for mitochondrial genetic diseases. The heterogeneous nature of mitochondria distribution to daughter cells results in an asystematic expression of the genetic disease in differing tissue types (Ashley *et al.*, 1989). Organ and tissue systems, such as brain, muscle, heart, kidney, liver and pancreatic islets which utilize OXPHOS as their primary energy source show a greater sensitivity to these genetic diseases (Wallace, 1992a, b).

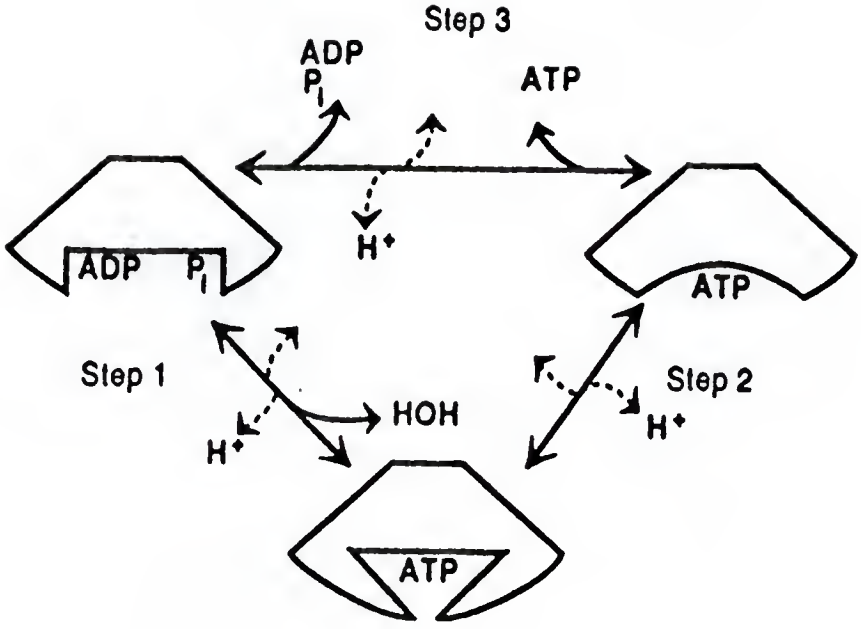

Figure 1-2. Model of the binding change mechanism and its relationship to energy supplied by proton translocation. Modified figure from Boyer (1993).

Mitochondrial genetic diseases display many clinical symptoms that correlate with damage in the organ and tissues systems listed above. The manifestations of mitochondrial genetic diseases include blindness, deafness, dementia, movement disorders, weakness, cardiac failure, diabetes, renal disfunction, and liver disease (Wallace, 1992a, b). Clinically the diseases usually present as a degenerative process with a progressive deterioration from onset. The degenerative nature of these genetic diseases can be attributed to a gradual loss of mitochondrial function that occurs over a person's lifetime. The process of OXPHOS is believed to contribute to the gradual loss of mitochondrial function through damaging mtDNA with oxygen free radicals.

The OXPHOS pathway is composed of five enzyme complexes containing multiple subunits. The first four enzyme complexes constitute the electron transport chain. NADH dehydrogenase (complex I), ubiquinol-cytochrome c oxidoreductase (complex III), and cytochrome c oxidase (complex IV) have subunits encoded in the mtDNA as well as the nuclear genome. Succinate dehydrogenase (complex II) is encoded solely in the nuclear genome and is not implicated in maternally inherited mitochondrial genetic diseases. The electron transport chain produces a proton electrochemical gradient which is utilized by F_1F_0 ATP synthase (complex V) to produce ATP.

Various abnormalities in mtDNA have been observed associated with mitochondrial genetic diseases. Deletions and insertions in the mtDNA genome have been associated with Kearns-Sayre syndrome (KSS), chronic external ophthalmoplegia plus (CEOP), and Pearson's marrow/pancreas syndrome. The mitochondrial genetic diseases myoclonic epilepsy and ragged-red fiber disease (MERRF); mitochondrial encephalomyopathy, lactic acidosis, and stroke-like symptoms (MELAS); and maternally inherited myopathy and cardiomyopathy (MMC) have been associated with point mutations in mitochondrial encoded tRNAs. The MERRF, MELAS and MMC mutations are postulated to act by inhibiting mitochondrial protein synthesis. Deletions, insertions, and point mutations in mitochondrial tRNAs have the effect of reducing or eliminating all or several of the proteins necessary for OXPHOS. This global effect on OXPHOS often results in morphologically abnormal mitochondria, and some of the more clinically severe manifestations of the mitochondrial genetic diseases (Wallace, 1992a, b).

Point mutations in mtDNA also result in mitochondrial genetic diseases by producing missense mutations in mitochondrial genes which impair their function. One example of this type of mitochondrial disease occurs in Leber's Hereditary Optic Neuropathy (LHON). Initially LHON was linked to a missense mutation in the gene for the ND4 protein which converted amino acid 340 from a conserved

arginine to a histidine. Additionally eight separate missense mutations have also been linked to LHON. The other missense mutations linked to LHON occur in other mitochondrial encoded subunits of NADH dehydrogenase (complex I) as well as one missense mutation in the *cyt b* gene, the mitochondrial encoded subunit for ubiquinol:cytochrome c oxidoreductase (complex III) (Singh *et al.*, 1989; Huoponen *et al.*, 1991; Howell *et al.*, 1991; Brown *et al.*, 1992).

The second genetic disease to be linked to a mitochondrial missense mutation is neurogenic muscle weakness, ataxia, and retinitis pigmentosa (NARP) (Holt *et al.*, 1990). The missense mutation is at nucleotide 8993 in the mtDNA *ATPase 6* gene. The mutation results in a change in *ATPase 6* amino acid 156 converting a conserved leucine to an arginine ($ATPase\ 6_{L156\rightarrow R}$). The mutation also resulted in a restriction fragment length polymorphism (RFLP) resulting in the appearance of an additional *AvaI* site in the mtDNA genome. The *AvaI* RFLP allowed the correlation between the severity of the disease and the percentage of mutant mtDNA genomes present in each patient. The mutation could also be followed by a *HpaII* RFLP.

The NARP mutation has also been linked to a second mitochondrial genetic disease. The mutation has been linked to some cases of maternally inherited Leigh's syndrome, or subacute necrotizing encephalopathy (SNE), by *AvaI* and *HpaII*

RFLP analysis (Tatuch *et al.*, 1992; Shoffner *et al.*, 1992; Ciafaloni *et al.*, 1993; Yoshinaga *et al.*, 1993). Leigh's syndrome is an early onset encephalopathy that often results in death at a young age. Leigh's syndrome was apparent only in patients with very high levels of the NARP mutation. The relationship between these genetic diseases is shown by the fact that the patient from the NARP pedigree that had very high levels of the mutation (>95%) exhibited clinical symptoms of Leigh's syndrome (Holt *et al.*, 1990). Additionally a patient in one of the Leigh's syndrome pedigrees with lower levels of the mutation present (<80%), exhibited clinical symptoms of NARP (Tatuch et al., 1992).

A second missense mutation at L156 has been reported by de Vries *et al.* (1993). The nucleotide mutation T8993→C was found instead of the T→G changed previously observed. The resulting mutation *ATPase* $6_{L156 \rightarrow P}$ could be followed by *HpaII* RFLP, but the *AvaI* RFLP was not present. The T8993→G mutation results in both restriction sites being formed, while T8993→C results in a *HpaII* site, shifted one base pair downstream from the T→G *HpaII* site. The NARP mutation reported by Yoshinaga *et al.* (1993) was tested only by *HpaII* RFLP, so a question exists as to which mutation is present.

Clinically the patients with NARP did not always exhibit elevated levels of lactic acid which supports the premise of a functional electron transport chain in some of the patients (Holt *et al.*, 1990). Neurological atrophy was

the prevalent phenotype of the disease indicating that the cellular energy thresholds were not being met in this tissue type. A defective ATP synthase (complex V) could account for this phenotype. Attempts to analyze cultured cell lines from patients gave results indicating no effect (Tatuch, *et al.*, 1992), or only a partial loss of F_1F_0 ATP synthase function (Tatuch & Robinson, 1993). Determination of the probable biochemical affect of the NARP mutations is presented in Chapter 5.

E. coli F_1F_0 ATP Synthase

Genetics

E. coli F_1F_0 ATP synthase is well characterized genetically. F_1F_0 is composed of eight different subunits in the following stoichiometry: $\alpha(3)$, $\beta(3)$, $\gamma(1)$, $\delta(1)$, and $\epsilon(1)$ in F_1, and $a(1)$, $b(2)$, and $c(10\pm1)$ in F_0. All subunits are encoded in the *unc* operon in *E. coli*. The order of genes is: *uncB* (*a*), *uncE* (*c*), *uncF* (*b*), *uncH* (δ), *uncA* (α), *uncG* (γ), *uncD* (β), and *uncC* (ϵ). An open reading frame termed *uncI* also resides 5′ with respect to *uncB* (*a*). The *uncI* open reading frame does not encode a known subunit of F_1F_0 ATP synthase. The *uncI* gene encodes a polypeptide which has been translated *in vitro* (Schneppe *et al.*, 1991). However, mRNA studies indicate that the RNA encoding *uncI* is quickly degraded from the polycistronic *unc* operon message,

and the rate of mRNA degradation may play a role in the differing protein levels of the F_1F_0 ATP synthase subunits (Schaefer *et al.*, 1989; Lagoni *et al.*, 1993). Differential translational control has been demonstrated for the unc operon message based on ribosome 'toe prints' (Schaefer *et al.*, 1989).

F_1 Subunits

The F_1 sector of ATP synthase houses the catalytic activity of the enzyme as discussed above. All five of the F_1 subunits, α, β, γ, δ, and ϵ, are required for both ATP synthesis and ATP-driven proton translocation *in vitro* (Dunn & Heppel, 1981) and *in vivo* (Downie *et al.*, 1979; Humbert *et al.*, 1983).

The α subunit. The α subunit is 513 amino acids long and has a deduced molecular weight of 55,300 daltons. It folds into a roughly ellipsoidal, globular structure (Gogol *et al.*, 1989a; Ishii *et al.*, 1993;Bianchet *et al.*, 1991). The α subunit can be divided into three functional regions, the membrane-binding region, the nucleotide-binding region, and the α/β signal transmission region (Senior, 1990). The membrane-binding region resides in the amino terminus of the α subunit, and may be involved in the association of the δ subunit with F_1. The depletion of the δ subunit from the F_1 sector results in the loss of the ability of F_1 to bind F_0. The function of this region is supported by proteolysis studies (Dunn *et al.*, 1980) and mutagenesis studies (Maggio

et al., 1988). The nucleotide-binding-domain is between amino acid positions α_{160} and α_{340} and proposed to be involved in the tight binding of ATP at a non-catalytic site. The nucleotide-binding domain function is supported by sequence homology with other nucleotide-binding proteins (Maggio *et al.*, 1987) and mutagenesis (Rao *et al.*, 1988). The proposed a α/β signal transmission region is believed to be involved in transmission of cooperativity between the catalytic nucleotide-binding sites. The α/β signal transmission region is located at amino acids positions α_{345} to α_{375} and its function supported by mutagenesis experiments (reviewed in Senior, 1990).

The β subunit. The β subunit is slightly smaller than the α subunit with 459 amino acids and a deduced molecular weight of 50,200 daltons. The β subunit appeared to be very similar to the α subunit in structural studies (Gogol *et al.*, 1989a; Ishii *et al.*, 1993; Bianchet *et al.*, 1991), and shares primary amino acid sequence homology with the α subunit (Walker *et al.*, 1984). The catalytic nucleotide-binding domain believed to be contained in the β subunit between amino acid positions β_{140} and β_{335} (Duncan *et al.*, 1986; Senior, 1988). Support for the β subunit containing the catalytic site of F_1 comes from affinity labeling with nucleotide analogs (reviewed by Senior, 1988) and mutagenesis analysis (reviewed by Futai *et al.*, 1989; Senior, 1990; Schnizer, 1993).

The γ subunit. The γ subunit consists of 286 amino acids with a deduced molecular weight of 31,400 daltons. The γ subunit displays conservation at the amino acid level in the amino-terminal and carboxyl-terminal regions (Futai *et al.*, 1989; Iwamoto *et al.*, 1990; Shin *et al.*, 1992). The γ subunit has also been localized to the central cavity of the α/β ring in F_1 by immuno-cryoelectron microscopy (Gogol *et al.*, 1989). The amino-terminal portion of the γ subunit was shown to reside in the cavity by using cryoelectron microscopy of monomaleimidonagold cross-linked to cysteines that had been incorporated into the γ subunit via site-directed mutagenesis of the *uncG* (γ) gene (Wilkens & Capaldi, 1992). Abrahams *et al.* (1993) proposed that the γ subunit may be responsible for a 90 Å long alpha-helix extending through the central cavity of F_1 (see above).

Aggeler and Capaldi (1992) also reported cross-linking via tetrafluorophenylazide maleimides (TFPAMs) of the α and β subunits to the mutant γ subunits containing cysteine substitutions. The mutant $\gamma_{S8\rightarrow C}$ subunit could be cross-linked to the β subunit, yielding different products with different ligands present (see above). The mutant $\gamma_{V286\rightarrow C}$ subunit cross-linked with the α subunit in an non-substrate dependent manner. Both cross-links inhibited F_1-ATPase activity at levels proportional to the cross-linking yield. The cross-linking results correlate with mutagenesis analysis of the γ subunit. The carboxyl-terminal region of

the γ was found to be important for ATPase activity (Iwamoto *et al.*, 1990), in agreement with the $\gamma_{V286\rightarrow C}/\alpha$ cross-link. Substitutions of arginine and lysine at γ_{M23} affect coupling between catalysis and proton translocation (Shin *et al.*, 1992), in agreement with ligand dependent $\gamma_{S8\rightarrow C}/\beta$ cross-links. Apparent ligand induced conformational changes indicates that the γ subunit may play a role similar to the ϵ subunit (see below).

The δ subunit. The δ subunit is an elongated and highly α-helical subunit of 177 amino acids with a deduced molecular weight of 19,300 daltons (Sternweis & Smith, 1977). The δ subunit is required for F_1 binding to F_o (Bragg *et al.*, 1973; Sternweis & Smith, 1977). The δ subunit can be cross-linked to the α and β subunits via the reactive cysteine δ_{C140} (Aggeler & Capaldi, 1992). The δ-α cross-link does not result in loss of F_1-ATPase activity (Brag & Hou, 1986; Tozer & Dunn, 1986; Mendel-Hartvig & Capaldi, 1991a). The amino-terminal and carboxyl-terminal regions of the δ subunit have been reported to be oriented toward F_1 (Mendel-Hartvig & Capaldi, 1991a).

The δ subunit has been shown to be involved in F_1 binding to F_o by mutagenesis analysis (Humbert *et al.*, 1983). Mutations in the δ subunit have also been implicated in affecting the stability of the F_1F_o ATP synthase complex (Stack & Cain, 1994) and DCCD sensitivity (Hazard & Senior, 1994). The δ subunit has also been suggested to open the

proton channel by interacting with F_O (Angov *et al.*, 1991).

The ϵ subunit. The ϵ subunit is a globular protein (Sternweis & Smith, 1980) of 138 amino acids with a deduced molecular weight of 15,000 daltons. Although structural data has not yet been reported, the ϵ subunit has been crystallized separately and in conjunction with the γ subunit (Codd *et al.*, 1992; Cox *et al.*, 1993). Binding of the ϵ subunit to F_1-ATPase (with or without the δ subunit present) results in inhibition of ATP hydrolysis activity (Laget & Smith, 1979; Sternweis & Smith, 1980; Dunn *et al.*, 1987). The ϵ subunit is also required for F_1 binding to F_O (Sternweis, 1978). The two functional domains of the ϵ subunit have localized to $\epsilon_{1\text{-}78}$ for F_1 binding to F_O, and $\epsilon_{80\text{-}90}$ for inhibition of F_1-ATPase activity (Kuki *et al.*, 1988). As mentioned above the detergent LDAO has also been proposed to effect the inhibitory action of the ϵ subunit (Lötscher *et al.*, 1984).

The ϵ subunit has also been reported by Capaldi and colleagues to undergo conformational changes that affect the subunit's rate of cleavage by trypsin, which results in activation of F_1-ATPase activity. The conformational change was controlled by the binding of ligands to F_1. Ligands ATP + EDTA, ADP + EDTA, AMP-PNP + Mg^{2+} resulted in a fast rate of trypsin cleavage. Ligands ATP + Mg^{2+} or ADP + P_i + Mg^{2+} resulted in a slow rate of trypsin cleavage. Nucleotide binding was required to elicit the conformation with a fast

rate of cleavage (EDTA, Mg^{2+}, Mg^{2+} + P_i, EDTA + P_i were equivalent to ATP + Mg^{2+}). The rate of trypsin cleavage with the ligands ADP and Mg^{2+} was high, but slowed by addition of phosphate (P_i). The concentration of P_i was determined to change the conformation of ϵ in a manner that correlated with high affinity binding of P_i to F_1 (Mendel-Hartvig & Capaldi, 1991a). The indication from the different ligands analysized is that the conformational change depends on whether ADP or ADP + P_i is present in the active site. This assumes Mg^{2+} is reguired for P_i binding, and that AMP-PNP mimics ADP in the catalytic site. The ϵ subunit could also be locked in either conformation by treatment of F_1F_0 ATP synthase with DCCD under the proper ligand conditions (Mendel-Hartvig & Capaldi, 1991b). The ligand induced conformational change of the ϵ subunit could also be followed by immuno-cryoelectron microscopy (Gogol *et al.*, 1990), as well as, differing cross-link product yields (Mendel-Hartvig & Capaldi, 1991a; Aggeler *et al.*, 1992). The ϵ subunit has been cross-linked via 1-ethyl-3-[3-(dimethylamino)propyl]-carbodiimide (EDC) to β (Mendel-Hartvig & Capaldi, 1991a), and cysteine substitution mutants to α and γ (Aggeler *et al.*, 1992).

The F_0 Subunits

The F_0 sector is made up of three subunits in *E. coli*. All three subunits, *a*, *b* and *c*, are required for coupled proton translocation (Schneider & Altendorf, 1985). The

stoichiometry of subunits is $a_1b_2c_{10\pm1}$ (Hermolin & Fillingame, 1989). As mentioned above, *E. coli* F_O is insensitive to oligomycin. In *E. coli*, proton translocation is usually inhibited by covalent modification of c_{D61} with DCCD.

The *a* subunit. The *a* subunit is a hydrophobic protein of 271 amino acids and deduced molecular weight of 30,276 daltons. However, the hydrophobic nature of the *a* subunit is thought to cause anomalous binding of sodium dodecyl sulfate (SDS), resulting in an apparent molecular weight around 23,000 daltons by SDS polyacrylamide gel electrophoresis (SDS PAGE). Hydropathy plots of the *a* subunit predict four-five potential membrane spanning regions. Predictions for the number of membrane spanning regions range from 5-8, and are discussed in greater detail below. Truncations of the *a* subunit result in loss of F_1F_O ATP synthase function if more than seven amino acids are removed from the carboxyl terminus (Eya *et al.*, 1991). However, missense mutations can also abolish enzyme function (Cain & Simoni, 1986).

The *a* subunit contains two regions strongly conserved at the amino acid level (see Figure 1-3). These regions of homology have been the basis for extensive site-directed mutagenesis analysis (Cain & Simoni, 1988, 1989; Eya *et al.*, 1988, 1991; Howitt *et al.*, 1988, 1993; Lightowlers *et al.*, 1987, 1988; Vik *et al.*, 1988, 1990, 1991, 1994; Chapter 4 and 6). An overview of the results of these studies is

presented in Chapter 7. The studies indicate that the *a* subunit is involved in proton translocation and coupling of the proton motive force to ATP catalysis. The amino acid a_{R210} is considered to be essential in proton conductance, with amino acids a_{E219} and a_{H245} also playing important roles.

The *b* subunit. The *b* subunit is a largely hydrophilic protein of 156 amino acids and a deduced molecular weight of 17,265 daltons. The *b* subunit is anchored to the membrane by one predicted membrane spanning region in its amino-terminal end. When this region is removed via a deletion in the *uncF* (*b*) gene, the hydrophilic portion of the *b* subunit, b_{sol}, is found to form a dimer (Dunn, 1992). The hydrophilic portion of the *b* subunit has been shown to play an important role in F_1 binding by proteolysis experiments (Hoppe *et al.*, 1983; Perlin *et al.*, 1983).

Mutagenesis experiments have resulted in mainly assembly phenotypes (Jans *et al.*, 1984, 1985; Porter *et al.*, 1985; McCormick & Cain, 1991). Mutations at b_{A79} result in assembly mutations, with an apparent dependence on expression levels (McCormick *et al.*, 1993). Additionally the $b_{A79\rightarrow K}$ mutation results in a unique phenotype that effects coupling of proton translocation to ATP catalysis. This mutation had a severe effect on ATP synthesis while maintaining substantial ability to actively transport protons with ATP hydrolysis. This is the clearest reported example of an asymmetrical effect on the coupling mechanism,

indicating that the *b* subunit plays a direct role in the mechanism. For this reason it is very interesting that mammalian mitochondria do not contain an analogous subunit. This indicates either a major change in the mechanism of coupling or a major change in the *b* subunit.

The *c* subunit. The proteolipid *c* subunit is an extremely hydrophobic protein of 79 amino acids with a deduced molecular weight of 8,288 daltons. It folds into a hairpin of two α-helices that span the membrane. A polar loop connects the two α-helices, and has been demonstrated to extend from the membrane on the cytoplasmic side (Girvin *et al.*, 1989; Hensel *et al.*, 1990). The structure of the *c* subunit has also been partially solved by NMR in a chloroform-methanol-water mixture (Girvin & Fillingame, 1993). (For *c* subunit reviews see Fillingame 1992a, b.)

As mentioned above DCCD binds to c_{D61} and inhibits proton conductance and the ATPase activity of F_1 bound to F_O. The amino acid c_{D61} is proposed to be near the center of the lipid bilayer, at least 10 Å inside the membrane surface (Mitra & Hammes, 1990). When site-directed mutagenesis is used to change c_{D61} to either a glycine or an asparagine, proton conductance is abolished. The carboxylic group of amino acid c_{D61} is considered essential for proton conductance, since activity is retained with a glutamate substitution (Miller *et al.*, 1990). The carboxylic group can also be moved to the other α-helix of the *c* subunit,

with retention of some activity in the double mutation $c_{A24\rightarrow D,D61\rightarrow G}$ (Miller *et al.*, 1990). Third-site suppressor mutants have also been isolated that improve the activity of the $c_{A24\rightarrow D,D61\rightarrow G}$ double mutation (see below).

The several amino acids located in the polar loop of the *c* subunit and are conserved in other proteolipid subunits. Structurally non-conservative amino acid substitutions at these positions result in a loss of ATP synthase function. The phenotype of these mutants is proposed to be the uncoupling of ATP catalysis from proton translocation (Mosher *et al.*, 1985; Miller *et al.*, 1989; Fraga & Fillingame, 1989, 1991). A reduction in F_1 binding affinity to F_O was also observed with some of the mutations, as well as, passive proton conductance when F_1 was apparently bound to F_O. Loss of F_1-ATPase DCCD sensitivity was also observed, while proton conductance was still inhibited by DCCD. The highly conserved amino acid positions c_{R41}, c_{Q42}, and c_{P43} were the most sensitive to mutagenesis (Fraga & Fillingame, 1991).

The *c* subunit also has two apparent roles, the conductance of protons and the coupling of F_1 to F_O. The mechanism of *c* subunit coupling appears to be mainly through the binding affinity of F_1 for F_O. The *c* subunit's effect on binding affinity would have to be mediated through another subunit if the hypothetical stalk region exist. Candidates for interaction with the *c* subunit are the *b* and

δ subunits.

Second-Site Suppressor Mutations in F_O

A second-site suppressor mutation occurs when the original deleterious mutation is complemented by a second mutation in another codon. Second-site suppressor mutations can reveal interactions between amino acids, potentially giving insight into tertiary structure if the second-site suppressor resides at a distance from the original mutation. If the suppressor occurs in another protein, then subunit interactions may also be revealed. Several suppressor mutation studies have been carried out in F_O subunits and are reviewed below.

Kumamoto and Simoni (1986a, 1986b) studied suppression of the mutation of $b_{G9\rightarrow D}$. The substitution did not completely block proton translocation but function of the complex was so low that the bacteria failed to grow on succinate minimal medium. A selection scheme was used to isolate suppressor mutations that occurred in other F_1F_O ATP synthase subunits. Suppressor mutations occurred in each of the other two F_O subunits. Two suppressor mutations occurred in the *a* subunit, $a_{P240\rightarrow A}$ and $a_{P240\rightarrow L}$. The *c* subunit suppressor mutation was $c_{A62\rightarrow S}$. Both suppressor mutations recovered only partial activity for F_1F_O ATP synthase. Biochemical analysis of the $b_{G9\rightarrow D}$ mutant, and the nature of the suppressor mutants, indicated that the suppressor mutants probably were correcting conformational changes

imposed by the initial mutant. The locations of the suppressor mutants imply that the *b* subunit interacts with the *a* subunit and the *c* subunit.

Cain and Simoni (1988) engineered an intra-gene suppressor mutation in the *a* subunit gene. This study involved the two amino acids a_{E219} and a_{H245}. Both amino acids were changed independently and together by site-directed mutagenesis. The mutant $a_{E219 \rightarrow H}$ had little activity while the mutant $a_{H245 \rightarrow E}$ had somewhat higher levels of activity. The second-site suppression was constructed by the production of the double mutation of $a_{E219 \rightarrow H, H245 \rightarrow E}$. The strain carrying the double mutation exhibited more F_1F_O ATP synthase activity than either of the individual mutants. The amino acid positions a_{E219} and a_{H245} are predicted to be on different membrane spanning segments (see below). The ability to exchange the amino acids at these two positions indicates not only interaction between the amino acids themselves, but interactions between the membrane spanning regions.

Miller *et al.* (1990) also isolated an internal second-site suppressor by investigating suppressors of the $c_{D61 \rightarrow G}$ mutation. The $c_{D61 \rightarrow G}$ mutation abolishes proton conductance and renders F_1F_O ATPase insensitive to DCCD inhibition (see above). Attempts to move the aspartic acid to amino acid positions near c_{61} failed to restore enzyme function, indicating precise requirements for the position of carboxylic acid in enzyme function. A second-site

suppressor mutation was isolated through limited medium selection. The $c_{A24\rightarrow D}$ mutation was found to suppress the $c_{D61\rightarrow G}$ phenotype, allowing 60% of normal enzyme function. Interaction between c_{A24} and c_{D61} had been demonstrated before with the DCCD insensitive mutant $c_{A24\rightarrow S}$ (Fillingame *et al.*, 1991). The $c_{A24\rightarrow D,D61\rightarrow G}$ double mutation has been used to align the positions of the two membrane spanning helices predicted in the *c* subunit. The ability to move the essential carboxylic acid to the other helix of the *c* subunit indicates that position c_{24} is in close proximity to position c_{61}. This conclusion has been supported by NMR structural data for the *c* subunit (Girvin & Fillingame, 1993).

The $c_{A24\rightarrow D,D61\rightarrow G}$ double mutation was also subjected to a limited medium selection process (Fraga *et al.*, 1994). Third-site suppressor mutants were found in the *c* and *a* subunits. Five mutations were found in the *c* subunit at amino acid positions c_{F53} (3), c_{M57} (1) and c_{G71} (1). Thirteen mutations were found in the *a* subunit at amino acid positions a_{D92} (1), a_{V198} (2), a_{A217} (3), a_{I221} (3), and a_{L224} (4). There were no clear trends in the type of amino acid substitutions isolated. Surprisingly, several of the suppressor mutations occurred in regions predicted to be outside the membrane hydrophobic core (see below). One possible explanation for this observation is that extra-membrane loops may play a role in the positioning of the membrane spanning regions. This is an interesting

hypothesis, since the majority of the third-site mutations in the *a* subunit are in positions that might affect the positioning of the membrane spanning region containing the essential amino acid a_{R210}.

The *a* Subunit of *E. coli* F_1F_O ATP Synthase

Conservation of the *a* Subunit

The *a* subunit shares homology at the amino acid level with all *a*-like F_1F_O ATP synthase subunits. This homology is most prevalent in the carboxyl-terminal region of the subunit. This region has also been found to play an important role in proton conductance (Cain & Simoni, 1988, 1989; Eya *et al.*, 1988, 1991; Howitt *et al.*, 1988; Lightowlers *et al.*, 1987, 1988; Vik *et al.*, 1990, 1991).

Figure 1-3 aligns the reported *a*-like amino acid sequences. Six-membrane spanning regions were defined based on the criteria of exclusion of non-conserved charge from a hypothetical hydrophobic core. Surprisingly, at least one amino acid was found to be completely conserved in five of the six predicted membrane spanning regions. Likewise non-conserved positively charged amino acids (mostly lysines) were used to define eight of the twelve hydrophobic-hydrophilic interfaces. The variation in size of one extra-membrane loop helps define two other interfaces. The other two interfaces

Code	Organism, Strain, Organelle	Reference
Ec =	*E. coli*	Walker *et al.*, 1984
Va =	*Vibrio alginolyticus*	Prot. Ident. Res., 1992
Bm =	*Bacillus megaterium*	Brusilow *et al.*, 1989
P3 =	thermophilic *Bacillus* strain PS3	Ohta *et al.*, 1988
OF =	*Bacillus firmus*, strain OF4	Ivey & Krulwich, 1991
Pm =	*Propionigenium modestum*	Esser *et al.*, 1990
Ab =	*Anabaena* sp. strain PCC-7120	Prot. Ident. Res., 1992
Sy =	*Synechococcus* sp. strain 6301	Cozens & Walker, 1987
Lw =	Liverwort (*Marchantia polymorpha*) chloroplast	Prot. Ident. Res., 1992
GP =	Garden pea chloroplast	Cozens *et al.*, 1986
Tb =	Common tobacco chloroplast	Prot. Ident. Res., 1992
So =	*Spinacia oleracea* chloroplast	Hennig & Herrman, 1986
Rr =	*Rhodospirillum rubrum*	Prot. Ident. Res., 1992
Sc =	Yeast (*Saccharomyces cerevisiae*) mitochondrion	Macino & Tzagoloff, 1980
Ch =	*Cochliobolus heterostrophus* mitochondrion	Prot. Ident. Res., 1992
Ni =	*Aspergillus* and *Emericella nidulans* mitochondrion	Grisi *et al.*, 1982
Ob =	*Oenothera berteriana* mitochondrion	Prot. Ident. Res., 1992
Rd =	Radish mitochondrion	Prot. Ident. Res., 1992
Wh =	Wheat mitochondrion	Prot. Ident. Res., 1992
Mz =	Maize mitochondrion	Dewey *et al.*, 1985
Rc =	Rice mitochondrion	Prot. Ident. Res., 1992
Dm =	Fruit fly (*Drosophila melanogaster*) mitochondrion	Prot. Ident. Res., 1992
Pl =	Sea urchin (*Paracentrotus lividus*) mitochondrion	Jacobs *et al.*, 1988
Xp =	*Xenopus laevis* mitochondrion	Roe *et al.*, 1985
Tr =	Cutthroat and Rainbow trout mitochondrion (fragment)	Prot. Ident. Res., 1992
Sm =	Chinook, Coho and Sockeye salmon mitochondrion (fragment)	Prot. Ident. Res., 1992
Ck =	Chicken mitochondrion	Prot. Ident. Res., 1992
CH =	Chinese hamster mitochondrion	Prot. Ident. Res., 1992
Ms =	Mouse mt	Bibb *et al.*, 1981
Bv =	Bovine mt	Anderson *et al.*, 1982
Hu =	Human mitochondrion	Anderson *et al.*, 1981

Figure 1-3. Alignment of *a*-like subunits. Proposed membrane spanning regions are boxed, and Roman numerals denote helix name. The *E. coli* amino acid position is listed above sequence. Homology used for alignment of sequence denoted by ∇.

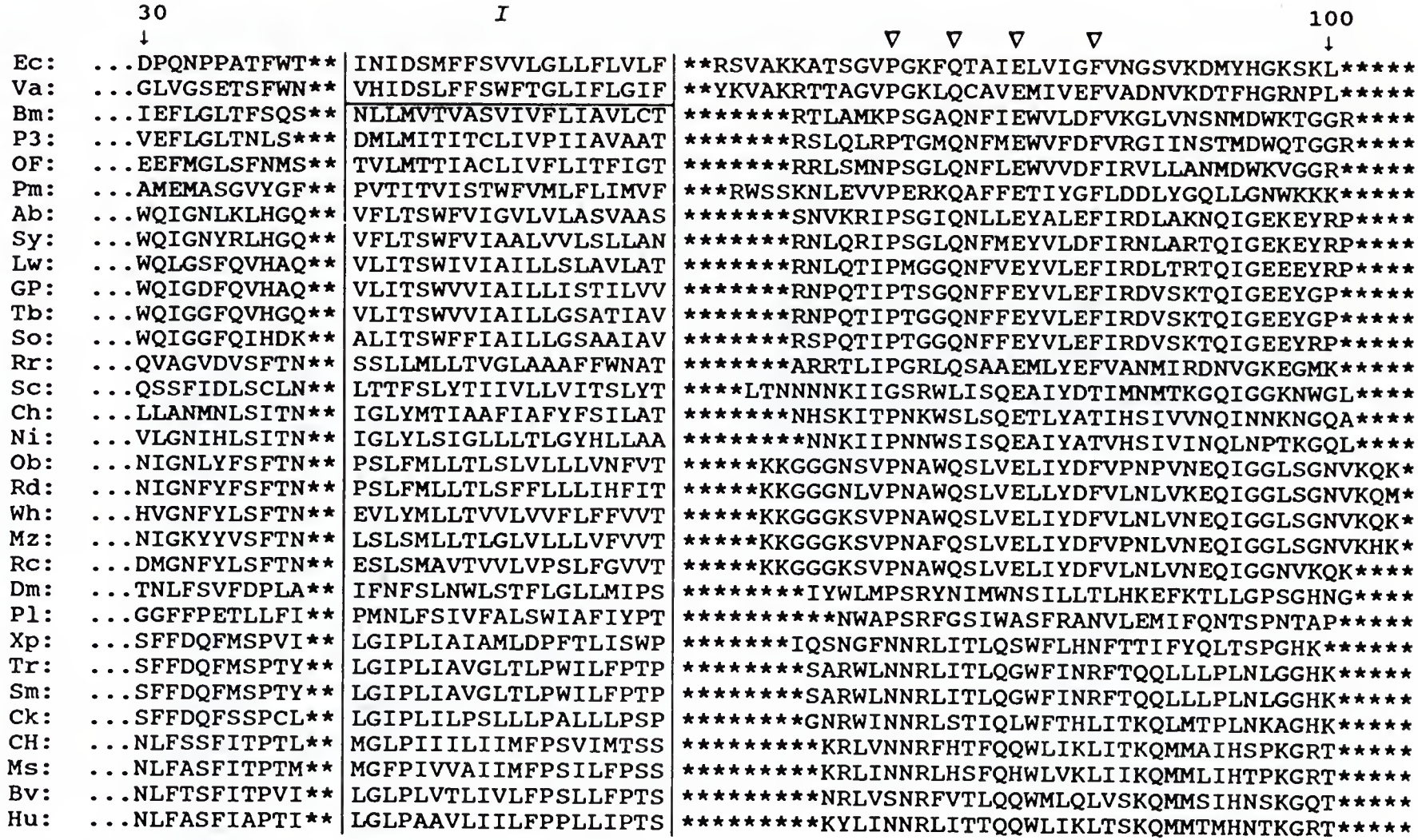

Figure 1-3--continued. Proposed membrane spanning regions are boxed, and Roman numerals denote helix name. The *E. coli* amino acid position is listed above sequence. Homology used for alignment of sequence denoted by ∇.

```
                101          II                                                  III          161
                 ↓           ∇     ∇  ∇                                    ∇     ∇           ↓
Ec:  **|IAPLALTIFVWVFLMNLMD|**LLPIDLLPYIAEHVLGLPALRVV**|PSADVNVTLSMALGVFILI|**
Va:  **|IAPLALTIFCWVFLMNVMD|**LVPIDFLPYPAEHWLGIPYLKVV**|PSADVNITMAMALGVFALM|**
Bm:  **|FLTLGVTLLMYIFVSNMLG|**********LPFAIVIDHNLWWKS**|PTADPAITLTLAVMVVVLS|**
P3:  **|FLTLGVTLIMYVFVANMLG|**********LPFSVHVNGELWWKS**|PTADATVTLAVMVVALTHY|**
OF:  **|FIVLAYALLFYVFVANMLG|********LPFELYNPTTHEVWWKS**|PTFDPVLTLTMAAFVVILT|**
Pm:  **|YFTYIGTLFLFLLISNIVS|***FFPIPGFSSENGVFSIAPALRT**|PTADLNTTVGLALLTTYSF|**
Ab:  **|WVPFVGTLFLFIFVSNWSG|********ALVPFKLIHLPEGELTA**|PTSDINTTVALALLTSLAY|**
Sy:  **|WVPFIGTLFLFIFLSNWSG|********ALIPWKLIKLPSGELAA**|PTSDINTTVALALLTSLAY|**
Lw:  **|WVPFIGTMFLFIFVSNWSG|********ALFPWRVFELPNGELAA**|PTNDINTTVALALLTSVAY|**
GP:  **|WVPFIGTLFLFIFVSNWSG|********ALLPWKIIKLPHGELAA**|PTNDINTTVALALLTSVAY|**
Tb:  **|WVPFIGTMFLFIFVSNWSG|********ALLPWKIIQLPHGELAA**|PTNDINTTVALALLTSVAY|**
So:  **|WVPFIGTMFLFIFVSNWSG|********ALLPWKIIQLPHGELAA**|PTNDINTTVALALLASVAY|**
Rr:  **|YFPYILTLFVFVFLGNMLG|**********************ML**|PYSFTFTSHIAVTAALAVG|**
Sc:  **|YFPMIFTLFMFIFIANLIS|**********************MI**|PYSFALSAHLVFIISLSIV|**
Ch:  **|YFPFMYTLFIFILINNLIG|**********************MV**|PYSFASTSHFILTFSLSFT|**
Ni:  **|YFPFIYALFIFILVNNLIG|**********************MV**|PYSFASTSHFILTFSMSFT|**
Ob:  **|FFPRISVTFTFSLFRNPQG|**********************MI**|PYSFTVTSHFLITLGLSFS|**
Rd:  **|FFPCILVTFLFLLFCNLQG|**********************MI**|PYSFTVTSHFLITLALSFS|**
Wh:  **|FFPRISVTFTFSLFRNPQG|**********************MI**|PFSFTVTSHFLITLALSFS|**
Mz:  **|FFPCISVTFTFSLFRNPQG|**********************MI**|PFSFTVTSHFLITLALSFS|**
Rc:  **|FFPRISVTFTFSLFRNPQG|**********************MI**|PFSFTVTSHFLITLALSFS|**
Dm:  **|STFIFISLFSLILFNNFMG|**********************LF**|PYIFTSTSHLTLTLSLALP|**
Pl:  **|WAGLITTVFIVILSANVLG|**********************LF**|PYAFTATSHISLTYSLGFP|**
Xp:  **|WALLLTSLMLLLMSLNLLG|**********************LL**|PYTFTPTTQLSLNMGLAVP|**
Tr:  **|WAALLTSLMLFLITLNMLG|**********************LL**|PYTFTPTTQLSLNMGLAVP|**
Sm:  **|WAALLTSLMLFLITLNMLG|**********************LL**|PYTFTPTTQLSLNMGLAVP|**
Ck:  **|WALLLTSLILMLLSINLLG|**********************LL**|PYTFTPTTQLSMNMALALP|**
CH:  **|WSLMLASLIIFIGSTNLLG|**********************LL**|PHTFTPTTQLSMNLGMAIP|**
Ms:  **|WTLMIVSLIMFIGSTNLLG|**********************LL**|PHTFTPTTQLSMNLSMAIP|**
Bv:  **|WTLMLMSLILFIGSTNLLG|**************************|PHSFTPTTQLSMNLGMAIP|**
Hu:  **|WSLMLVSLIIFIATTNLLG|**********************LL**|PHSFTPTTQLSMNLAMAIP|**
```

Figure 1-3--continued. Proposed membrane spanning regions are boxed, and Roman numerals denote helix name. The *E. coli* amino acid position is listed above sequence. Homology used for alignment of sequence denoted by ∇.

```
          162                                IV                                V                  222
           ↓                                 ∇    ∇                            ∇  ∇∇  ∇   ∇    ↓
Ec:  ***LFYSIKMKGIGGFTKELTLQPF***|NHWAFIPVNLILEGV|**SLLSKP**|VSLGLRLFGNMYAGELIF|**
Va:  ***IYYSIKVKGLGGFAKELALHPF***|NHPLMIPFNLLIEVV|**SLLAKP**|LSLGMRLFGNMFAGEVVF|**
Bm:  ******HYYGIKMRGFSAYTKDYFK***|PMAFLFPLKIIEEFA|******NT**|LTLGLRLYGNIYAGEILL|**
P3:  ********YGVKMKGASDYLRDYTR***|PVAWLFPLKIIEEFA|******NT**|LTLGLRLFGNIYAGEILL|**
OF:  ******HYYGIKIQGFGKYLKGYIT***|PVPFLLPFKIIEEFA|******NT**|LTLGMRLFGNVYAKEILM|**
Pm:  ******IAASFRTSGFFGFFKGLFE***|PMPLMFPINLAGEFA|******KP**|TNISIRLFGNMFAGMVIL|**
Ab:  *******FYAGFSKKGLGYFGNYVQ***|PVSFMLPFKIIEDFT|******KP**|LSLSFRLFGNILADELVV|**
Sy:  *******FYAGFSRKGLGYFGNYVH***|PTPVMLPFKILEDFT|******KP**|LSLSFRLFGNILADELVV|**
Lw:  *******FYAGLHKKGLSYFGKYIQ***|PTPVLLPINILEDFT|******KP**|LSLSFRLFGNILADELVV|**
GP:  *******FYAGISKKGLAYFGKYIQ***|PTPILLPINILEDFT|******KP**|LSLSFRLFGNILADELVV|**
Tb:  *******FYAGLTKKGLGYFGKYIQ***|PTPILLPINILEDFT|******KP**|LSLSFRLFGNILADELVV|**
So:  *******FYAGLTKKGLGYFGKYIQ***|PTPILLPINILEDFT|******KP**|LSLSFRLFGNILAEDLVV|**
Rr:  *IFIAVTIIGFARHGFHYFRMFFPHG**|APLLTAPLLIPIELI|**SYLSRP**|FSLSVRLFANMTVGHIML|**
Sc:  *IWLGNTILGLYKHGWVFFSLFVPAG**|TPLPLVPLLVIMETL|**SYIARA**|ISLGLRLGSNILAGHLLM|**
Ch:  *VVLGATVLGFKEHGLKFFSLFVPAG**|CPLGLLPLLVLIEFI|**SYLARN**|VSLGLRLAANILSGHMLL|**
Ni:  *IVLGATFLGLQRHGLKFFSLFVPSG**|CPLGLLPLLVLIEFI|**SYLSRN**|VSLGLRLAANILSGHMLL|**
Ob:  *IFIGITIVGFQRNGLHFLSFSLPAG**|VPLPLAPFLVLLELI|**PHCFRA**|LSSGIRLFANMMAGHSSV|**
Rd:  *IFIGITIVGFQRHGLHFFSFLLPAG**|VPLPLAPFLVLLELI|**SYCFRA**|LSLGIRLFANMMAGHSLV|**
Wh:  *IFIGITIVGFQRHGLHFFSFLLPAG**|VPLPLAPFLVLLELI|**SYCFRA**|LSLGIRLFANMMAGHSLV|**
Mz:  *IFIGITIVGFQRHGLHFFSFLLPAG**|VPLPLAPFLVLLELI|**SHCFRA**|LSSGIRLFANMMAGHSSV|**
Rc:  *IFIGITIVGFQRHGLHFFSFLLPAG**|VPLPLAPFLVLLELI|**SHCFRA**|LSSGIRLFANMMAGHSSV|**
Dm:  *LWLCFMLYGWINHTQHMFAHLVPQG**|TPAILMPFMVCIETI|**SNIIRP**|GTLAVRLTANMIAGHLLL|**
Pl:  *IWMAVNILGFYLAFNSRLSHLVPQG**|TPSALIPLMVWIETL|**SLFAQP**|IALGLRLAANLTAGHLLI|**
Xp:  **LWLATVIMASKPTNYALGHLLPEG**|TPTPLIPVLIIIETI|**SLFIRP**|LALGVRLTANLTAGHLLI|**
Tr:  *LWLATVIIGMRNQPTAALGHLLPEG**|TPVPLIPVLIIIETI|**SLFIR***|PALGVRLTANLTAGHQLI|**
Sm:  *LWLATVIIGMRNQPTAALGHLLPEG**|TPVPLIPVLIIIETI|**SLFIR***|PALGVRLTANLTAGHQLI|**
Ck:  *LWLATLLTGLRNQPSASLGHLLPEG**|TPTPLIPALIMIETT|**SLLIRP**|LALGVRLTANLTAGHLLI|**
CH:  *PWAGAVILGFRHKMKDSLAHFLPQG**|TPIPLIPMLVIIETI|**SLFIQP**|MALAVRLTANITAGHLLM|**
Ms:  *LWAGAVITGFRHKLKSSLAHFLPQG**|TPISLIPMLIIIETI|**SLFIQP**|MALAVRLTANITAGHLLM|**
Bv:  *LWAGAVITGFRNKTKASLAHFLPQG**|TPTPLIPMLVIIETI|**SLFIQP**|MALAVRLTANITAGHLLI|**
Hu:  *LWAGTVIMGFRSKIKNALAHFLPQG**|TPTPLIPMLVIIETI|**SLLIQP**|MALAVRLTANITAGHLLM|**
```

Figure 1-3--continued. Proposed membrane spanning regions are boxed, and Roman numerals denote helix name. The *E. coli* amino acid position is listed above sequence. Homology used for alignment of sequence denoted by ∇.

```
           223                                             VI                  271
            ↓                                   ▽        ▽▽  ▽  ▽   ▽           ↓
Ec:  *********ILIAGLLPWWSQWILNVP********* | WAIFHILIITLQAFIFMVLTIVYL | **SMASEEH
Va:  *********ILCAAMLPWYLQWMGSLP********* | WAIFHILVITIQAFVFMMLTIVYL | **SMAHEDP...
Bm:  *******SLLAGLATTGFLGTIGAAIPMLL****** | WQGFSIFVGAIQAFIFTMLTMVYL | **SHKVSSD...
P3:  *****GLLASLGTHYGVLGAVGASQFPIMV****** | WQAFSIFVGTIQAFIFTMLTMVYM | **PHKVKS
OF:  *******ILLVTAGTSGLIGMFGAFLPLIV****** | WQAFGLFIGAIQAYIFAMLAMVYM | **AHKVESH
Pm:  *************GLLYKAAPVLIPAPL******** | HLYFDLFSGVVQSFVFIMLTMVYI | **QGSIGDA...
Ab:  *************AVLVLLVPLFVPLP********* | VMAFPLFTSAIQALIFATLAAAYI | **GEAMEDH...
Sy:  *************AVLVLLVPLFVPLP********* | AMILGLFTSAIQALIFATLAASYI | **GEAVEEH...
Lw:  *************AVLISLVPLVVPIP********* | MMFLGLFTSAIQALIFATLAAAYI | **GESMEGH...
GP:  *************VVLVSLVPLVVPIP********* | VMFLGLFTSGIQALIFATLAAAYI | **GESMEGH...
Tb:  *************VVLVSLVPLVVPIP********* | VMLLGLFTSGIQALIFATLAAAYI | **GESMEGH...
So:  *************VVLVSLVPLVVPIP********* | VMFLGLFTSGIQALIFATLAAAYI | **GDSLDGH...
Rr:  ***KVLAGFVIMLGVVGGVVPFAVVLG********* | VTVLEFFIAALQAYVFTILTCIYL | **NDAINMH
Sc:  ***VILAGLTFNFMLINLFTLVFGFVPLAMILA*** | IMILEFAIGIIQSYVWTILTASYL | **KDTLYLH
Ch:  ***NILSGFTYNIMSSGIIFFILGLLPLAFIIA*** | FSGLELGIAFIQSQVFVVLSCSYI | **KDALELH
Ni:  ***SILSGFTYNIMTSGILFFFLGLIPLAFIIA*** | FSGLELAIAFIQAQVFVVLTCSYI | **KDGLDLH
Ob:  ***KILSGFAWTMLCMNDLFYFIGDLGPLFIVLA** | LTGPELGVAISQAYVSTISICIYL | **NDATNLH...
Rd:  ***KILSGFAWTMLCMNEIFYFIGALGPLFIVLA** | LTGLELGVAILQAYVFTILICIYL | **NDAINLH
Wh:  ***KILSGFAWTMLFLNNIFYFIGDLGPLFIVLA** | LTGLELGVAISQAHVSTISICIYL | **NDATNLH...
Mz:  ***KILSGFAWTMLFLNNIFYFLGDLGPLFIVLA** | LTGLELGVAISQAHVSTISICIYL | **NDATNLH...
Rc:  ***KILSGFAWTMLFLNNIFYFIGDLGPLFIVLA** | LTGLELGVAILQAHVSTISICIYL | **NDAINLH...
Dm:  ******TLLGNTGSSMSYMLMTFLLMAQIA****** | LLVLESAVAMIQSYVFAVLSTLYS | **SEVN
Pl:  *****FLLSTAIWLLSSSLMVSSIPIFVIFVL**** | LFILEIGVACIEAYVFTALVHFYL | **QQNV
Xp:  *****QLIATAAFVLLSIMPTVAILTSIVLFL**** | LTLLEIAVAMIQAYVFVLLLSLYL | **QENV
Tr:  ******ATAAFVLLPMMPTVAILTSIVLFL****** | LTLLEIAVAMIQAYVFVLLLSLYL | **QENV
Sm:  ******ATAAFVLLPMMPTVAILTSIVLFL****** | LTLLEIAVAMIQAYVFVLLLSLYL | **QENV
Ck:  *****QLISTATIALLPMMPSISALTALILFL**** | LTILEVAVAMIQAYVFVLLLSLYL | **QENI
CH:  *****HLIGGATLVLTSISLPTAMITFIILIM**** | LTILEFAVALIQAYVFTLLVSLYL | **HDNT
Ms:  *****HLIGGATLVLMNISPPTATITFIILLL**** | LTILEFAVALIQAYVFTLLVSLYL | **HDNT
Bv:  *****HLIGGATLALMSISTTTALITFTILIL**** | LTILEFAVAMIQAYVFTLLVSLYL | **HDNT
Hu:  *****HLIGSATLAMSTINLPSTLIIFTILIL**** | LTILEIAVALIQAYVFTLLVSLYL | **HDNT
```

Figure 1-3--continued. Proposed membrane spanning regions are boxed, and Roman numerals denote helix name. The *E. coli* amino acid position is listed above sequence. Homology used for alignment of sequence denoted by ▽.

were defined by more subjective methods. Five of the six hydrophobic membrane spanning regions were 18 to 24 amino acids long. Predicted membrane spanning region IV is defined as only 15 amino acids. This membrane spanning region does not follow the criteria used to define the other regions, however its existence is supported by alkaline phosphatase data (see below).

Additionally, the first extra-membrane loop was also found to contain amino acid homology. The amino acids a_{P72}, a_{Q76}, a_{E80}, and a_{F85} were found to be conserved in all bacterial and chloroplast *a*-like subunits. Predictions of secondary structure indicate that these amino acids may form an amphipathic α-helix. Deletion of this extra-membrane region results in loss of enzyme function (Lewis & Simoni, 1992). The importance of this loop is also supported by the third-site suppressor mutations mention above (Fraga & Fillingame, 1994), for one of the mutations isolated was in a_{D92}. The amino acid a_{E80} also appears to be conserved in the mitochondria of fungi and plants. One possible function of this region is interaction with the *b* subunit. This conservation is lost in the *a*-like subunits from organisms that do not have a *b*-like subunit embedded in the membrane sector.

Topology of the *a* Subunit

Models for the topology of the a subunit have predicted 5 to 8 membrane spanning regions. Hydropathy plots of the

E. coli a subunit predict 5 hydrophobic regions large enough to span the membrane. Vik and Dao (1992) used computer hydropathy plots from the yeast *a*-like subunit and the *E. coli a* subunit to predict six membrane spanning regions. The alignment presented in Figure 1-3 is the first to use all the *a*-like subunits to determine a consensus for hydrophobic regions (see above). The alignment data was used to construct a hypothetical topology model of the *a* subunit (Figure 1-4).

Two groups have produced *phoA/uncB* (alkaline phosphatase/subunit *a*) fusions to study the topology of the *a* subunit. Bjorbaek *et al.* (1990) predicts eight membrane spanning regions with both termini extending into the cytoplasm. Lewis *et al.* (1990) also predicts eight spanning regions but with both termini on the periplasmic side of the membrane. The production of a *phoA* fusion at the carboxyl terminus lends more credibility to the latter model. Additionally, the Bjorbaek *et al.* (1990) *phoA* fusion data can be more easily incorporated into the Lewis *et al.* model than the Lewis *et al.* (1990) data into the Bjorbaek *et al.* model. The Lewis *et al.* model also predicted transmembrane spanning regions too short to span a lipid bilayer by the traditional α-helix. Non-α-helix structure was proposed for the shorter transmembrane regions. Alternately a structural shortening of the distance protons must be transported across the membrane was also proposed. Analysis of the data

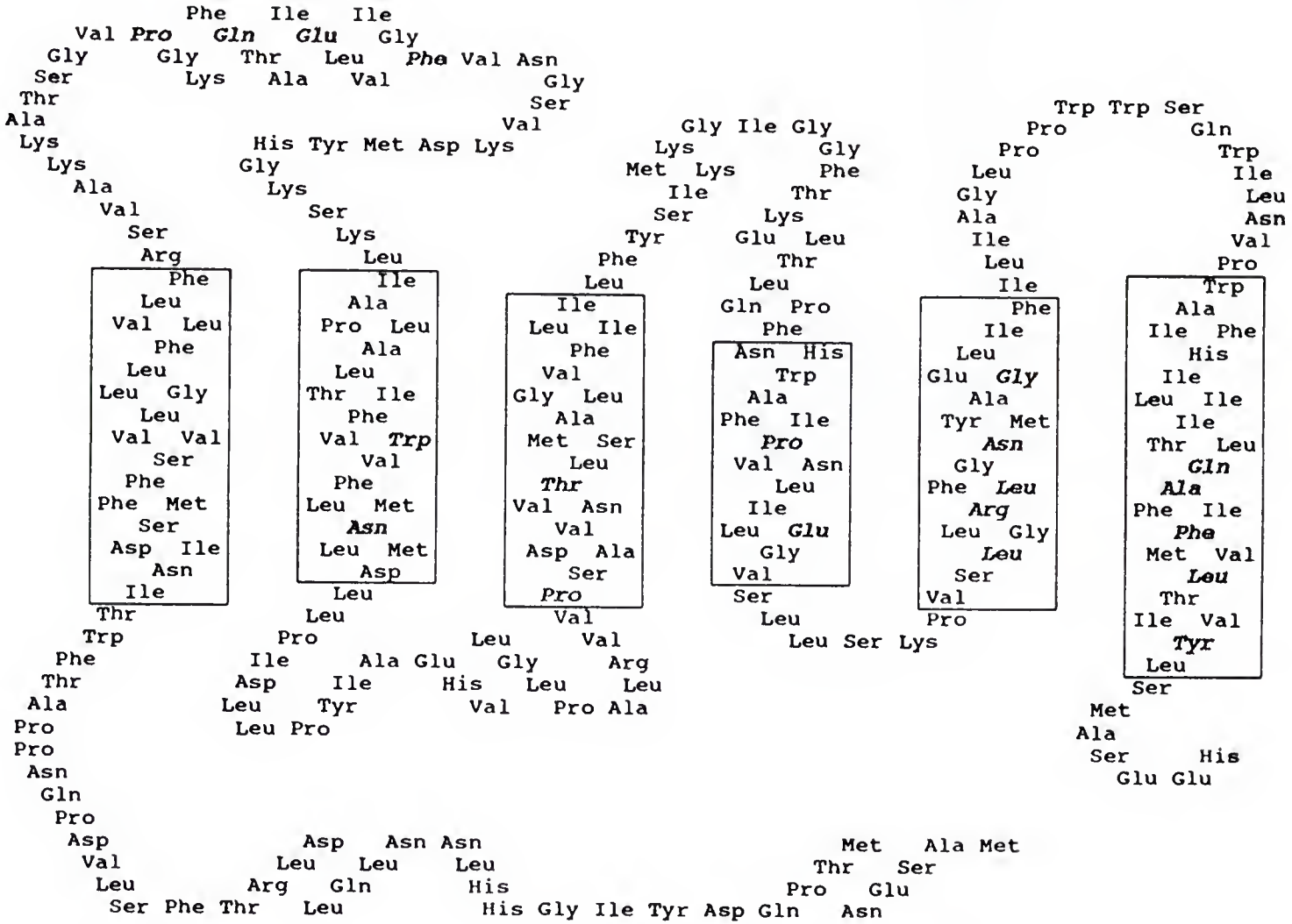

Figure 1-4. Proposed topology model of the *a* subunit. The model incorporates the observations from the alignment in Figure 1-3, and is consistent with alkaline phosphatase/subunit *a* fusion data (see text).

from both experiments can also be used to support a model with six membrane spanning regions. The ambiguity of the alkaline phosphatase technique can explain the differing interpretations of fusion protein data. Evidence for the amino-terminus being located on the periplasmic facing of the membrane was obtained via β-galactosidase fusions with the *a* subunit (Lewis & Simoni, 1992).

Significance of the *a* Subunit

F_1F_0 ATP synthase is of biological importance to the bioenergetics of all aerobic organisms. The *a* subunit is essential for the function of F_1F_0 ATP synthase. The importance of F_1F_0 ATP synthase and the *a* subunit were demonstrated by the NARP mutation in human mitochondrial genetic diseases. High levels of the NARP mutation in the *a*-like subunit in human mitochondria correlates with a clinical phenotype of neurological atrophy. The phenotype is consistent with a reduction in cellular energy levels resulting in the death of nerve cells.

The *a* subunit is also essential to the mechanism of proton translocation. The mechanism of proton transport is probably similar to the mechanism of transporting other ions. This is supported by the F_1F_0 ATP synthase of *P. modestum*, which transports sodium ions as well as protons. Ion transport is a vital part of all biological systems, and very little is known about how it is accomplished and controlled.

The *a* subunit may also play a role in coupling proton translocation with ATP catalysis. How energy is converted from an electrochemical gradient into the chemical bond energy of ATP is one of the primary unanswered question concerning the chemiosmotic hypothesis.

The conservation of all F_1F_0 ATP synthases at the functional and structural level indicate that the *E. coli* F_1F_0 ATP synthase can be used as a model for investigating the function of the *a* subunit. This work encompasses the investigation of amino acids in the *a* subunit involved in proton translocation (Chapter 4). The biochemical effects of the *ATPase 6* gene mutations, that result in the human mitochondrial genetic disease NARP, were also determined by modeling the mutations in the *E. coli a* subunit (Chapter 5). Modeling of sequence variations that occur in the *a*-like subunits of chloroplast and alkaliphilic bacteria revealed a role for the *a* subunit in coupling proton translocation with ATP catalysis (Chapter 6).

CHAPTER 2
EXPERIMENTAL PROCEDURES

Molecular Techniques

Materials

T-4 DNA ligase, T-4 polynucleotide kinase, Taq polymerase, and restriction endonucleases were supplied by Bethesda Research Laboratories (Bethesda, MD) and New England Biolabs (Beverly MA). Taq-Traq sequencing system was the product of Promega (Madison, WI). AmpliTaq Cycle Sequencing Kit was purchased from Perkin Elmer Cetus (Norwalk, CT). Radionucleotides were purchased from Amersham Corp. (Arlington Heights, IL) or ICN Biomedicals, Inc. (Costa Mesa, CA). Lysozyme was supplied by Sigma Chemical Co. (St. Louis, MO). Difco Laboratories (Detroit, MI) was the source of bacterial growth media. Proteinase K was purchased from Amresco (Solon, OH). All other reagents and chemicals were obtained from Sigma or Fisher Scientific (Orlando, FL). Oligonucleotides were synthesized in the core facility of the Interdisciplinary Center for Biotechnology Research at the University of Florida.

Organisms, Media and Growth Conditions

Bacterial strains and plasmids are listed in Table 2-1. Luria broth containing 0.2% w/v glucose (LBG) was used as the primary medium for DNA purification unless otherwise noted. The concentration of chloramphenicol in liquid medium was 15-20 μg/ml and 30 μg/ml in solid medium. Liquid cultures were aerated by continuous mixing on an orbital shaker or in a roller drum. Incubations were performed at 37°C.

DNA Preparation

Large quantities of plasmid DNA were purified using a CsCl step gradient (Garger *et al.*, 1983) and smaller quantities were prepared by the rapid screen method (Birnboim & Doly, 1979). Plasmid DNA for sequencing was prepared by a modification of the rapid screen method. Cells were grown in 10 ml Terrific Broth [1.2% bacto-tryptone (w/v), 2.4% bacto-yeast extract (w/v), 0.04% glycerol (v/v), 0.17 M KH_2PO_4 and 0.072 M K_2HPO_4] overnight (Tartof & Hobbs, 1987). Cells were lysed and plasmid DNA was recovered essentially as described by Birnboim and Doly (1979). The plasmid DNA was treated with 10 units of RNAse-It (Stratagene, La Jolla, CA) for 30 min, and then treated with Proteinase K overnight in the presence of 25 mM EDTA. The solution was extracted twice with phenol:chloroform (1:1) and twice with chloroform. The DNA was precipitated 0by the addition of 0.5 volume of 7.5 M ammonium acetate and

Table 2-1
List of Strains and Plasmids

Strain/ plasmid	Genotype/description	Source/ Reference
1100	*bglR thi-1 rel-1* HfrPO1	Humbert *et al.*, 1983
1100ΔBC	$[a, c, b, \delta, \alpha, \gamma, \beta, \epsilon]_{del}$	
BC2000	a_{del} (*uncB2000*), c_{SD} in 1100 background	Cain & Simoni, 1986
MC4100	F⁻ Δ*lacU169 araD139 thiA rpsL relA*	Kumamoto & Simoni, 1986
PH105	a_{del} (*uncB2000*) in 1100 background	Chapter 3
RH305	$a_{V239\rightarrow A,P240\rightarrow W,W241\rightarrow end}$ (*uncB205*) *recA56* srl::Tn*10* in 1100 background	Humbert *et al.*, 1983
pBDC1	Ap^r *a*	Cain & Simoni, 1986
pBDC26	Cm^r $a_{L207\rightarrow W,E219\rightarrow K}$	Cain & Simoni, 1989
pBR325	Ap^r Cm^r Tet^r	NEB[a]
pMAK705	Cm^r ori^{ts}	Hamilton *et al.*, 1989
pPH11	Cm^r a_{del} (*uncB2000*)	Chapter 2
pPH12	Cm^r *a*	Chapter 2
pPH13	Cm^r a_{del}, *c*, *b*, δ, α, γ, β, ϵ	Chapter 2
pPH15	Cm^r a_{del}, *c*, *b*, δ^-	Chapter 2
pUNCB4.70 -4.71	Cm^r a_{L207} NARP mutations pBDC26 based plasmids	Chapter 5
pUNCB5.01 -5.04	Cm^r a_{Q252} mutations pPH12 based plasmids	Chapter 4
pUNCB5.10 -5.16	Cm^r a_{F256} mutations pPH12 based plasmids	Chapter 4
pUNCB5.20 -5.23	Cm^r a_{L259} mutations pPH12 based plasmids	Chapter 4
pUNCB5.30 -5.36	Cm^r a_{Y263} mutations pPH12 based plasmids	Chapter 4
pUNCB5.40 -5.41	Cm^r a_{G218} mutations pBDC26 based plasmids	Chapter 6
pUNCB5.42 -5.44	Cm^r a_{H245} mutations pPH12 based plasmids	Chapter 6

[a]New England Biolabs (Beverly, MA)

3 volumes of ethanol and recovered by centrifugation at 12,000 x g for 20 min. The pellet was rinsed with 70% ethanol, dried under a vacuum and suspended in TE buffer [10 mM Tris-HCl, 1 mM EDTA, pH 8.0].

Genomic DNA was isolated by the method of Porter *et al.* (1985). A 5 ml culture of the desired strain was harvested, then suspended in 0.4 ml of GTE Buffer [50 mM glucose, 25 mM Tris 10 mM EDTA, pH 8] containing fresh lysozyme [2 mg/ml] and incubated at 4°C for 30 minutes. Samples were heated to 70°C for 3 min, and lysed by adding 0.8 ml 1% SDS with gentle mixing. Samples were cooled to 4°C, then extracted by gentle mixing with 1.2 ml phenol. Genomic DNA was collected by spooling DNA at the interface of 2 volumes of ethanol layered over the aqueous sample. The spooled DNA was rinsed with 80% ethanol and allowed to dry for a few minutes before suspension in TE buffer. An aliquot of the preparation was extracted with phenol, and then extracted with ethyl ether to remove the phenol. The DNA was precipitated in 2 volumes of ethanol, and dissolved in TE buffer. Aliquots of the DNA were used for either Southern analysis or for genomic sequencing.

PCR Amplification of DNA

Polymerase Chain Reaction (PCR) was used to amplify genomic DNA isolated from strain RH305 ($a_{uncB205}$) for sequencing of the *uncB205* mutation. The *uncB* gene was amplified using oligonucleotide primers (GGTGCTGGTGGTTCAGATACTGGCAC, CCAGTTTGTTTCAGTTAAAACGTAGTAGTGTTGG) under standard PCR

conditions (Saiki, 1990). The reaction mixture consisted of: 100 μM dNTP's, 20 pmol of each primer, 1 ng of genomic DNA template, 2.5 U of Taq polymerase, in Taq polymerase Buffer [10 mM Tris-HCl, 50 mM KCl, 1.5 mM $MgCl_2$, 0.001% (w/v) gelatin, pH8.8]. Genomic DNA was amplified with 30 cycles of the following temperature steps: 95°C for 30 seconds, 65°C for 30 seconds, 72°C for 1 minute. PCR products were extracted with chloroform to remove mineral oil and precipitated with 2 volumes of ethanol. The nucleotide sequence of the PCR product was determined using cycle sequencing according to the protocol from AmpliTaq Cycle Sequencing Kit (Perkin Elmer Cetus, Norwalk, CT), as described below.

Restriction Digest

Restriction endonuclease digestions were carried out under conditions specified by the vendor. Conditions for digestions involving more than one restriction endonuclease were chosen to prevent any non-specific activities.

Restriction digested DNA used for ligations, mutagenesis or nucleotide sequencing was handled as follows. Digested DNA was diluted to 50 μl or 100 μl with TE buffer and extracted with 1 volume of phenol/chloroform, followed by two extractions with 1 volume chloroform. The DNA was precipitated at room temperature for an hour in 2.5 M ammonium acetate and 67% ethanol (by addition of 0.5 volumes of 7.5 M ammonium acetate and 3.0 volumes of ethanol). The

precipitated DNA was pelleted (12,000 x g, 30 min) and dried under vacuum to remove excess ammonium acetate. When small amounts of DNA were digested, 20 μg of tRNA was added to the precipitation step to increase recovery.

DNA digested for analysis via gel electrophoresis was handled differently. Upon completion of restriction digestion, loading dye [1% bromophenol blue, 1% xylene cyanol, 50% glycerol] was added at 1/10 volume of reaction. The sample was loaded into a well in an agarose horizontal gel (usually 0.8% agarose) then subjected to electrophoresis. DNA was visualized following staining with ethidium bromide via UV light. Samples were stored at -20°C upon completion of the digest if not used immediately in electrophoresis experiments (Sambrook *et al.*, 1989).

Southern Analysis

DNA fragments size fractionated in a 0.6% agarose gel were transferred through capillary action in 10X SSC onto Gene Screen hybridization transfer membrane (NEN; Boston, MA). DNA was cross-linked to Gene Screen membrane by UV light. Prehybridization was in hybridization buffer [7% SDS, 1% BSA, 1 mM EDTA, 0.5 M NaH_2PO_4, pH 7.2] for 10 minutes at 65°C. Hybridization was initiated by addition of radiolabled probe in hybridization buffer, and incubation was allowed to continue over night. The probe was made from the 1.1 kilobase *SalI* fragment generated from the digestion of plasmid pEMS54 (*unc* operon), and radiolabeled according to the random primers

kit (BRL) directions. The hybridization membrane was washed with buffer [1mM EDTA, 40 mM NaH_2PO_4, pH 7.2] until non-specific bound radiolabled probe was removed. This was accomplished by monitoring radiation released into the wash buffer. The signal was visualized by exposing Kodak XAR 5 film to the hybridization membrane overnight (autoradiography).

Ligations and Transformations

Ligations were preformed by three different protocols, depending on the source of the ligase and the type of ligation. For 'sticky-end' ligations using NEB T4 ligase, 1 μg of DNA was incubated with 0.2 μl of ligase (80 U) in 50 μl of ligation buffer [40 mM Tris-HCl, 10 mM $MgCl_2$, 10 mM DTT, 0.5 mM ATP, pH 7.5]. The reaction was incubated over night at 16°C to facilitate annealing of restriction site overhangs. Insert to vector ratios were 1, 3 and 10 fold molar excess. For 'blunt-end' ligations 4.5 μl of NEB T4 ligase (1800 U) in ligation buffer was incubated at room temperature to increase T4 ligase efficiency. When BRL T4 ligase was used for sticky-end ligations a different protocol was used. The DNA concentration was dropped to 0.1 μg, and only 0.1 U of BRL ligase was used in a 20 μl reaction volume with BRL ligase buffer [50 mM Tris-HCl, 10 mM $MgCl_2$, 1 mM DTT, 1 mM ATP, 5% (w/v) polyethylene glycol-8000, pH 7.6]. The incubation was one hour at room temperature. The insert to vector ratios

were 1, 3 and 5 fold molar excess. The ligation reaction was usually diluted 5 fold with TE before use.

Competent cells were prepared by harvesting a mid-logarithmic phase culture by centrifugation (8000 x g, 5 min, 4°C) and treating the *E. coli* with cold (4°C) 50 mM $CaCl_2$. Treatment was with 0.5 volume of cold 50 mM $CaCl_2$ for 45 minutes, followed by storage in 0.1 volume of cold 50 mM $CaCl_2$ for 4 to 24 hours before use.

Transformations were performed as follows. Competent cells were added to DNA (1/3 to 1/2 of a ligation reaction mixture, 1 μl of a plasmid preparation) and incubated at 4°C for a half an hour. The cells were then heat shocked at 42°C for two minutes. LBG medium was added to the cells and they were allowed to grow aerobically by incubation of the cultures for 1 to 2 hours at 37°C. The cells were then harvested by centrifugation and spread on LBG solid medium containing the appropriate antibiotic.

Strain MC4100 (Table 2-1) was used for transforming ligation reactions, and conditions were optimized for its efficiency. Transformations into other strains for specific applications used DNA from plasmid preparations.

Plasmid Construction

Plasmid pPH1. Plasmid pPH1 (*Amp*^{r}, *Cm*^{r}; 5.1 kb) was constructed from plasmid pBR325 (*Tet*^{r}, *Amp*^{r}, *Cm*^{r}) (Table 2-1), by removing the 375 bp *BclI/BamHI* fragment. This was accomplished by digestion of plasmid pBR325 with *BclI* and

BamHI, and circularizing by ligation. The deletion of the *BclI/BamHI* fragment was confirmed by restriction site mapping and the loss of tetracycline antibiotic resistance.

Plasmid pPH4. Plasmid pPH4 (*a*, *Cm*^{r}; 5.4 kb) was constructed by ligating the 1070 bp *AatII/AseI* fragment containing the *uncB* (*a*) gene from pBDC1 (Cain & Simoni, 1986), into the 4.36 kb *AseI/AatII* fragment of pPH1 (*Amp*^{r}, *Cm*^{r}). The construction of the plasmid was confirmed by restriction site mapping, loss of ampicillin resistance, and the ability to complement the *uncB205* mutation in strain RH305.

Plasmid pPH5. Plasmid pPH5 (*a*, *Cm*^{r}; 4.6 kb) was constructed by digesting plasmid pPH4 (*a*) with *NarI* restriction endonuclease, and then circularizing the 4638 bp fragment of the plasmid under sticky-end ligation conditions. The 4 *NarI* restriction sites present in plasmid pPH4 (*a*) were reduced to one in plasmid pPH5 (*a*). The deletion of the DNA between the *NarI* sites was confirmed by restriction site mapping.

Plasmid pPH6. Plasmid pPH6 (*a*, *Cm*^{r}; 4.6 kb) was constructed by destroying the *ClaI* and *HindIII* restrictions sites in plasmid pPH4 (*a*, *Cm*^{r}). This was accomplished by digesting pPH4 with *ClaI* and *HindIII*, then incubating with DNA polymerase I (Klenow fragment) and dNTP's to fill in the 3' recessed ends left by the restriction enzymes. The DNA was circularized by ligating under blunt-end conditions (see above). The construction was confirmed by restriction site

mapping, and the plasmid was shown to complement the *uncB205* mutation in strain RH305.

Plasmid pPH7. Plasmid pPH7 (*a*, *Cm*^{r}; 4.6 kb) was constructed by removing the *NarI* restriction sites from pPH4 (*a*). This was accomplished by digestion with *NarI* followed by filling the recessed ends with DNA polymerase I (Klenow fragment) and dNTP's. The DNA was circularized under blunt-end ligation conditions. The removal of the *NarI* restriction sites from the plasmid also decreased the number *AhaII* restriction sites, facilitating the construction of plasmid pPH9.

Plasmid pPH9. Plasmid pPH9 (*a*$^-$, *Cm*^{r}; 4.4 kb) was constructed to remove the first *AhaII* restriction site in the *uncB* (*a*) gene. Plasmid pPH7 (*a*) was digested to completion with restriction enzyme *AatII* and partially with restriction enzyme *AhaII*. The larger fragment was isolated, containing the cleavage of only the first *AhaII* restriction site in *uncB* (*a*) gene and the *AatII* restriction site. The fragment was treated with DNA polymerase I (Klenow fragment) and dNTP's to fill-in the 3' recessed ends. The plasmid was circularized under blunt-end ligation conditions. Plasmid pPH9 (*a*$^-$) now contained only one *AhaII* restriction site in the carboxyl terminal region of an incomplete *uncB* (*a*) gene.

Plasmid pPH10. Plasmid pPH10 (*a*$^-$, *Cm*^{r}; 4.4 kb) was constructed by cassette mutagenesis (see below) as follows. Plasmid pPH9 (*a*$^-$) was digested with the restriction enzymes

BclI and *AhaII*. A synthetic oligonucleotide cassette containing silent mutations that generated *ClaI* and *HindIII* restriction sites was ligated to the --kb *BclI/AhaII* fragment of plasmid pPH9 (a^-) (Figure 2-1). Plasmid pPH10 (a^-) carried an incomplete *uncB* (*a*) gene containing unique restriction sites that could be used for site-directed cassette mutagenesis.

Plasmid pPH11. Plasmid pPH11 (*a*, Cm^r; 4.0 kb) was made by the digestion of plasmid pPH5 (*a*) with *BamHI*, and then the 4.0 kb fragment was circularized by sticky-end ligation. Construction of plasmid pPH11 (a_{del}) was confirmed by restriction site mapping and loss of complementation of strains PH105 and RH305 on succinate minimal medium.

Plasmid pPH12. Plasmid pPH12 (*a*; Cm^r; 4.6 kb) was made to restore the disrupted *uncB* (*a*) gene of plasmid pPH10 (a^-) using the *uncB* (*a*) gene from plasmid pPH6 (*a*). Both plasmids were digested with the restriction enzymes *PstI* and *AvaI* and the appropriate DNA fragment isolated. The 2.2 kb *PstI/AvaI* fragment of plasmid pPH6, containing the amino-terminal section of the *uncB* (*a*) gene and the chloramphenicol resistance gene, was ligated with the 2.4 bp *PstI/AvaI* fragment of plasmid pPH 10, containing the plasmid origin of replication and the carboxyl-terminal section of the *uncB* (*a*) gene. Plasmid pPH12 contained the complete *uncB* (*a*) gene with the silent mutations for the unique restriction sites *ClaI* and *HindIII* (Figure 2-1). The construction was confirmed by

A

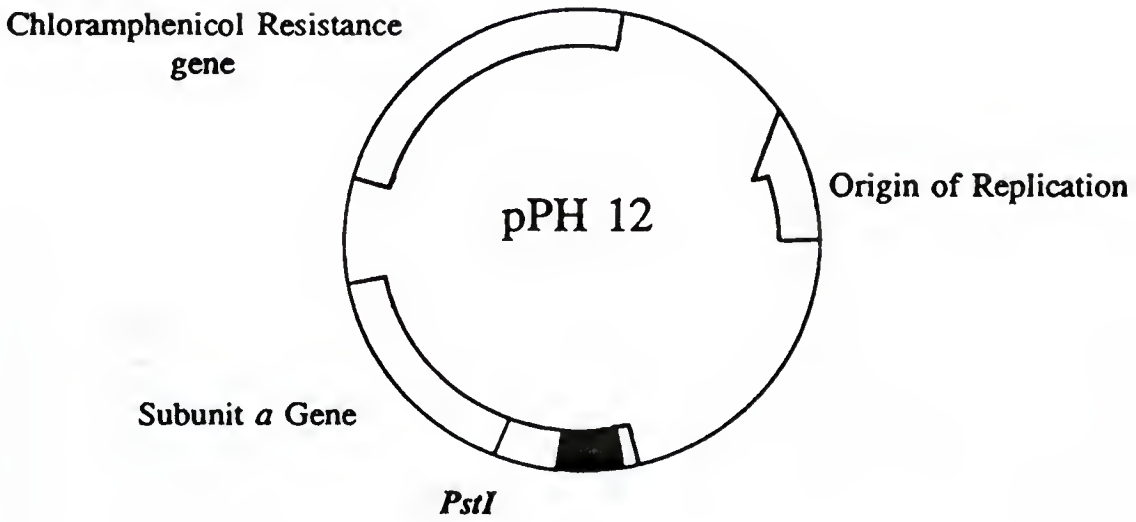

B

```
247                                                                 268
 L   I   I   T   L   Q   A   F   I   F   M   V   L   T   I   V   Y   L   S   M   A   S
CTG ATC ATT ACG CTG CAA GCT TTC ATC TTC ATG GTG TTA ACG ATC GTA TAC TTA TCG ATG GCG TCT
GAC TAG TAA TGC GAC GTT CGA AAG TAG AAG TAC CAC AAT TGC TAG CAT ATG AAT AGC TAC CGC AGA
 BclI                HindIII                                        ClaI    AhaII
```

Figure 2-1. Plasmid pPH12 (*a*) that was used to construct site-directed mutations in the *uncB* (*a*) gene by cassette mutagenesis. A. Diagram of plasmid pPH12 (*a*). B. The region of the *uncB* (*a*) gene in which silent changes were constructed for plasmid pPH12 (*a*). Numbers above the protein sequence denote amino acid position, restriction recognition sequences are denoted below DNA sequence.

restriction site mapping and complementation of the *a* subunit deficient strains PH105 and RH305.

Plasmid pPH13. Plasmid pPH13 (a_{del},*c*,*b*,δ,α,γ,β,ϵ, Cm^r; 13.6 kb) was constructed by ligating the 2.1 kb *BamHI/XbaI* fragment from pAP55 (*a*,c_{SD},*b*,δ,α,γ,β,ϵ), *unc* promoter, *uncI* and part of the *uncB* (*a*) gene, with the 11.5 kb *BamHI/XbaI* fragment from pEMS54 (*a*,*c*,*b*,δ,α,γ,β,ϵ), containing part of *uncB* (*a*), *uncE* (*c*), *uncF* (*b*), *uncH* (δ), *uncA* (α), *uncG* (γ), *uncD* (β), *uncC* (ϵ), the Cm resistance gene, and origin of replication for plasmid pACYC184. The resulting plasmid contained the complete *unc* operon minus the 617 bp *BamHI* fragment from *uncB* (*a*), which was confirmed by restriction site mapping.

Plasmid pPH15. Plasmid pPH15 (a_{del}, *c*, *b*, δ^-, Cm^r; 6.9 kb) was constructed by ligation of the 2.2 kb *HindIII/ClaI* fragment from plasmid pPH13 (a_{del},*c*,*b*,δ,α,γ,β,ϵ) into plasmid pMAK705 digested with *HindIII* and *ClaI*. Plasmid pMAK705 was kindly provided by Sidney R. Kushner (University of Georgia).

Cassette Site-Directed Mutagenesis

Cassette site-directed mutagenesis requires that restriction endonuclease sites bracket the region of interest. These restriction sites should be unique in the mutagenesis vector. The segment of DNA between the restriction sites constitutes the 'cassette', which can now be replaced following restriction enzyme digestion, and

ligation with a synthetic double-stranded oligonucleotide cassette. The double stranded oligonucleotide cassettes were made by annealing complementary synthetic oligonucleotides that encoded the desired mutation(s) and generated sticky-ends compatible with the restriction fragment ends. The cassette allows for multiple changes, including incorporation of 'doped' nucleotides at a given position(s). Use of a 'doped' cassette results in a mixture of oligonucleotides which are identical except for the positions reflecting ambiguous synthesis. From this type of mutagenesis cassette many changes at a given codon can be constructed at once, resulting in an array of amino acid substitutions. Each clone from an experiment of this type was sequenced to determine which mutation had been constructed.

Several cassettes and cassette mutagenesis plasmids were used in this thesis and are detailed in each chapter. Figure 2-1 shows the cassette used to construct plasmid pPH12 resulting in the *HindIII* and *ClaI* sites incorporated into the carboxyl terminal region of the *uncB* (*a*) gene.

PCR Mutagenesis

PCR assisted mutagenesis was used to construct mutants in Chapter 6. The basic protocol was as follows. A sense primer was designed upstream of the restriction site *PstI* in the *uncB* (*a*) gene (Figure 2-1). An antisense mutagenic primer was designed that contained the $a_{H245\rightarrow G}$ mutation. This

primer also encompassed the *BclI* restriction site in the *uncB* (*a*) gene (see Figure 2-1). The *BclI* restriction site was 3′ with respect to the $a_{H245\rightarrow G}$ mutation, allowing the PCR product containing the mutation to be ligated into the *uncB* (*a*) gene. Standard PCR conditions were used (see above) to amplify DNA from the wild-type plasmid pPH12 (*a*) and the mutagenic plasmids pUNCB5.40 ($a_{G218\rightarrow D}$) and pUNCB5.41 ($a_{G218\rightarrow K}$) separately (Figure 2-1; Chapter 6, Table 6-1). The PCR products were ligated into pPH12 (*a*) using the restriction enzymes *PstI* and *BclI* (by the protocols detailed above), and the nucleotide sequence was confirmed across the whole cloned region using the the AmpliTaq system (see below).

Sequencing Reactions

Taq-Traq. DNA sequencing was carried out using the Taq-Traq sequencing system for the mutations in chapter 4. Briefly, 2-4 μg of plasmid DNA in a total volume of 18 μL was denatured by alkali treatment with 2 μL of 2 N NaOH for 5 min at room temperature. Base was neutralized by mixing with 2 μL of 3 M ammonium acetate (pH 4.8). DNA was precipitated in 75 μL of ethanol at -70°C for 10 min, and microfuged (12,000 xg) for 15-30 min. The DNA pellet was rinsed with 200-500 μL of cold 75% ethanol and dried under vacuum for 5-10 min. DNA pellet was suspend in 10-16 μL of water, stored on ice and used as quickly as possible to minimize the renaturing of DNA strands. The denatured DNA template was added to 2 pmol of sequencing primer, 5 μL of

TAQ polymerase 5X reaction buffer, and 2 μL of the extension mix to give a volume of 25 μL. The primer was annealed to the template for 10 min at 50°C. 2 μL of radioactivity (dATPα^{35}S: 1,000 Ci/mmol, 10 μCi/μL) and 1 μL of TAQ polymerase (sequencing grade) were added, mixed, and incubated at annealing temperature for 2 min. 6 μL of the extension mixture was aliquotted into the four termination tubes (labeled A C G T) containing the appropriate terminating ddNTP, mixed and incubate at 70°C for 5 min. The reaction was stopped by adding 4 μL of the Stop Solution. If not used immediately, samples were stored at -20°C and used within 2 weeks. Samples were heated to 95°C for 2 min before size fractionation by electrophoresis in a 6% acrylamide, urea denaturing, sequencing gel (Garoff & Ansorge, 1981).

AmpliTaq. Cycle sequencing was done according to the protocol from AmpliTaq Cycle Sequencing Kit (Perkin Elmer Cetus, Norwalk, CT). Approximately 1 μg of Plasmid DNA that had been previously digested with *PvuII* (see above) in a total volume of 15 μl was added to AmpliTaq buffer with 2 pmol of primer; end-labeled with ATP-γ-^{32}P and kinase, then purified over a Nensorb-20 column (New England Nuclear; Wilmington, DE). The mixture was split into 4 tubes containing the appropriate ddNTP and amplified with 20 cycles of the following temperature steps: 15 sec at 95°C, 1 min at 50°C, 1 min at 72°C; followed by 10 cycles of the

following temperature steps: 15 sec at 95°C, 1 min at 72°C. Reactions were stored at 4°C until stop solution was added. If not used immediately, samples were stored at -20°C and used within 5 days. Samples were heated to 95°C for 2 min before size fractionation by electrophoresis in a 6% acrylimide, urea denaturing, sequencing gel (Garoff & Ansorge, 1981).

Membrane Preparations

Materials

Difco Laboratories (Detroit, MI) was the source of bacterial growth media. Deoxyribonuclease I was purchased from Sigma Chemical Co. (St. Louis, MO). All other reagents and chemicals were obtained from Sigma or Fisher Scientific (Orlando, FL).

Cell Fractionation

Preparation of subcellular fractions was as described previously (Klionsky *et al.*, 1983). *E. coli* were inoculated into LBG (500 ml) and grown to a cell density of approximately 150 Klett units. The cells were harvested by centrifugation (5000 x g, 5 min), washed with TM buffer (50 mM Tris-HCl, 20 mM $MgSO_4$, pH 7.5) and suspended in 7 ml of TM buffer containing DNase I (10 μg/ml). Cells were disrupted at 14000 psi in a French pressure cell. Debris and unbroken cells were removed by two successive

centrifugation (8000 x g, 5 min). The particulate membrane fraction and soluble cytoplasmic fractions were separated by high speed centrifugation (150,000 x g, 1.5 h).

Membranes used for proton conduction studies were prepared by suspending the membrane pellet in 1.5 ml of TM buffer by use of ground glass homogenizers. The suspended membranes were then diluted to a total volume of 7 ml with TM buffer then pelleted again by high speed centrifugation (150,000 x g, 1 hr). Pellets were suspended as above in 1.2 ml of TM buffer. Samples were centrifuged (12,000 x g, 5 min) to remove any remaining cell debris and the supernate was transferred to a new tube for use in fluorescence assays.

Membranes used for F_1 stripping experiments were suspended in SB buffer [1mM Tris-HCl, 0.5 mM EDTA, 2.5 mM 2-mercaptoethanol, 10% (v/v) glycerol, pH 8.0]. The stripped membranes prepared for analysis in chapter 4 were diluted to a total volume of 7 ml with SB buffer then pelleted again by high speed centrifugation (150,000 x g, 1 hr). The stripped membranes prepared for analysis in chapter 5 and 6 were diluted to a total volume of 7 ml with SB buffer and gently agitated for 1 hr before being pelleted again by high speed centrifugation (150,000 x g, 1 hr). All stripped membranes preparations were suspended and diluted in SB buffer as above and gently agitated overnight. Stripped membranes were recovered by centrifugation (150,000 x g, 1 h) and then

suspended in 1.2 ml of TM buffer. The membranes were centrifuged (12,000 x g, 5 min) to remove any remaining cell debris.

Three seperate procedures were used to prepare membranes used for measuring F_1 ATPase hydrolysis activity. The method used in chapter 3 and 4 involved simply suspending the membrane pellet from subcellular fractionation in 1.2 ml of TM buffer. Membranes for ATPase hydrolysis activity from the first part of chapter 5, considering the $a_{L207\rightarrow R}$ mutation, were prepared by an improved method. The membrane pellets were suspended in PSB buffer (5mM Tris-HCl, 0.5mM EDTA, 15% (v/v) glycerol, 2.5 mM 2-mercaptoethanol, 6 mM p-aminobenzamidine, pH 7.5) diluted and gently agitated for one hour before being pelleted again by high speed centrifugation (150,000 x g, 1 hr). The membrane pellets were once again suspended in PSB buffer, diluted up to 7 ml, and gently agitated overnight prior to pelleting by high speed centrifugation (150,000 x g, 1 hr). The last step was to suspend the membrane pellet in 1.2 ml of TM buffer. The membranes prepared for the second part of chapter 5, the $a_{L207\rightarrow P}$ mutation, and the membranes for Chapter 6 were prepared in the same manner with two modifications to improve the dissociation of uncoupled F_1 ATPase. First, the membrane 'washing' step, suspending the membrane pellets in PSB buffer and gently agitating for one hour prior to pelleting, was performed twice. Second, after the final

suspension in 1.2 ml of TM buffer, the membranes were centrifuged (12,000 x g, 5 min) to remove any remaining cell debris. All steps performed at 4°C.

Protein Assay

Protein concentrations were measured using the modified Lowry procedure of Markwell *et al.* (1978). An aliquot of membrane vesicles was diluted 1:10 or 1:5 with TM buffer. Aliquots of 5, 15 and 25 μL were taken from the dilution for assaying. A standard curve of bovine serum albumin (BSA) was used with a concentration range of 5 to 100 μg of protein. Duplicate samples were incubated in 3 ml of alkaline copper [100 parts reagent A (2.0% Na_2CO_3, 0.4% NaOH, 0.16% sodium potassium tartrate, 1% SDS) to one part reagent B (4% $CuSO_4$)] for 15 to 60 minutes at room temperature. Color was developed by adding 0.3 ml of Folin-Ciocalteu phenol reagent (diluted 1:1 with distilled water immediately prior to addition) and incubating 45 min at room temperature. Absorbance at 660 nm was read in a Pharmacia spectrophotometer, and the duplicate samples averaged. Protein concentrations were determined from the linear range of the standard curve by using a linear regression program. Membrane protein concentrations were usually 15 to 30 mg/ml for unstripped membranes and 2 to 5 mg/ml for stripped membranes.

Storage Conditions

Membrane preparations were stored at 4°C and most biochemical assays were preformed within 24 hours of the cells being lysed. If the membranes were to be stored for a period longer than 24 hours, the preparations were quick frozen in liquid nitrogen and kept at - 80°C. Frozen membranes were then thawed in a 37°C water bath before use.

Assays

Materials

Pyruvate kinase and lactate dehydrogenase were purchased from Sigma Chemical Co. (St. Louis, MO). 9-Amino-6-chloro-2-methoxyacridine (ACMA) was purchased from Molecular Probes (Eugene, OR). ECL Western blotting detection system, and Anti-rabbit Ig linked to horseradish peroxidase were from Amersham corp. (Arlington Heights, IL). All other reagents and chemicals were obtained from Sigma or Fisher Scientific (Orlando, FL).

Growth Characteristics

Minimal media employed for growth studies consisted of minimal-A salts (Miller, 1972) supplemented with either glucose or succinate (0.2% w/v) as specified in the text.

Growth on succinate was determined by visual inspection of colony size after 2 - 4 days growth at either 37°C or 42°C. The scale by which colony size was rated is wild-type

or near wild-type colonies (+++), clearly smaller colonies with substantial growth (+), minute colonies that were barely visible but present (±), and no visible colonies (-). Plasmids carrying *a* subunit site-directed mutations were transformed into *E. coli a* subunit defective strains PH105 and RH305. Mutant strains were grown on succinate media multiple times and plasmids carrying mutations were transformed into each strain at least twice. Growth on succinate characteristics were used to check for reversions to wild-type phenotypes (especially in strain RH305 for reasons detailed in chapter 3).

Growth yields of strains were determined turbidimetrically by a Klett-Summerson colorimeter, and yields were reported in Klett units. Minimal A medium (Miller, 1972) supplemented with 5mM glucose was used unless otherwise indicated. The cultures were aerated by continuous mixing on an orbital shaker at 37°C.

Anaerobic Growth

Anaerobic growth conditions were sustained with the GasPak H_2 + CO_2 generating system in an anaerobic jar. Glucose minimal medium agar plates were incubated under vacuum, followed by preincubation under anaerobic conditions. Colonies were streaked on to the plates. The plates were then placed into the anaerobic jar, in which the O_2 content had been reduced with CO_2 subliming from crushed dry ice. Anaerobic conditions were obtained (GasPak O_2

indicator strip) before the minimal medium plates were placed in a 37°C incubator. Strains were incubated for 48 hours before colony size was scored.

ATP-Driven Proton Translocation

Chapter 4 and 5. Membrane energization was assayed by fluorescence quenching of 9-amino-6-chloro-2-methoxyacridine (ACMA) (Aris *et al.*, 1985). Membrane vesicle concentration was 250 μg protein/ml buffer [50 mM MOPS and 10 mM $MgCl_2$, pH 7.3] in a volume of 3 ml buffer. ACMA was added to final concentration of 1 μM, and a Perkin-Elmer Model LS3B Fluorescence spectrometer was used to measure the change in ACMA fluorescence over time. Samples were first treated with NADH (0.5 mM) resulting in fluorescence quenching due to an acidification of the vesicles driven by the electron transport chain. NADH driven quenching was used to test the integrity of the membrane preparation (usually not shown in figure). Fluorescence was recovered by poisoning the electron transport chain with KCN (0.5 mM). After the fluorescence had recovered ATP (0.4 mM) was added to assay ATP-driven vesicle acidification. Fluorescence was once again recovered using nigericin (0.05 μM) to collapse the proton gradient. Treatment of fractionated membranes with 50 μM DCCD for 15 minutes at 37°C was used for inhibition of F_1F_O ATP synthase proton translocation.

Chapters 5 and 6. Membrane energization was done essentially as described above with the following

modifications. Membrane concentration was 150 μg of membrane protein/ml buffer [50 mM Tris and 10 mM $MgCl_2$, pH 7.5]. Fluorescence quenching was driven by addition of 500 μM ATP, and addition of 100 μM DCCD was used to recover the fluorescence by inhibiting F_1F_0 ATP synthase proton translocation. Analysis of pH conditions and ATP concentrations affect on proton pumping (Chapter 6) were done essentially the same, but membrane integrity was not confirmed with NADH for each ATP concentration. However, each membrane preparation was tested for NADH-driven fluorescence quenching in a separate trace. Additionally, the buffer used was pH 7.2 instead of pH 7.5. Both these changes were made to increase the apparent rate of the relative fluorescence change (see Chapter 6).

Passive Proton Conductance

Membrane vesicles stripped of F_1 (described above) were acidified with NADH (0.5 mM) to test passive proton conductance in mutant *a* subunit F_0 sectors. Wild-type F_0 sectors exhibit passive proton conductance, which decreases NADH driven ACMA fluorescence quenching by collapsing the generated proton gradient. Stripped membrane vesicles were analyzed under the same conditions as indicated for the intact membrane vesicles of the same mutant strains.

ATPase Activity

Inorganic phosphate assay. ATPase activity was measured by the release of inorganic phosphate from the

hydrolysis of ATP. Inorganic phosphate was assayed by the acid-acetone-molybdate method of Heininen and Lahti (1981). Inorganic phosphate complexes with the molybdate in an acid form that absorbs light at 335 nm in organic solvent. The molybdate-phosphate complex was stabilized by the addition of citric acid, and will degrade very slowly. The citric acid also complexes with all the free molybdate, preventing ATP hydrolysis by the acid in the mixture from interfering with the assay of enzymatic activity. Moreover, the F_1-ATPase activity was abolished by the acidic mixture, so addition of the enzyme assay buffer to the acid-acetone-molybdate solution stopped the enzyme reaction.

Phosphate contamination was minimized by use of new or acid washed glassware to prevent interference with the assay. ATPase activity was measured under the following conditions: 70 μg membrane vesicle protein, in 3.5 ml of buffer [50 mM Tris-HCl, 1 mM $MgCl_2$, pH 9.1] at 37°C. At time zero 3 mM ATP was added and aliquots of the enzyme solution taken at 1, 2, 5, 10, 15, 20 minutes and were added to the acid-acetone-molybdate solution, effectively stopping enzymatic ATP hydrolysis. A time zero aliquot was used to blank out background phosphate contamination. Inorganic phosphate concentrations at each of the time points were determined by comparison of absorbance to the absorbance of a phosphate standard curve. Specific activity was expressed as μmol of ATP hydrolyzed/min/mg membrane protein.

Coupled assay. ATP hydrolysis was also measured by a coupled assay to regenerate ATP in the system. Membranes (15 or 30 μg protein) were added to the assay buffer (2mM $MgCl_2$, 25 mM KCl, 5mM KCN, 25 mM Tris-HCl, 5 units/ml pyruvate kinase, 5 units/ml lactate dehydrogenase, 2.5 mM phosphoenol pyruvate, and 0.5mM NADH, pH 8.0) and monitored by absorbance at 350 nm for loss of NADH upon addition of ATP-$MgCl_2$ (2mM). One mol of ATP was assumed to be hydrolysis for each mol of NADH oxidized. Specific activity was expressed as μmol of ATP hydrolyzed/min/mg of membrane protein. Treatment of fractionated membranes with 50μM DCCD for 1 hour at room temperature was used to inhibit F_1F_O ATPase activity. DCCD insensitive activity was considered to be non-specific binding of F_1-ATPase to the membrane.

Western analysis. Twenty μg of membrane vesicle protein samples were size fractionated by SDS-PAGE using a 10% tris-tricine acrylamide gel (Schägger & Jagow, 1987) in a Bio-Rad Mini Protean II Electrophoresis System. Samples were subjected to electrophoresis till the bromophenol blue tracking dye reached the bottom of the gel. Protein was transfered from the gel to nitrocellulose in a tris-glycine transfer buffer [20 mM Tris-HCl, 150 mM glycine, 20% methanol, pH8.3] with a Bio-Rad Mini Trans-Blot Electrophoretic system at constant amperage of 100 mAmps for 16 hrs at 4°C (Towbin *et al.*, 1979). Nitrocellulose blots were stained with Fast Green and the sample lanes were cut

out and blocked in a buffer of 5% Carnation non-fat dried milk in TBS [10 mM Tris-HCl, 150 mM NaCl, 0.02% sodium azide, pH 7.2] for 2 hrs at room temperature (Tamarappoo *et al.*, 1992). Nitrocellulose blots were then incubated with 1/500 dilution of anti-F_1 antibodies (Brusilow *et al.*, 1981; generously provided by R. D. Simoni) or a 1/5000 dilution of anti-*b* antibodies (Deckers-Hebestreit *et al.*, 1992; McCormick *et al.*, 1993; Stack & Cain, 1994; generously provided by K. Altendorf) in blocking buffer for 1.5 hrs. Blots were washed with TBS-Tween 20 [TBS + 0.3% Tween 20], then incubated with 1/50,000 dilution of Anti-rabbit Ig linked to horseradish peroxidase (Amersham) for 45 min in blocking buffer. Blots were washed again with TBS-Tween 20, then the ECL Western blotting detection system (Amersham) was used to visualize the antibody blots. Autoradiographs using Hyperfilm (Amersham) were exposed for 5 - 30 min.

CHAPTER 3
CONSTRUCTION OF DELETION STRAIN PH105

Introduction

The strain traditionally used for studies of the *a* subunit, strain RH305, carries the *uncB205* mutation in a *recA*⁻ background (see Table 2-1). The chromosomal *uncB205* mutation has been mapped by recombination to the 3′ one-third of the *uncB (a)* gene and can be suppressed by an amber tRNA suppressor mutation (B. D. Cain personal communication). The *uncB205* mutation was sequenced from strain RH305 by K. McCormick and determined to consist of the following mutations: V239→A, P240→W and W241→end (TAG stop codon). The ability of strain RH305 ($a_{uncB205}$) to undergo reversion to a wild-type phenotype by an amber tRNA suppressor or by reversion of the stop codon, made the strain less than ideal for propagating *uncB* (*a*) mutation plasmids through extended cell divisions. This was especially true for *uncB* (*a*) mutations that impaired F_1F_O ATP synthase function, because the mutant strain was placed under selective pressure to produce reversion or amber suppressor mutation. A wild-type or near wild-type

background of *a* subunits produced from reversion or tRNA suppression in strain RH305 ($a_{uncB205}$) would obscure the phenotype of an *a* subunit encoded by a mutant plasmid that effected activity. This in turn would have led to inaccurate biochemical characterization of the mutants effect on activity.

The construction of an *uncB* (*a*) gene deletion strain would solve the problem of amber suppressors found in strain RH305 ($a_{uncB205}$). The *uncB* (*a*) gene deletion strain BC2000 reported by Cain and Simoni (1986), was found to have low expression of F_1 subunits. This was thought to have been due to a mutation in the Shine-Dalgarno sequence of the *uncE* (*c*) gene (designated c_{SD}). The mutation originated in plasmid pRPG54 which was the first *unc* operon expression plasmid (Solomon & Brusilow, 1988). A derivative of plasmid pRPG54 was used to construct strain BC2000 (a_{del}, c_{SD}). The mutation resulted in a polar phenotype reducing expression of the rest of the *unc* operon genes. Plasmid pEMS54 was constructed to correct the altered *uncE* (*c*) Shine-Dalgarno sequence found in plasmid pRPG54 (Schaefer *et al.* 1989). Plasmid pEMS54 was used as the source of the *unc* operon in the construction of strain PH105 (a_{del}) so that the reduced expression of F_1 subunits could be avoided.

Results

Construction of Strain PH105

The *uncB* (*a*) deletion strain PH105 was constructed via homologous recombination between the chromosome of strain 1100 and plasmid pPH15 (a^-,c,b,δ^-) essentially as described by Hamilton *et al*. (1989). Plasmid pPH15 (a^-,c,b,δ^-) carries the *uncB* (*a*) gene deletion of 617 bp between the two *BamHI* sites located in the *uncB* (*a*) gene, as well as, the temperature sensitive origin of replication from plasmid pMAK705. Strain 1100 carrying plasmid pPH15 (a^-,c,b,δ^-) was grown at the non-permissive temperature for plasmid replication (44°C) in the presence of the chloramphenicol (Cm). The bacteria were passed three times to log phase in order to obtain a co-integrate via homologous recombination between the plasmid and the genome. The culture was then returned to a permissive temperature for plasmid replication (30°C) in the presence of Cm. This step allowed a low frequency secondary recombination event excising the plasmid from the genome. Theoretically resolution of the co-integrate should yield cells with either the normal *uncB* (*a*) gene or the constructed deletion of the *uncB* (*a*) gene in the genome. After three passes the culture was then returned to the non-permissive temperature for plasmid replication (44°C). Antibiotic was withdrawn to remove the pressure to retain the plasmid. The final step was designed to cure the

bacteria of the plasmid, since the plasmid is incapable of undergoing replication at 44°C. Finally, aliquots of the culture were plated onto LBG media at different dilutions. Of 41 colonies tested 3 did not grow on Cm media indicating resolution of the co-integrate and curing of the plasmid. One colony was also unable to support growth on minimal medium supplemented with succinate, a non-fermentable carbon source (Chapter 2). This colony was designated strain PH105 (a_{del}) and was tested by complementation and Southern analysis.

Complementation Analysis of Strain PH105

Strain PH105 (a_{del}) was tested for complementation by plasmids containing different *unc* operon genes (Table 3-1). Plasmid pAP55 (*a, c, b,* δ, α, γ, β, ϵ) carried all the genes of the *unc* operon, and complemented strain PH105 (a_{del}) for growth on succinate minimal medium. Plasmid pPH13 (*c, b,* δ, α, γ, β, ϵ) carried the *unc* operon minus the *uncB* (*a*) gene and did not complemented strain PH105 (a_{del}) for growth on succinate minimal medium. Plasmid pPH12 (*a*) carried only the *uncB* (*a*) gene, and complemented strain PH105 (a_{del}) for growth on succinate minimal medium. The results of the complementation study indicated that a mutation in the *uncB* (*a*) gene was present in strain PH105 (a_{del}), and the mutation was complemented by a wild-type *uncB* (*a*) gene carried on a plasmid. None of the other *unc* operon genes carried on a plasmid were sufficient for complementation of strain PH105

Table 3-1
Complementation Analysis

Strain/ Plasmid	Subunits Present strain/plasmid	Growth on Succinate[a]
PH105	a_{del}/none	-
PH105/pAP55	a_{del}/*a, c, b,* δ, α, γ, β, ϵ	+++
PH105/pPH13	a_{del}/*c, b,* δ, α, γ, β, ϵ	-
PH105/pPH12	a_{del}/*a*	+++
RH305	$a_{uncB205}$/none	-
RH305/pPH13	$a_{uncB205}$/*c, b,* δ, α, γ, β, ϵ	-
RH305/pPH12	$a_{uncB205}$/*a*	+++
1100ΔBC	unc_{del}/none	-

[a]Growth on minimal A medium supplemented with succinate. Colonies were scored after 48 hours at 37°C on the as follows: wild-type growth (+++) or no growth (-).

(a_{del}). Identical results were observed in the complementation studies of the control *uncB* (*a*) gene mutation strain RH305 ($a_{uncB205}$) (Table 3-1).

Southern Analysis of Strain PH105

Confirmation that the *uncB* (*a*) deletion was incorporated into strain PH105 (a_{del}) was shown by Southern analysis. Samples of wild-type strain 1100 and strain PH105 (a_{del}) chromosomal DNA were digested with the restriction endonuclease *PstI* and probed with the *SalI* fragment from the *unc* operon (Figure 3-1). The Southern analysis showed the predicted restriction fragment length polymorphism (RFLP) in strain PH105 (a_{del}), demonstrating the loss of a *PstI* site located between the two *BamHI* restriction sites in the *uncB* (*a*) gene (see Figure 3-1). The result demonstrated that strain PH105 (a_{del}) contains the 617 bp deletion from the *uncB* (*a*) gene.

Comparison of Strain PH105 and Strain RH305

As demonstrated above strain PH105 (a_{del}) and strain RH305 ($a_{uncB205}$) failed to grow on succinate minimal A media. However, when the two strains were compared using biochemical assays, an obvious difference between them became apparent. There was a reduction in the specific activity of ATP hydrolysis associated with membrane vesicles isolated from the strain PH105 (a_{del}). A similar level of activity was also observed in strain PH105 (a_{del}) carrying plasmid pPH12 (*a*). Table 3-2 shows the specific activity

A

B

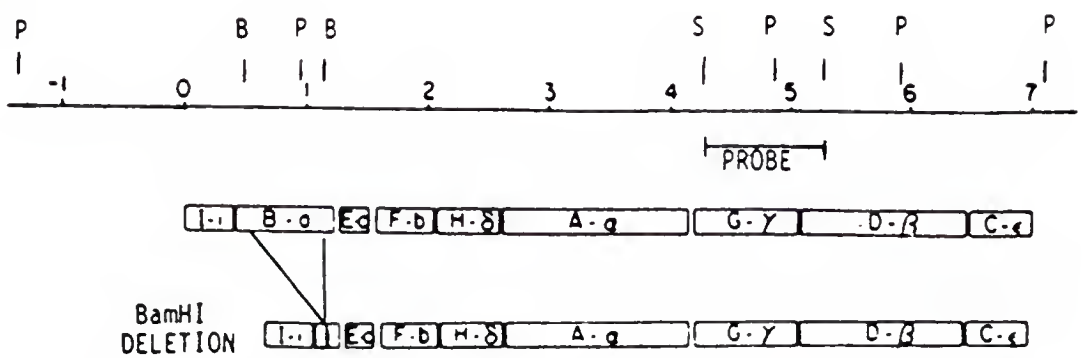

Figure 3-1. Southern analysis of strain PH105 (a_{del}) and its parent strain 1100. Panel A. Autoradiograph of Southern blot. Panel B. Shows the arrangement of the *unc* operon with its restriction map. The genomic DNA was digested with *PstI*. The probe was the *SalI* fragment indicated by the bar. Key: P = *PstI*; B = *BamHI*; S = *SalI*.

Table 3-2
Membrane Associated ATPase Activities

Strain/ Plasmid	Mutation	ATPase specific activity[a] (μmol ATP/min/mg protein)
PH105	a_{del}	0.40 ± .07
PH105/pPH12	*a*	0.48 ± .09
RH305	$a_{uncB205}$	1.05 ± .04
RH305/pPH12	*a*	0.92 ± .14

[a]ATPase specific activity is the average of at least two separate experiments. The activity of strain RH305 ($a_{uncB205}$)/plasmid pPH12 (*a*) is indicative of a wild-type strain. ATP hydrolyzed was determined by measuring release of inorganic phosphate over a time course. Assays were performed at pH 9.1 (see Chapter 2).

for membrane bound ATP hydrolysis for strains PH105 (a_{del}) and strain RH305 ($a_{uncB205}$). Apparently, the reduction in specific activity is due to a reduction in the amount of F_1 ATPase present in strain PH105 (a_{del}) as compared to strain RH305 ($a_{uncB205}$).

This deficiency was further demonstrated in the fluorescence assay for ATP driven proton translocation. Figure 3-2 displays the ACMA fluorescence traces for NADH driven and ATP membrane energization. The traces for strain PH105 (a_{del}) carrying plasmids pPH12 (a) and pPH4 (a), showed fluorescence quenching approximately half the level of pPH12(a) in strain RH305 ($a_{uncB205}$) or strain PH105 (a_{del}) carrying the plasmid pEMS54 ($a,c,b,\delta,\alpha,\gamma,\beta,\epsilon$). Strain PH105 ($a_{del}$) carrying the plasmid pEMS54 ($a,c,b,\delta,\alpha,\gamma,\beta,\epsilon$) displayed twice as much ATP driven fluorescence quenching activity as strains of PH105 (a_{del}) carrying plasmids pPH12 (a) or pPH4 (a). This indicated that strain PH105 (a_{del}) carrying the plasmid pEMS54 ($a,c,b,\delta,\alpha,\gamma,\beta,\epsilon$) had significantly higher levels of F_1F_O ATP synthase activity. Strain RH305 ($a_{uncB205}$) carrying plasmid pPH12 (a) had a similar level of ACMA fluorescence quenching as strain PH105 (a_{del}) carrying plasmid pEMS54 ($a,c,b,\delta,\alpha,\gamma,\beta,\epsilon$), indicating comparable levels of F_1F_O ATP synthase. The difference between strain RH305 ($a_{uncB205}$) carrying pPH12 (a) and strain PH105 (a_{del}) carrying pPH12 (a) indicated that strain PH105 (a_{del}) was producing lower levels of other F_1F_O ATP synthase

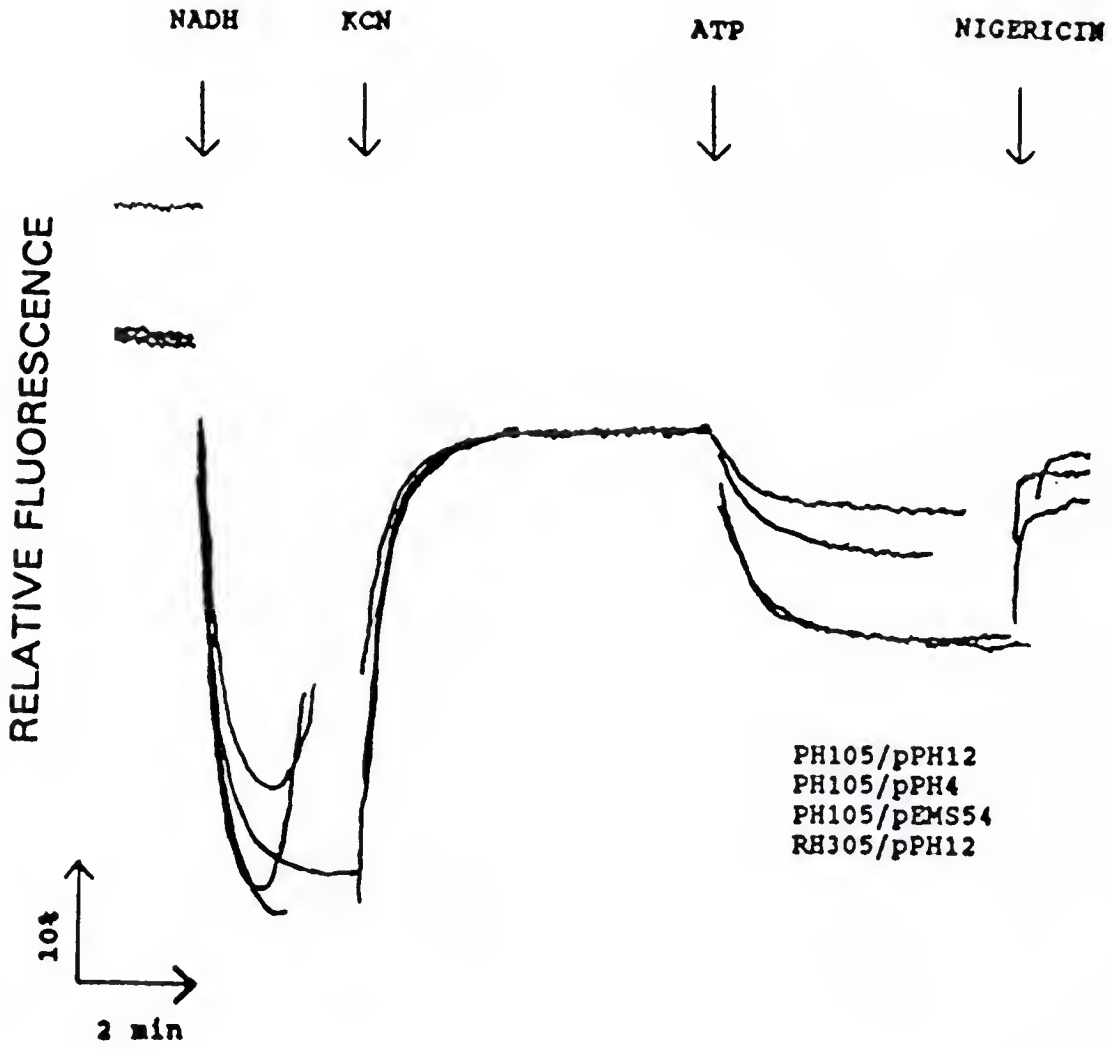

Figure 3-2. Energization of membrane vesicles determined by fluorescence quenching of ACMA. Reduced fluorescence indicates establishment of a proton gradient across the membrane via electron transport (NADH) or F_1F_o ATP synthase (ATP). ACMA was added to a final concentration of 1 μM. Membrane vesicles were at a concentration of 250 μg protein/ml of buffer (50 mM MOPS and 10 mM $MgCl_2$, pH 7.3). The reagents were added to final concentrations of: NADH 0.5 mM; KCN 0.5 mM; ATP 0.4 mM; nigericin 0.05 μM. the strain/plasmid combinations are listed under the traces in the order of ATP driven fluorescence quenching levels.

subunits compared to strain RH305 ($a_{uncB205}$). The NADH-driven quenching data for strain PH105 (a_{del}) carrying plasmid pPH12 (*a*) are also reduced indicating the membranes of this particular preparation were leaky. This probably accounted for the difference in ACMA fluorescence quenching observed between strain PH105 (a_{del}) carrying plasmid pPH12 (*a*) and strain PH105 (a_{del}) carrying plasmid pPH4 (*a*). The manipulation of the promoter for the *uncB* (*a*) gene in plasmid pPH12 (*a*) may have reduced the expression of the *uncB* (*a*) gene (Chapter 2), but the high levels of ACMA fluorescence quenching exhibited by strain RH305 ($a_{uncB205}$) carrying pPH12 (*a*) indicate that this not the case.

Western Analysis of Strain PH105 and Strain RH305

To look directly at the expression of subunits of F_1F_O ATP synthase, Western blots were done using anti-*b* antibodies (Deckers-Hebestreit *et al.*, 1992; McCormick *et al.*, 1993; Stack & Cain, 1994) and anti-F_1 antibodies (Brusilow *et al.*, 1981). Figure 3-3 shows the results of the Western blot. A reduction in the amount of the *b* subunit was seen in strain PH105 (a_{del}) as compared to strain RH305 ($a_{uncB205}$). Whether plasmid pPH12 (*a*) was present or not made no apparent difference to the amount of the *b* subunit present in strain PH105 (a_{del}). Strain RH305 ($a_{uncB205}$) exhibited a reduced level of the *b* subunit present compared to strain RH305 ($a_{uncB205}$) carrying plasmid pPH12 (*a*). The lower molecular weight band observed on the Western may have

A

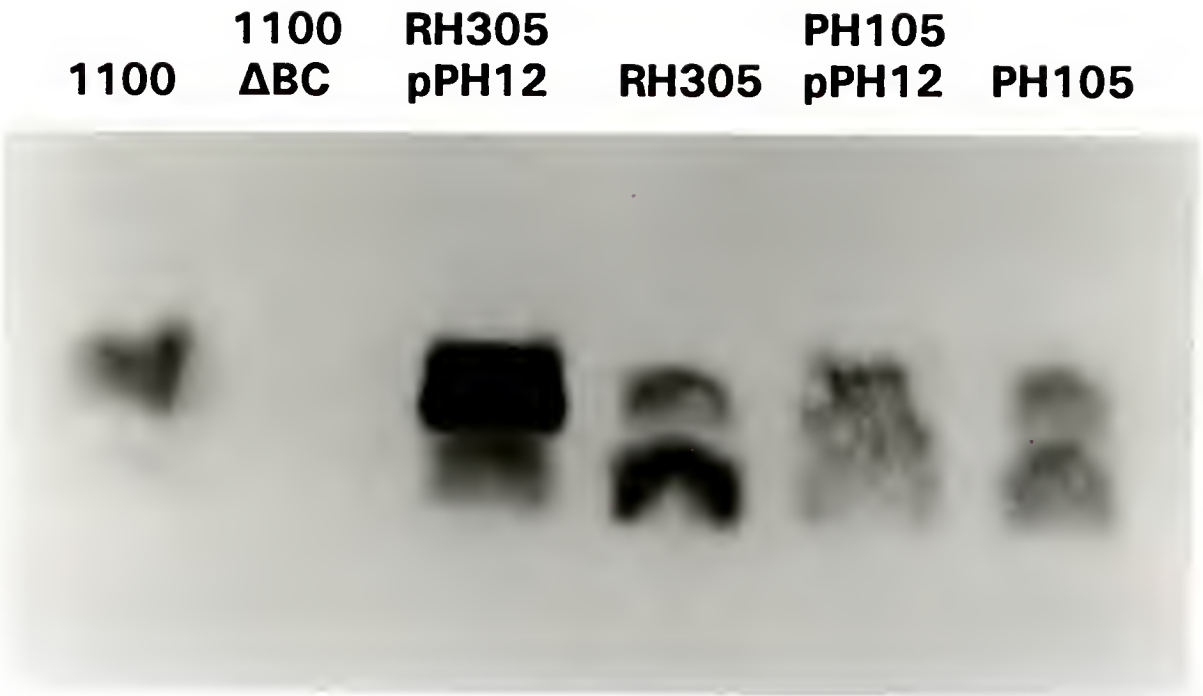

Figure 3-3. Western analysis of strain RH305 ($a_{uncB205}$) and strain PH105 (a_{del}). Strain 1100, positive control. Strain 1100ΔBC, negative control. Plasmid pPH12 (*a*). Panel A: anti-*b* antibody. Panel B: anti-F_1 antibody. See Chapter 2 for details.

B

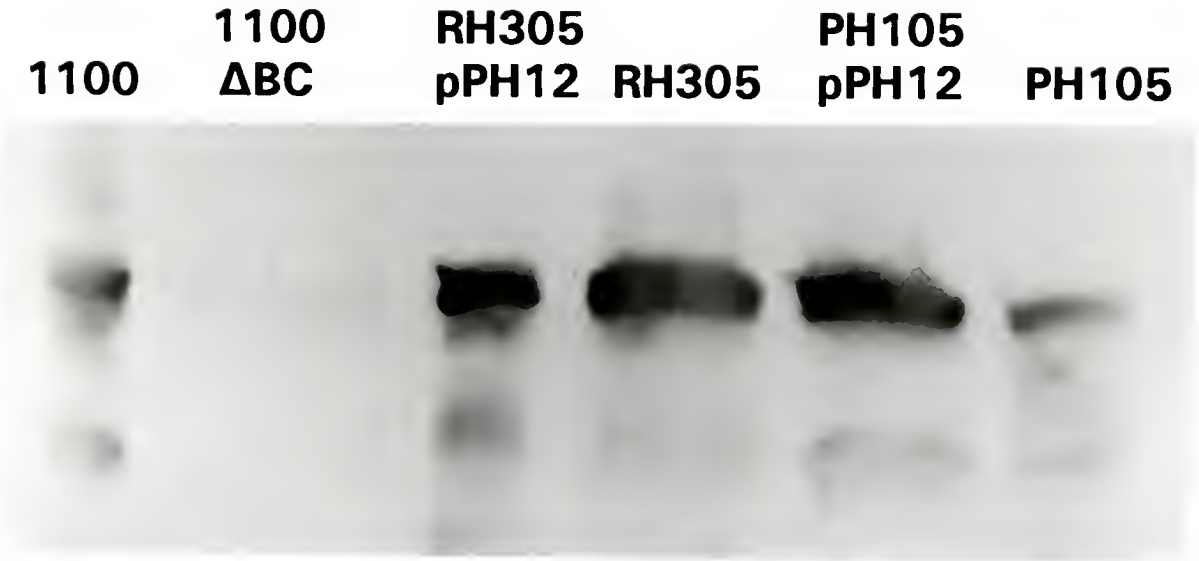

Figure 3-3--continued. Strain 1100, positive control. Strain 1100ΔBC, negative control. Plasmid pPH12 (*a*). Panel A: anti-*b* antibody. Panel B: anti-F_1 antibody. See Chapter 2 for details.

been a degradation product of the *b* subunit (McCormick, 1993). Strains 1100 (wt) and 1100ΔBC (unc_{del}) were run as positive and negative controls, respectively. The reduced levels of the *b* subunit present in strain 1100 (wt) may be the result of a poor transfer efficiency (Figure 3-3A).

The reduction in the expression of F_1 subunits (mainly α and β, with a weak signal for γ) was not as dramatic between the two strains. The levels of F_1 subunits present in each strain correlate with differences observed between the strains in membrane associated F_1-ATPase activity, though not at as great a level. The difference in levels of F_1 subunits present in strain RH305 ($a_{uncB205}$) as compared to strain RH305 ($a_{uncB205}$) carrying plasmid pPH12 (*a*) did not correlate with membrane associated F_1-ATPase activities observed. This may be attributed to a difference in membrane vesicle preparation. The amount of F_1 subunits present increases when plasmid pPH12 (*a*) was present in either strain. This is in contrast to the observation of *b* subunit levels in strain PH105 (a_{del}) in the absence or presence of plasmid pPH12 (*a*) (Figure 3-3A). Strain 1100 and strain 1100ΔBC are positive and negative controls, respectively. A light background signal observed in strain 1100ΔBC was probably due to contaminating proteins in the purified F_1 sector used in the preparation of the anti-F_1 antibodies (Figure 3-3B).

Discussion

The observations from the data indicate that strain PH105 (a_{del}) possesses a reduced level of F_1F_O ATP synthase subunits as compared to strain RH305 ($a_{uncB205}$). The reduced amount of F_1F_O subunits is probably because the subunit's expression levels have been altered. The 617 bp deletion of the *uncB* (*a*) gene probably effects the expression of the *uncE* (*c*) gene in a similar manner as the altered Shine-Dalgarno sequence observed in the *uncE* (*c*) gene (Solomon & Brusilow, 1988; Schaefer *et al.* 1989). That changes in the sequence of the mRNA effect the expression of the *uncE* (*c*) gene was demonstrated by Fillingame (1993) where a 7 bp deletion, 100's of bp from the translational start site, effected the levels of *c* subunit present. The effect of mRNA sequence on expression levels of the *uncE* (*c*) have been reported by McCarthy *et al.* (1985). The deletion of the 617 bp from the mRNA of the *unc* operon could effect the regulation of the *uncE* (*c*) gene. Alternately the 617 nucleotide deletion from the mRNA may effect its stability resulting in reduced expression due to reduced mRNA levels (Schaefer *et al.* 1989; Lagoni *et al.*, 1993). The observation of similar phenotypes for strain BC2000 (a_{del}, c_{SD}) and strain PH105 (a_{del}) indicates that the *uncE* (c_{SD}) mutation is not responsible for the polar phenotype on F_1 expression.

While this reduction in F_1F_0 ATP synthase subunits is detrimental to the biochemical assays of *a* subunit mutants, it appears to supply a more sensitive test for the effects of *a* subunit mutants *in vivo*. Consequently strain PH105 (a_{del}) was used for studying the growth characteristics of *a* subunit mutants, and strain RH305 ($a_{uncB205}$) was used for membrane vesicle preparation to perform biochemical analysis on *a* subunit mutants. Growth studies with strain PH105 (a_{del}) may reveal phenotypes that might be obscured by the truncated *a* subunit of strain RH305 ($a_{uncB205}$). The difference in levels of F_1F_0 ATP synthase subunits in strain PH105 (a_{del}) and strain RH305 ($a_{uncB205}$) may also affect growth phenotypes. An example of this is demonstrated by the $a_{L207\rightarrow P}$ mutant, which exhibited a phenotype dependent on the concentration of F_1 subunits (Chapter 5). Since strain PH105 (a_{del}) will have limited potential for recombination with *a* subunit plasmids carrying mutations, and is not subject to amber tRNA suppressor mutations, strain PH105 (a_{del}) will prove useful in the selection of second-site mutations.

CHAPTER 4
MUTAGENIC ANALYSIS OF CONSERVED AMINO ACIDS a_{Q252} THROUGH a_{Y263} IN THE *a* SUBUNIT

Introduction

The primary amino acid sequence of the carboxyl-terminal one-third of the *a* subunit bears striking homology with similar subunits from the mitochondrial and chloroplast F_1F_0 ATP synthases (Walker *et al.*, 1984). This evolutionary conservation consists of two regions of strong homology predicted to be located in the last two membrane spanning regions of the *a* subunit (Chapter 1). Cain & Simoni suggested both conserved regions were important in proton translocation (1986). This chapter will focus on the conserved amino acids in the second region of homology (Figure 4-1), which has not been as extensively studied as the first region.

The first evidence for the role of the *a* subunit in proton translocation came from the isolation of missense mutations which impaired proton translocation while apparently allowing assembly of an intact F_1F_0 ATP synthase complex (Cain & Simoni, 1986). In order to investigate the specific amino acids which might participate in the

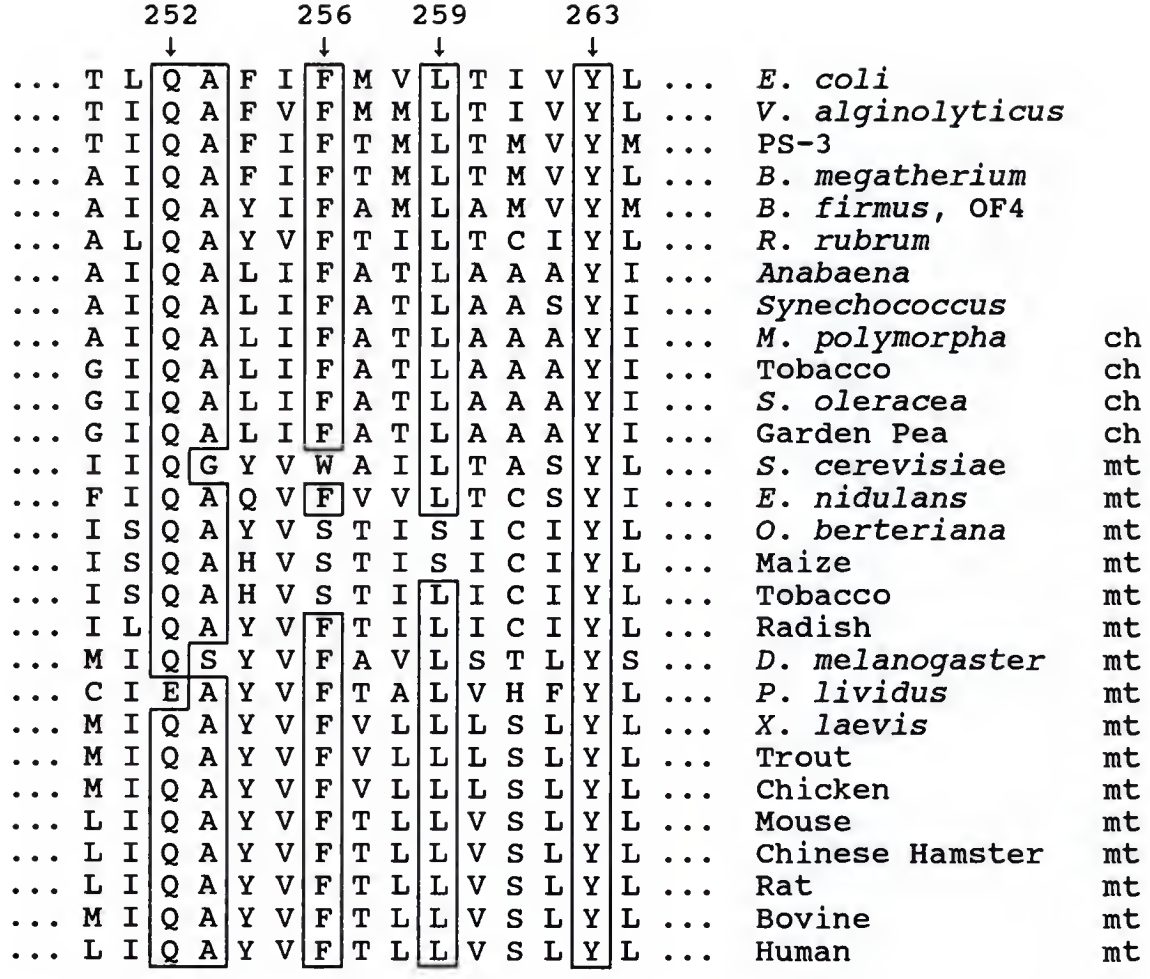
252
256
259
263
... T L Q A F I F M V L T I V Y L ... E. coli
... T I Q A F V F M M L T I V Y L ... V. alginolyticus
... T I Q A F I F T M L T M V Y M ... PS-3
... A I Q A F I F T M L T M V Y L ... B. megatherium
... A I Q A Y I F A M L A M V Y M ... B. firmus, OF4
... A L Q A Y V F T I L T C I Y L ... R. rubrum
... A I Q A L I F A T L A A A Y I ... Anabaena
... A I Q A L I F A T L A A S Y I ... Synechococcus
... A I Q A L I F A T L A A A Y I ... M. polymorpha ch
... G I Q A L I F A T L A A A Y I ... Tobacco ch
... G I Q A L I F A T L A A A Y I ... S. oleracea ch
... G I Q A L I F A T L A A A Y I ... Garden Pea ch
... I I Q G Y V W A I L T A S Y L ... S. cerevisiae mt
... F I Q A Q V F V V L T C S Y I ... E. nidulans mt
... I S Q A Y V S T I S I C I Y L ... O. berteriana mt
... I S Q A H V S T I S I C I Y L ... Maize mt
... I S Q A H V S T I L I C I Y L ... Tobacco mt
... I L Q A Y V F T I L I C I Y L ... Radish mt
... M I Q S Y V F A V L S T L Y S ... D. melanogaster mt
... C I E A Y V F T A L V H F Y L ... P. lividus mt
... M I Q A Y V F V L L L S L Y L ... X. laevis mt
... M I Q A Y V F V L L L S L Y L ... Trout mt
... M I Q A Y V F V L L L S L Y L ... Chicken mt
... L I Q A Y V F T L L V S L Y L ... Mouse mt
... L I Q A Y V F T L L V S L Y L ... Chinese Hamster mt
... L I Q A Y V F T L L V S L Y L ... Rat mt
... M I Q A Y V F T L L V S L Y L ... Bovine mt
... L I Q A Y V F T L L V S L Y L ... Human mt

Figure 4-1. Alignment of amino acid sequence in the last proposed membrane spanning segment. Numbers at the top of the sequence denote the amino acid position in *E. coli*. Abbreviations 'ch' and 'mt' stand for chloroplast and mitochondrion respectively. Amino acids positions that are highly conserved (> 80%) have been boxed. Amino acid positions like a_{I251}, a_{I255}, and a_{L264} have mainly conservative variations. For a more complete alignment, including full names, species designation and references see Figure 1-3.

translocation mechanism, a large number of missense mutations have been constructed using site directed mutagenesis by many investigators (Cain & Simoni, 1988, 1989; Eya *et al.*, 1988, 1991; Howitt *et al.*, 1988; Lightowlers *et al.*, 1987, 1988; Vik *et al.*, 1988, 1990, 1991). By analyzing the phenotypes of multiple mutations at single positions it has been possible to establish the relative importance of many of the conserved amino acids for the function of the enzyme.

Although the topology of the *a* subunit of F_1F_0 ATP synthase is not known, the membrane spanning segment proximal to the carboxyl-terminus of the *a* subunit is thought to extend from about a_{H245} through a_{S268} (Fillingame, 1992a; Vik & Dao, 1992). Evidence from localization of enzymatic activities of *a* subunit-alkaline phosphatase fusion products suggests the possibility of a shorter membrane spanning segment between a_{F254} and a_{S268} (Lewis *et al.*, 1990). In Chapter 1 membrane spanning segments were predicted based on alignment of conserved amino acids and exclusion of non-conserved charged amino acids. By these criteria the hydrophobic domain of the last membrane spanning segment would be a_{W241} to a_{L264}. The choice of a_{W241} as the beginning of the region is partly based on the evidence that a_{G218}, a_{E219} and a_{H245} are spatially close to each other (Cain & Simoni, 1988; Chapter 6).

The carboxyl-terminal membrane spanning region of the *a* subunit is essential for enzyme function since removal of all or part of this segment results in the apparent loss of F_1F_0 ATP synthase activity, such as occurs in strains carrying the $a_{W235\rightarrow end}$, $a_{Q252\rightarrow end}$, and $a_{Y263\rightarrow end}$ mutations (Cain & Simoni, 1986; Eya *et al.*, 1988, 1991; Vik *et al.*, 1991). Primary sequence comparisons between the *a* subunit present in the *E. coli* enzyme and the corresponding subunits in other F_1F_0 ATP synthases indicates that several amino acids in the carboxyl-terminal membrane span are among those most strongly conserved in F_1F_0 ATP synthases.

This chapter encompasses the construction and biochemical analysis of site-directed mutations in the second region of the *a* subunit sequence homology at amino acid positions a_{Q252}, a_{F256}, a_{L259}, and a_{Y263} (Figure 4-1). Amino acid position a_{Y263} exhibits complete evolutionary conservation. However, amino acid position a_{Q252} has one sequence deviation to a glutamate, reported in the sea urchin species *Paracentrotus lividus* (Jacobs *et al.*, 1988). Amino acid positions a_{F256} and a_{L259} are highly conserved, but deviations in their amino acid sequence homology have also been reported. Additionally, assuming that this membrane spanning domain is in an α-helical conformation these amino acids are positioned on the same face of the helix as a_{H245}. Since a_{H245} apparently interacts with the predicted membrane spanning domain containing a_{G218} and a_{E219} (Cain & Simoni,

1988; Chapter 6), mutations in a_{Q252}, a_{F256}, a_{L259}, and a_{Y263} might be expected to effect this interaction. This hypothesis is supported by the observation that substitutions of basic amino acids at each of these amino acid positions significantly reduced F_1F_0 ATP synthase function. This is what would be expected if the last two membrane spanning domains interacted along this face of an α-helix.

Results

Generation of *uncB* (*a*) Mutations

Site-directed mutations were constructed at amino acid positions a_{Q252}, a_{F256}, a_{L259}, and a_{Y263} using a novel cassette site-directed mutagenesis plasmid pPH12 (Chapter 2). The *uncB* (*a*) gene carried on plasmid pPH12 contained silent mutations with unique *HindIII* and *ClaI* restriction sites. Together with a *BclI* site present in the native *uncB* (*a*) gene, these restriction endonuclease sites flanked the codons targeted for mutagenesis (Figure 4-2).

The mutations generated by mutagenesis of plasmid pPH12 with each of the cassette oligonucleotides are listed in Table 4-1. Twenty-two mutations in the *uncB* (*a*) gene were recovered at the four sites. Four missense mutations altered a_{Q252}, seven amino acid substitutions affected a_{F252}, three missense mutations appeared at a_{L259}, and seven

Figure 4-2. Oligonucleotides used for cassette mutagenesis and the sequence from plasmid pPH12 (a). Numbers above amino acid sequence denote amino acid positions. Restriction enzymes below DNA sequence denote the beginning of the corresponding restriction recognition sequence. The mutants shown above each cassette represent potential mutants. Amino acids in brackets represent mutants that were not isolated. Numbers in brackets denote oligonucleotide number listed in Table 4-1.

Table 4-1
Mutations Generated in the *uncB* (*a*) Gene

Oligonucleotide	Isolates sequenced	Mutant codons	Plasmid	Mutation
18/17	4	GAA	pUNCB5.01	$a_{Q252 \rightarrow E}$
		AAA	pUNCB5.04	$a_{Q252 \rightarrow K}$
19/20	7	TTA	pUNCB5.02	$a_{Q252 \rightarrow L}$
		GTA	pUNCB5.03	$a_{Q252 \rightarrow V}$
27/28	15	TAC	pUNCB5.10	$a_{F256 \rightarrow Y}$
		CTC	pUNCB5.11	$a_{F256 \rightarrow L}$
		CAC	pUNCB5.12	$a_{F256 \rightarrow H}$
		TGC	pUNCB5.13	$a_{F256 \rightarrow C}$
		GTC	pUNCB5.14	$a_{F256 \rightarrow V}$
		GAC	pUNCB5.15	$a_{F256 \rightarrow D}$
		CGC	pUNCB5.16	$a_{F256 \rightarrow R}$
49/48	9	GGC	pUNCB5.20	$a_{L259 \rightarrow G}$
		CAC	pUNCB5.21	$a_{L259 \rightarrow H}$
		CGC	pUNCB5.22	$a_{L259 \rightarrow R}$
		TAA	pUNCB5.23	$a_{L259 \rightarrow end}$
25/26	21	TTC	pUNCB5.30	$a_{Y263 \rightarrow F}$
		TGC	pUNCB5.31	$a_{Y263 \rightarrow C}$
		TGG	pUNCB5.32	$a_{Y263 \rightarrow W}$
		TCC	pUNCB5.33	$a_{Y263 \rightarrow S}$
		CTG	pUNCB5.34	$a_{Y263 \rightarrow L}$
		CCC	pUNCB5.35	$a_{Y263 \rightarrow P}$
		CGG	pUNCB5.36	$a_{Y263 \rightarrow R}$

substitutions were found at a_{Y263}. In addition, mutagenesis of a_{Y263} produced a mutant plasmid that contained a nonsense mutation at position a_{L259} due to a fortuitous deletion of a thymidine nucleotide in the a_{L259} codon.

Effects of *uncB* (*a*) mutations on Cell Growth

The efficiency of F_1F_0 ATP synthase in *E. coli* was examined by correlation to growth yield of mutant strains in glucose-limited medium. Growth on succinate-based medium was also studied since F_1F_0 ATP synthase is necessary for OXPHOS.

E. coli strain PH105 (a_{del}) carrying an internal deletion of 617 base pairs of the *uncB* (*a*) gene was constructed to serve as the host strain for growth studies (see Chapter 3). The mutant *uncB* (*a*) gene plasmids were transformed into strain PH105 (a_{del}) in order to study the capacity of the plasmids to complement the chromosomal deficiency.

Each strain, PH105 (a_{del}) harboring an *a* subunit plasmid, was streaked onto solid succinate minimal-A medium. The missense mutation plasmids pUNCB5.04 ($a_{Q252\rightarrow K}$), pUNCB5.16 ($a_{F256\rightarrow R}$), pUNCB5.22 ($a_{L259\rightarrow R}$) and the nonsense mutation plasmid pUNCB5.23 ($a_{L259\rightarrow end}$) all failed to support growth on succinate (Table 4-2). Similarly, these strains attained cell densities in glucose-limited liquid medium comparable to strain PH105 with no plasmid. The results were consistent

Table 4-2
Growth Properties of *a* Subunit Mutants

Strain/ Plasmid	Strain/ Plasmid Mutation	Growth on succinate[a] 37°C	42°C	Growth yield on glucose[b] 2mM	5mM
PH105	Deletion	-	-	29	64
pPH12	Wild type	+++	+++	46	98
pUNCB5.01	$a_{Q252\rightarrow E}$	+++	+++	43	94
pUNCB5.02	$a_{Q252\rightarrow L}$	+	-	35	77
pUNCB5.03	$a_{Q252\rightarrow V}$	+	-	34	74
pUNCB5.04	$a_{Q252\rightarrow K}$	-	-	31	70
pUNCB5.10	$a_{F256\rightarrow Y}$	+++	+++	46	102
pUNCB5.11	$a_{F256\rightarrow L}$	+++	+++	46	101
pUNCB5.12	$a_{F256\rightarrow H}$	+++	+	48	98
pUNCB5.13	$a_{F256\rightarrow C}$	+++	+++	46	96
pUNCB5.14	$a_{F256\rightarrow V}$	+++	+++	40	81
pUNCB5.15	$a_{F256\rightarrow D}$	+	+	36	87
pUNCB5.16	$a_{F256\rightarrow R}$	-	-	31	69
pUNCB5.20	$a_{L259\rightarrow G}$	+++	-	42	89
pUNCB5.21	$a_{L259\rightarrow H}$	+++	+	42	87
pUNCB5.22	$a_{L259\rightarrow R}$	-	-	33	70
pUNCB5.23	$a_{L259\rightarrow end}$	-	-	31	69
pUNCB5.30	$a_{Y263\rightarrow F}$	+++	+++	47	95
pUNCB5.31	$a_{Y263\rightarrow C}$	+++	+	46	93
pUNCB5.32	$a_{Y263\rightarrow W}$	+++	+++	46	92
pUNCB5.33	$a_{Y263\rightarrow S}$	+++	+	42	89
pUNCB5.34	$a_{Y263\rightarrow L}$	+++	+++	40	89
pUNCB5.35	$a_{Y263\rightarrow P}$	+++	+	41	92
pUNCB5.36	$a_{Y263\rightarrow R}$	+	-	38	79

[a]Colony size after 48 h of incubation at the indicated temperatures on solid succinate (0.2% w/v) minimal medium A. Growth was scored as normal colonies (+++) comparable to the wild type control strain, smaller than normal colonies (+) and no visible colonies (-).

[b]Growth yield (Klett units) in 2 mM and 5 mM glucose minimal medium A was monitored turbidimetrically using a Klett-Summerson colorimeter.

with loss of biologically significant levels of F_1F_0 ATP synthase.

Mutant plasmids, such as pUNCB5.02 ($a_{Q252\rightarrow L}$) and pUNCB5.03 ($a_{Q252\rightarrow V}$), supported the development of very small colonies on succinate medium and intermediate densities in the glucose-limited medium suggesting reduced F_1F_0 ATP synthase function. Interestingly, plasmid pUNCB5.36 ($a_{Y263\rightarrow R}$) also supported limited growth. This was the only plasmid in the present collection encoding a mutation substituting a positively charged amino acid which allowed detectable enzyme function *in vivo*. Plasmid pUNCB5.35 ($a_{Y263\rightarrow P}$) promoted growth at a level marginally less than wild type. Apparently, a_{Y263} accommodates most mutations with little loss of enzyme activity.

Vik *et al.* (1991) had previously reported that some missense mutations of a_{Y263} displayed temperature sensitivity. As shown in Table 4-2, incubation at 42°C resulted in reduced growth phenotypes not only for a_{Y263} mutations, but for mutations in the other three positions as well. The most dramatic example of this temperature sensitivity was plasmid pUNCB5.20 ($a_{L259\rightarrow G}$) which supported wild type like growth at 37°C, but was unable to promote visible growth at 42°C. The loss of growth on succinate at the elevated temperature is likely due to the individual amino acid substitutions destabilizing the structure of the F_0 complex.

In summary, the growth studies indicate that substitutions in a_{Q252} exhibited the most pronounced effects in cell growth. The severity of growth inhibition seemed to diminish as the amino acid positions neared the carboxyl-terminus of the *a* subunit. The latter point has been demonstrated by the observation that missense mutations affecting a_{Y263} were not sufficient for abolition of F_1F_0 ATP synthase function (Table 4-2; Eya *et al.*, 1991; Vik *et al.*, 1991).

ATP Synthase Proton Pumping

ATP driven acidification of inverted *E. coli* membrane vesicles can be used as measure of the capacity of F_1F_0 ATP synthase to carry-out proton translocation coupled to ATP hydrolysis. The acidification of the membrane vesicles derived from strain RH305 ($a_{uncB205}$) harboring the *a* subunit mutation plasmids was followed by observing the ATP-dependent quenching of the fluorescent dye ACMA (see Chapter 2). Electron transport chain mediated NADH-dependent quenching was also determined for each preparation to ensure vesicle integrity. Membrane vesicles were prepared from each strain with an *a* subunit mutation plasmid which apparently resulted in a defect in F_1F_0 ATP synthase based on the growth characteristics.

The ability of membranes from the mutant strains to promote vesicle acidification was determined by comparing the quenching of ACMA fluorescence between the mutant

strains and the positive control membranes from strain RH305 ($a_{uncB205}$) with plasmid pPH12 (*a*). Membranes derived from cells with plasmids pUNCB5.04 ($a_{Q252\rightarrow K}$), pUNCB5.16 ($a_{F256\rightarrow R}$), and pUNCB5.23 ($a_{L259\rightarrow R}$) exhibited no significant vesicle acidification suggesting an apparent loss of proton pumping activity (Figure 4-3A). Vesicle acidification in the range of 25% to 50% of the positive control were observed in membranes from cells carrying plasmids pUNCB5.36 ($a_{Y263\rightarrow R}$), pUNCB5.03 ($a_{Q252\rightarrow V}$), pUNCB5.15 ($a_{F256\rightarrow D}$) and pUNCB5.02 ($a_{Q252\rightarrow L}$). As expected, studies of membranes from cells carrying plasmid pUNCB5.01 ($a_{Q252\rightarrow E}$) resulted in vesicle acidification similar to membranes from the positive control.

To determine if the ATP-dependent fluorescence quenching was due to F_1F_0 ATP synthase, the strains exhibiting detectable vesicle acidification were treated with the F_0 proton translocation inhibitor DCCD. In every instance, treatment with DCCD reduced fluorescence quenching below detectable levels indicating that F_1F_0 ATP synthase was responsible for the observed vesicle acidification (Figure 4-3B).

The vesicle acidification data showed that the mutant strains that apparently reduced *in vivo* synthesis of ATP, also reduced the ability of F_1F_0 ATP synthase to pump protons *in vitro*.

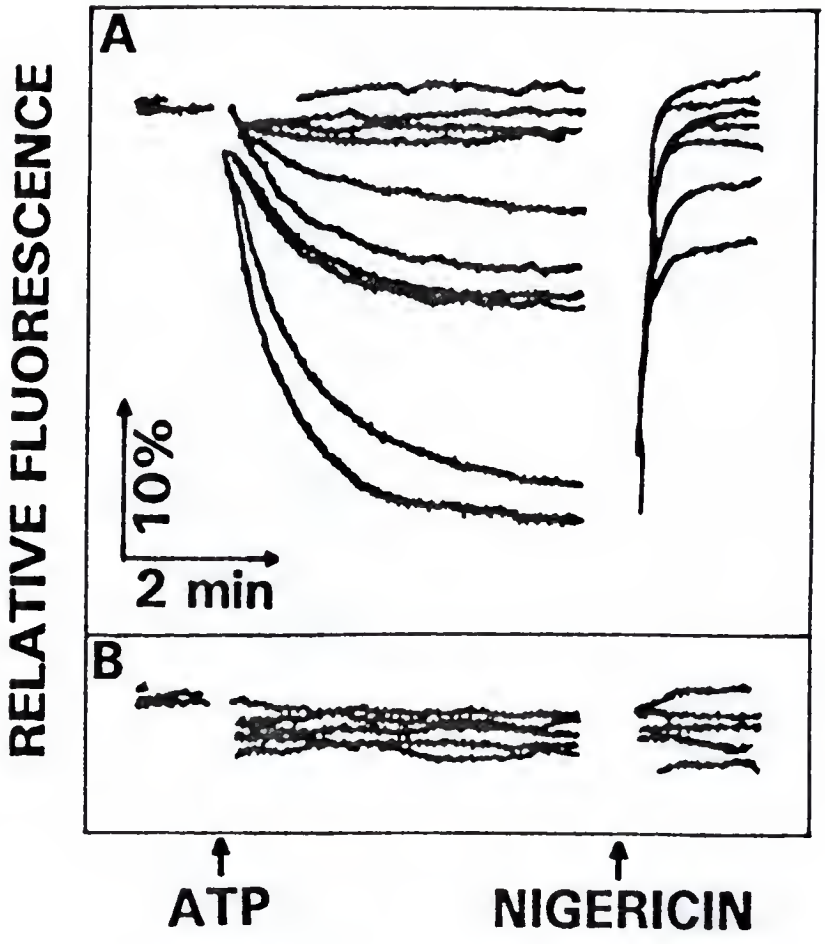

Figure 4-3. Energization of membrane vesicles determined by fluorescence quenching of ACMA. ACMA was added to a final concentration of 1 μM. Membrane vesicles were at a concentration of 250 μg of protein/ml buffer (50 mM MOPS and 10 mM $MgCl_2$, pH 7.3). Arrows mark the addition of reagents to final concentrations of: ATP 0.4 mM; nigericin 0.05 μM. A. ATP-driven membrane energization. The traces represent the following mutant strains in descending order: RH305 ($a_{uncB205}$), $a_{F256\rightarrow R}$, $a_{L259\rightarrow R}$, $a_{Q252\rightarrow K}$, $a_{Y263\rightarrow R}$, $a_{Q252\rightarrow V}$, $a_{F256\rightarrow D}$, $a_{Q252\rightarrow L}$, pPH12 (a), and $a_{Q252\rightarrow E}$. B. Membrane energization following treatment of membranes with 50μM DCCD. The traces represent the following mutant strains in descending order: $a_{Q252\rightarrow V}$, $a_{Q252\rightarrow L}$, $a_{Y263\rightarrow R}$, pPH12 (a), $a_{Q252\rightarrow E}$, and $a_{F256\rightarrow D}$.

F_O-Mediated Passive Proton Conductance

To determine if a mutation specifically affected F_O-mediated proton translocation, the permeability of membrane vesicles stripped of F_1 was examined. The stripping of F_1 from membranes derived from wild type cells results in F_O functioning as a passive proton conductor, allowing the collapse of an imposed electrochemical gradient. A mutation affecting F_O-mediated proton translocation typically reduced the capacity of F_O to collapse proton gradients.

An electrochemical gradient was imposed by addition of NADH as a substrate for NADH dehydrogenase driven vesicle acidification. The stripped membranes from cells harboring plasmid pPH12 (*a*) displayed little ACMA fluorescence quenching upon addition of NADH demonstrating F_O proton conductance (Figure 4-4). Similarly, analysis of stripped membranes from cells carrying plasmid pUNCB5.01 ($a_{Q252\rightarrow E}$) revealed abundant proton permeability. However, stripped membranes from cells with reduced growth phenotypes resulted in significant ACMA quenching indicating impairment of F_O-mediated proton conductance.

In summary, the studies of proton translocation were consistent with the mutational effects on cell growth being attributable to a reduction in ATP synthase activity due to a reduction in F_1F_O proton translocation.

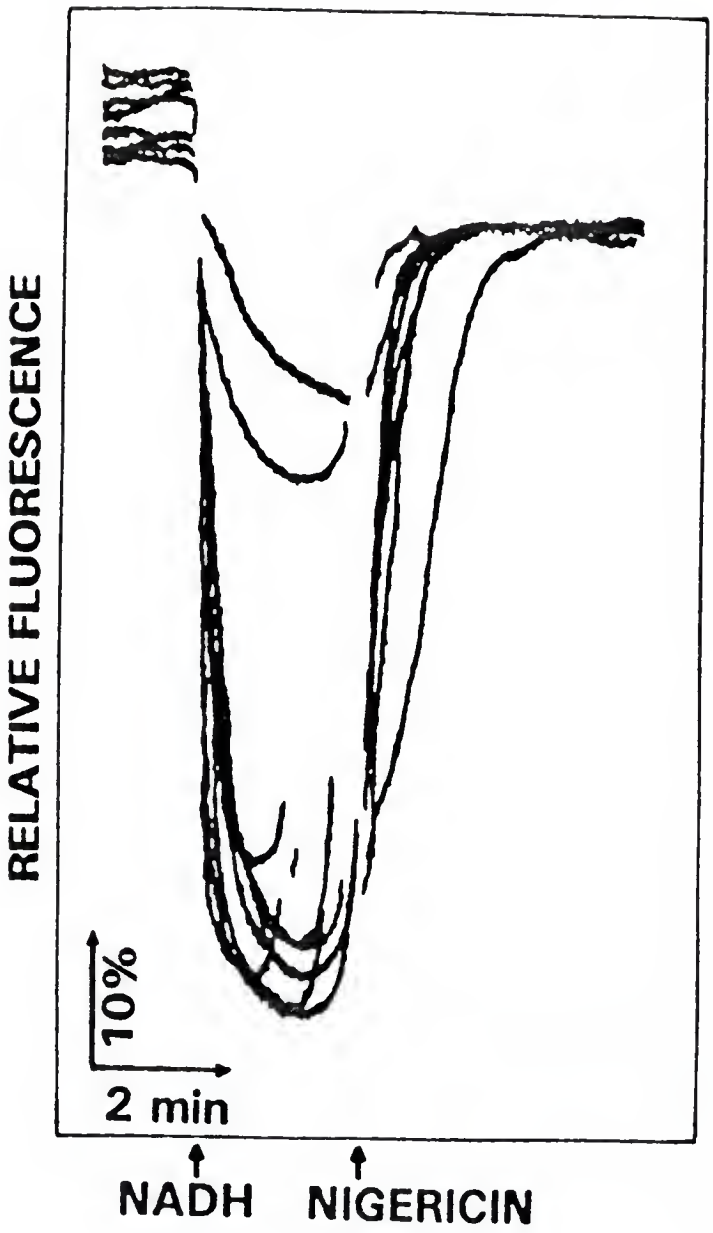

Figure. 4-4. Proton impermeability of stripped membranes from a subunit mutant strains. Assays were performed as described in Chapter 2. ACMA was added to a final concentration of 1 μM. Stripped membrane vesicle were at a concentration of 250 μg of protein/mls buffer (50 mM MOPS and 10 mM $MgCl_2$, pH 7.3). Arrows mark the addition of NADH (0.5 mM) and nigericin (0.05 μM). The traces represent the following mutant strains in descending order: $a_{Q252\rightarrow E}$, pPH12 (a), $a_{Q252\rightarrow L}$, $a_{F256\rightarrow D}$, $a_{Y263\rightarrow R}$, $a_{L259\rightarrow R}$, $a_{Q252\rightarrow V}$, RH305 ($a_{uncB205}$), $a_{F256\rightarrow R}$, and $a_{Q252\rightarrow K}$.

ATP Hydrolysis Activity

Reduction in the ability of membranes from mutant strains to carry-out ATP dependent vesicle acidification can be attributed to a reduction in the activity of F_1F_o ATP synthase or to a reduction in the number of functional F_1F_o ATP synthases in the membrane. Mutations in the *a* subunit have been shown to affect F_1F_o ATP synthase by either perturbing F_o assembly via a structural defect or through alteration of an amino acid important in proton translocation. The DCCD-sensitive F_1 ATPase activity present on membranes isolated from positive control and mutant strains can be utilized as a measure of the amount of coupled F_1F_o ATP synthase present. Membrane-associated, DCCD-sensitive F_1 ATPase activity was assayed by measuring the ATPase activity of membrane vesicles both treated and untreated with 50 μM DCCD for 1 hour at room temperature. The difference in ATPase activities was termed DCCD sensitive ATPase activity and indicates the amount of F_1-ATPase activity bound to the F_o sector. This was sometimes referred to as coupled F_1F_o ATPase activity, but results in Chapter 6 indicate that 'coupled' may not be technically correct. By comparing the DCCD sensitive ATPase activity of the positive control strain and *a* subunit mutant strains, the structural integrity of the F_1F_o ATP synthase complex in the mutant strains can be determined. However, some *a* subunit mutations display DCCD insensitivity, which exhibit

a phenotype similar to mutants with unbound F_1-ATPase activity. (Cain & Simoni, 1989; Eya *et al.*, 1991).

Substitutions at position a_{Q252} were analyzed to determine the activity of coupled F_1F_0 ATP synthase. The percentage of DCCD-sensitive ATP hydrolysis activity (Table 4-3; a = 49%, $a_{Q252\rightarrow E}$ = 46%, $a_{Q252\rightarrow L}$ = 39%, $a_{Q252\rightarrow V}$ = 29%, $a_{Q252\rightarrow K}$ = 0%, a_{del} = 10%) coorelated with the growth characteristics observed for the substitutions at a_{Q252} (Table 4-2). Membranes derived from strain RH305 carrying plasmids pUNCB5.01 ($a_{Q252\rightarrow E}$), pUNCB5.02 ($a_{Q252\rightarrow L}$), and pUNCB5.03 ($a_{Q252\rightarrow V}$) possessed significant levels of DCCD-sensitive ATP hydrolysis activity, though slightly reduced from wild-type levels, indicating significant F_1 association with F_0. The percentage of DCCD sensitive activity is reduced in the $a_{Q252\rightarrow L}$ and $a_{Q252\rightarrow V}$ mutants , which coorelates with there partial phenotype. Study of membranes from strain RH305 with plasmid pUNCB5.04 ($a_{Q252\rightarrow K}$) revealed virtually no DCCD-sensitive F_1 ATPase activity suggesting an interruption of productive coupling in F_1F_0 ATP synthase.

Discussion

This Chapter reports the first missense mutations in this region of the *a* subunit which appeared to be sufficient to abolish F_1F_0 ATP synthase activity. All previously reported missense mutations in this area of the *a* subunit

Table 4-3
Properties of *a* Subunit Mutations at a_{Q252}

Plasmid	Plasmid mutation	ATPase specific activity[a] Total	DCCD sensitive[b]
pPH12	*a*	0.80±.08	0.39±.05
pUNCB5.01	$a_{Q252 \rightarrow E}$	0.65±.03	0.30±.01
pUNCB5.02	$a_{Q252 \rightarrow L}$	0.77±.02	0.30±.01
pUNCB5.03	$a_{Q252 \rightarrow V}$	0.73±.06	0.21±.00
pUNCB5.04	$a_{Q252 \rightarrow K}$	0.76±.08	0.00±.00
pPH11	a_{del}	0.60±.03	0.06±.02

[a]Specific activity = μmol ATP hydrolyzed/mg protein/min determined at pH 8.0. Values are the average of two assays done at two different protein concentrations.

[b]DCCD sensitive activity = specific activity lost after treatment with 50 μM DCCD for one hour at room temperature.

allowed detectable levels of enzyme function (Eya *et al.*, 1991; Vik *et al.*, 1991).

Generally, as the carboxyl-terminus is approached in the last membrane spanning segment of the *a* subunit, mutations appear to have progressively less profound effects. In the case of the final conserved position a_{Y263}, missense mutations which specify the substitutions of radically different amino acids, such as proline and arginine, do not abolish F_1F_O ATP synthase activity (Table 4-1, Vik *et al.*, 1991). The apparent ability of a_{Y263} to be substituted by any amino acid may be due to its proposed proximity to the edge of the membrane spanning region. The evidence for this proximity is that the truncated mutant $a_{S265\rightarrow end}$ forms an active F_1F_O ATP synthase (Eya *et al.*, 1991). This would allow charged substitutions at a_{Y263} to move outside of the hydrophobic environment of the membrane, but still allow reduced amounts of enzyme activity. In contrast, mutations resulting in the replacements of a_{Q252}, a_{F256} and a_{L259} with basic amino acids are sufficient for the apparent loss of enzyme function. In each of these mutant strains, proton translocation through the F_O sector is decreased beyond detectable levels. It seems likely that the introduction of charged amino acids into a membrane spanning region may result in a conformational change sufficient to perturb proton translocation. The mutants $a_{Q252\rightarrow K}$, $a_{F256\rightarrow D}$, $a_{F256\rightarrow R}$, and $a_{L259\rightarrow R}$ support this hypothesis, while the reduced activity of $a_{Y263\rightarrow R}$ can be attributed to a shifting of the membrane spanning

domain that permits function. This is also true if these amino acid positions are interacting with proposed membrane spanning domain V of the *a* subunit. As discussed above unpaired charged amino acids would be expected to disrupt a protein-protein interaction between membrane spanning domains. This hypothesis is supported by the positively charged amino acid substitutions.

Changes at a_{Q252} indicate a role beyond merely stabilizing a membrane span. In the case $a_{Q252\rightarrow E}$, a change to a charged amino acid, no significant effect was observed. In contrast two non-charged substitutions, $a_{Q252\rightarrow L}$ and $a_{Q252\rightarrow V}$, substantially reduce activity. These data suggest that a_{Q252} may play an important structural role in the formation of a functional F_O complex.

Another interpretation of the a_{Q252} mutant data, is that this amino acid effects the character of a hypothetical proton channel or binding site (Chapter 1). If this was the case then a negatively charged amino acid would have little effect on the flow of proton, while a hydrophobic amino acid might slow the flow and a positive charge block proton translocation altogether. Additionally a_{Q252} may interact with another amino acid known to be necessary for proton translocation. The predicted position for a_{Q252} in membrane spanning segment VI is approximately in the center of the membrane hydrophobic region (Chapter 1). This would place a_{Q252} in a position from which it could influence a_{R210} in proposed membrane spanning segment

V of the *a* subunit or c_{D61} from the *c* subunit. Both a_{R210} and c_{D61} have been shown to be essential for proton translocation. This hypothesis is supported by the reduction in DCCD sensitive activity seen with a_{Q252} mutants. The reduction may also be due a_{Q252} influencing c_{D61}. A significant reduction in DCCD sensitivity, without a reduction in membrane bound F_1 ATPase activity, was reported by Eya *et al.* (1991) for the mutants $a_{Q252 \rightarrow E}$ and $a_{Q252 \rightarrow L}$, indicating an amino acid interaction rather than a structural destabilization causes the loss of DCCD sensitivity.

Many of the amino acid changes in the carboxyl-terminal region of the *a* subunit allow appreciable F_1F_O ATP synthase activity. However, the fact that many of these mutations display temperature sensitivity also supports the hypothesis that the carboxyl-terminal membrane spanning segment plays a structural role in F_O, and possibly in forming a proton channel or binding site (Table 4-2).

This Chapter, coupled with earlier work by others, completes the mutational analysis based on homology alignment for the purpose of locating conserved amino acids essential for proton translocation in the carboxyl-terminal region of the *a* subunit. Designing of mutagenesis experiments based on evolutionary conservation asks the questions, which if any of the conserved amino acid positions are involved in proton translocation, and what are their roles. These questions have to a large part been answered by the multitude of missense

mutations created in the *a* subunit (Cain & Simoni, 1986, 1988, 1989; Eya *et al.*, 1988, 1991; Howitt *et al.*, 1988, 1993; Lightowlers *et al.*, 1987, 1988; Paule & Fillingame, 1989; Vik *et al.*, 1988, 1990, 1991; Chapter 4). An overview of missense mutations in the *a* subunit is presented in Chapter 7, and discusses the above questions. Because these questions have been addressed different criteria were used for designing the site-directed mutagenesis experiment in Chapter 6.

CHAPTER 5
BACTERIAL MODEL FOR HUMAN MITOCHONDRIAL DISEASE

Introduction

Mitochondrial myopathies are maternally inherited genetic defects in OXPHOS. Loss of OXPHOS results in cell death from a drop in cellular energy levels. The disruption of OXPHOS can be the result of a general deficiency, such as loss of mitochondrial protein synthesis through loss of DNA template or translational machinery. Mitochondrial myopathies of this type usually result in morphological changes in the mitochondrion (see Chapter 1). The mode of action by which energy production is lost in this type of mitochondrial myopathy is a loss of the enzyme complexes of OXPHOS. A missense mutation in one of the subunits of an OXPHOS complex would not necessarily result in structural abnormalities, nor would its biochemical effect be easy to investigate. Because of the difficulty in assaying biochemical effects of mutants in mitochondria, the ability to model a missense mutation in a bacterial system is preferable.

The nature of mitochondrial genetics makes determining the biochemical effect of a missense mutation very

difficult, even with cell lines. Diseases of the mitochondrial genome not only display maternal inheritance (Gyllensten *et al.*, 1991), but their pathology is complicated due to heteroplasmy arising from mitotic segregation of the mtDNA defect in somatic cells (Ashley *et al.*, 1989). Additionally, missense mutations that abolish the activity of an OXPHOS complex will almost never be 100% of the mtDNA population, given the cell's dependence on OXPHOS. The combination of these effects is likely to distort biochemical results by the introduction of a sub-population of cells with improved OXPHOS.

Holt *et al.* (1990) first reported that a mutation in the mtDNA *ATPase 6* gene encoding a subunit of F_1F_0 ATP synthase was linked to maternally inherited neurogenic muscle weakness, ataxia, and retinitis pigmentosa (NARP). A restriction fragment length polymorphism (RFLP) in mtDNA from the NARP family allowed a direct correlation between the severity of the disease and the percentage of mutant mtDNA genomes present in each patient. A single mutation was detected at nucleotide 8993 in the mtDNA and resulted in a change in the *ATPase 6* gene converting leucine 156 to arginine (*ATPase* $6_{L156\rightarrow R}$). The *ATPase* $6_{L156\rightarrow R}$ mutation has also been observed in patients from four families diagnosed with maternally inherited Leigh's syndrome or subacute necrotizing encephalopathy (Tatuch *et al.*, 1992; Shoffner *et al.*, 1992; Ciafaloni *et al.*, 1993; Yoshinaga *et al.*,

1993). Like the NARP patients, the severity of disease in patients with Leigh's syndrome was correlated to the percentage of mtDNA carrying the *ATPase* $6_{L156\rightarrow R}$ mutation. A second missense mutation at the same nucleotide has also been reported (de Vries *et al.*, 1993; Schon personal communication). The new mutation, T8993→C, was reported associated with Leigh's syndrome, and results in the missense mutation *ATPase* $6_{L156\rightarrow P}$. Neurological atrophy was the prevalent symptom in affected patients suggesting that cellular energy thresholds were not maintained in neural tissues.

Biochemical studies of the *ATPase* $6_{L156\rightarrow R}$ yielded little detailed information. Analysis of cultured skin fibroblast and muscle mitochondria from a Leigh's syndrome patient by Tatuch *et al.* (1992) revealed no significant reduction in oligomycin sensitive ATPase activity. Tatuch and Robinson (1993) were able to show partial reductions in ATP synthesis and oligomycin sensitive ATP hydrolysis with three lymphoblast cell lines carrying the *ATPase* $6_{L156\rightarrow R}$ mutation as greater than 95% of the mtDNA. Analysis of isolated mitochondria from a cell culture of fibroblast, containing high copy numbers of the *ATPase* $6_{L156\rightarrow P}$ mutation, revealed no apparent changes in oligomycin sensitive ATPase activity (Eric Schon, personal communication). The results of these inconclusive studies of the two NARP mutations using mitochondria from cultured cells demonstrated the need for a

better model to understand the biochemical effects of these two missense mutations.

This chapter details the construction of a bacterial model for the two NARP mutations. Mutations analogous to the NARP mutations were constructed in the *a* subunit of F_1F_0 ATP synthase from *E. coli* based on the alignment of conserved amino acids in 'a-like' (*ATPase 6*-like) sequences (Figure 5-1). The analogous mutations were $a_{L207\rightarrow R}$ and $a_{L207\rightarrow P}$. Their phenotypes correlated with the general observations from the tissue culture studies, however a greater understanding of the biochemical properties of each of the missense mutations was obtained.

Results

The $a_{L207\rightarrow R}$ Mutation

As noted in Chapter 2, OXPHOS is required for utilization of tricarboxylic acid cycle intermediates as carbon sources for aerobic growth, so growth of mutant strains on succinate-based medium is a sensitive test for F_1F_0 ATP synthase function *in vivo*. To analyze the *ATPase* $6_{L156\rightarrow R}$ mutation the comparable mutation $a_{L207\rightarrow R}$ was constructed via cassette site-directed mutagenesis (Chapter 2; Figure 5-2) in the mutant plasmid pUNCB4.70. The recombinant plasmid pUNCB4.70 ($a_{L207\rightarrow R}$) and the control plasmids pPH12 (*a*) and pPH11 (a_{del}) were studied by complementation of the *a* subunit

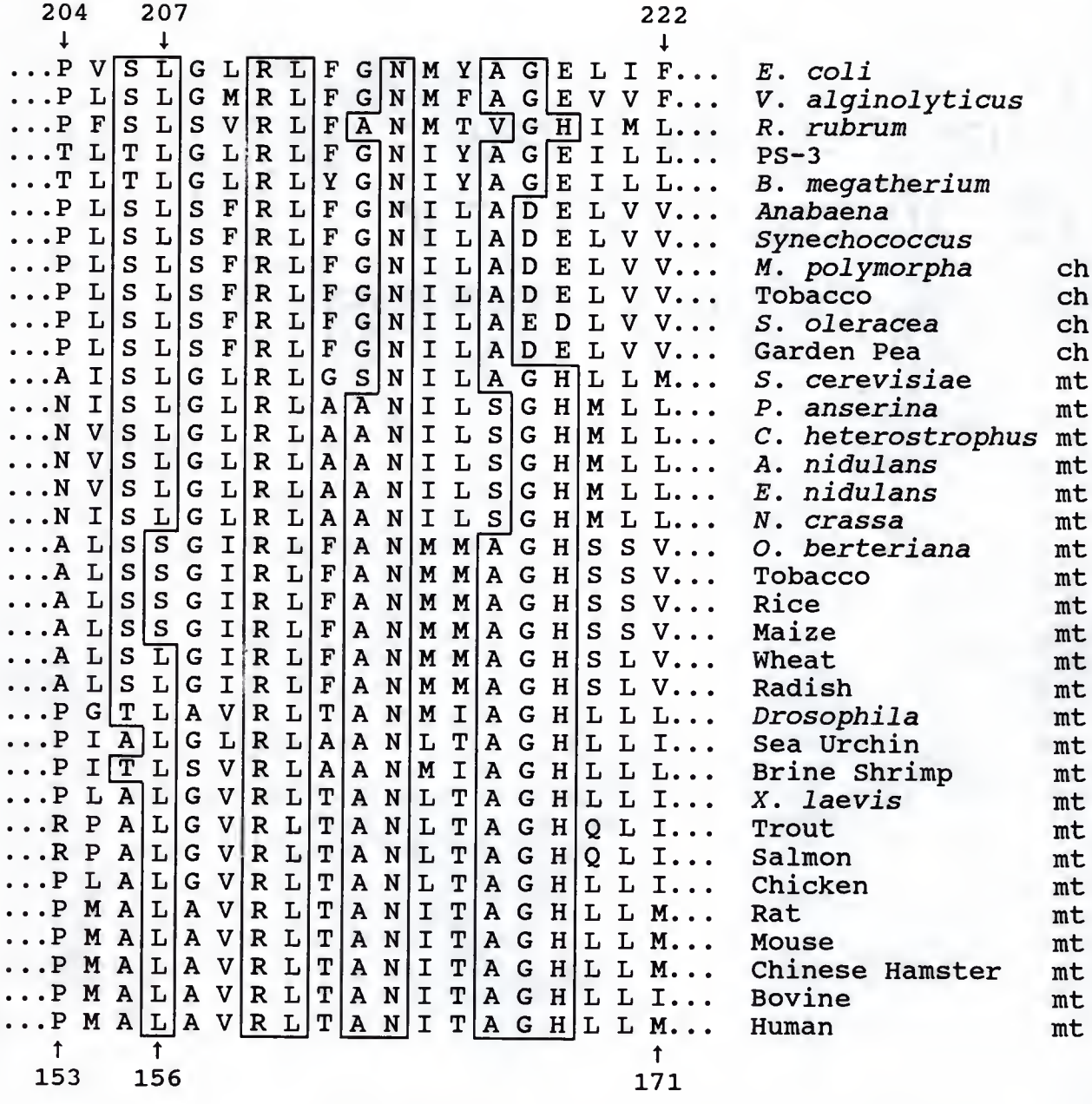
204
207
222
...P V S L G L R L F G N M Y A G E L I F... E. coli
...P L S L G M R L F G N M F A G E V V F... V. alginolyticus
...P F S L S V R L F A N M T V G H I M L... R. rubrum
...T L T L G L R L F G N I Y A G E I L L... PS-3
...T L T L G L R L Y G N I Y A G E I L L... B. megatherium
...P L S L S F R L F G N I L A D E L V V... Anabaena
...P L S L S F R L F G N I L A D E L V V... Synechococcus
...P L S L S F R L F G N I L A D E L V V... M. polymorpha ch
...P L S L S F R L F G N I L A D E L V V... Tobacco ch
...P L S L S F R L F G N I L A E D L V V... S. oleracea ch
...P L S L S F R L F G N I L A D E L V V... Garden Pea ch
...A I S L G L R L G S N I L A G H L L M... S. cerevisiae mt
...N I S L G L R L A A N I L S G H M L L... P. anserina mt
...N V S L G L R L A A N I L S G H M L L... C. heterostrophus mt
...N V S L G L R L A A N I L S G H M L L... A. nidulans mt
...N V S L G L R L A A N I L S G H M L L... E. nidulans mt
...N I S L G L R L A A N I L S G H M L L... N. crassa mt
...A L S S G I R L F A N M M A G H S S V... O. berteriana mt
...A L S S G I R L F A N M M A G H S S V... Tobacco mt
...A L S S G I R L F A N M M A G H S S V... Rice mt
...A L S S G I R L F A N M M A G H S S V... Maize mt
...A L S L G I R L F A N M M A G H S L V... Wheat mt
...A L S L G I R L F A N M M A G H S L V... Radish mt
...P G T L A V R L T A N M I A G H L L L... Drosophila mt
...P I A L G L R L A A N L T A G H L L I... Sea Urchin mt
...P I T L S V R L A A N M I A G H L L L... Brine Shrimp mt
...P L A L G V R L T A N L T A G H L L I... X. laevis mt
...R P A L G V R L T A N L T A G H Q L I... Trout mt
...R P A L G V R L T A N L T A G H Q L I... Salmon mt
...P L A L G V R L T A N L T A G H L L I... Chicken mt
...P M A L A V R L T A N I T A G H L L M... Rat mt
...P M A L A V R L T A N I T A G H L L M... Mouse mt
...P M A L A V R L T A N I T A G H L L M... Chinese Hamster mt
...P M A L A V R L T A N I T A G H L L I... Bovine mt
...P M A L A V R L T A N I T A G H L L M... Human mt
153
156
171

Figure 5-1. Alignment of *a*-like (*ATPase 6*-like) subunits. The sequences shown (see Chapter 1 for references) are from the region of homology that contains the *ATPase* $6_{L156\rightarrow R}$ and *ATPase* $6_{L156\rightarrow P}$ mutations. The numbers on the top of the figure refer to the amino acid position in the *E. coli a* subunit, while the numbers on the bottom denote the amino acid positions in the human mitochondrion *ATPase 6* subunit. Symbols: mt, mitochondrion; ch, chloroplast.

pBDC26 ($a_{L207\rightarrow W,\ E219\rightarrow K}$)

```
204       207                                        219
 P  V  S  W  G  L  R  L  F  G  N  M  W  A  G  K  L
CCAGTTTCATGGGGTTTGCGACTGTTCGGTAACATGTATGCCGGTAAGCTT
GGTCAAAGTACCCCAAACGCTGACAAGCCATTGTACATACGGCCATTCGAA
BstXI                                             HindIII
```

pUNCB4.70 ($a_{L207\rightarrow R}$)

```
          207                                        219
           R  G  L  R  L  F  G  N  M  W  A  G  E
       ACGCGGTTTGCGACTGTTCGGTAACATGTATGCCGGCG
   AAAGTGCGCCAAACGCTGACAAGCCATTGTACATACGGCCGCTCGA
                                        NaeI
```

pUNCB4.71 ($a_{L207\rightarrow P}$)

```
          207                                        219
           P  G  L  R  L  F  G  N  M  W  A  G  E
       ACCCGGGTTGCGACTGTTCGGTAACATGTATGCCGGTG
   AAAGTGGGCCCAACGCTGACAAGCCATTGTACATACGGCCACTCGA
        SmaI
```

Figure 5-2. Plasmid pBDC26 ($a_{L207\rightarrow W,\ E219\rightarrow K}$) and the oligonucleotide cassettes used to make the mutant plasmid pUNCB4.70 ($a_{L207\rightarrow R}$) and plasmid pUNCB4.71 ($a_{L207\rightarrow P}$). Amino acid sequence and position is listed above the DNA sequence. Italicized amino acids represent those mutated from the wild-type sequence. Restriction sites are denoted below the DNA sequence at the start of the recognition sequence.

defective *E. coli* strain RH305 ($a_{uncB205}$) and strain PH105 (a_{del}) (Chapter 3). Plasmid pPH12 (*a*) complemented strain RH305 for growth on succinate medium (Table 5-1). In contrast, cells carrying either plasmid pPH11 (a^-) or plasmid pUNCB4.70 ($a_{L207\rightarrow R}$) failed to grow indicating that the $a_{L207\rightarrow R}$ mutation was sufficient for loss of biologically significant OXPHOS activity (Table 5-1). The results were identical for both *a* subunit deficient strains.

The activity of F_1F_0 ATP synthase was studied *in vitro* in order to establish the biochemical basis for the loss of ATP synthase function. Inverted membrane vesicles were prepared from the strains carrying both mutant and control plasmids and, the capacity of the mutant F_1F_0 ATP synthase to transport protons was measured by studying ATP-dependent vesicle acidification. The acidification of the membrane vesicles was followed by the quenching of the fluorescent dye ACMA (Figure 5-3). The membranes derived from cells with plasmid pUNCB4.70 ($a_{L207\rightarrow R}$) exhibited fluorescent quenching comparable to that from the negative control membranes. It was clear that the $a_{L207\rightarrow R}$ mutation resulted in a profound inhibition of proton translocation through F_1F_0 ATP synthase.

In support of this conclusion, the inability to transport protons was further shown to result from a defect in the F_0 portion of the enzyme complex by studying passive proton conductance. The F_1 portion of ATP synthase was

Table 5-1
Properties of the $a_{L207\rightarrow R}$ Mutation

Plasmid[a]/ Strain	Mutation	Growth on succinate[b]	ATPase specific activity[c] (μmol ATP/mg protein/min) Membrane bound	DCCD sensitive[d]
pPH12	a^+	+++	0.75 ± .10	0.32 ± .05
pPH11	a^-	-	0.58 ± .08	0.09 ± .03
pUNCB4.70	$a_{L207\rightarrow R}$	-	0.42 ± .05	0.04 ± .01
1100ΔBC[e]	$F_1F_O^-$	-	0.19 ± .00	0.01 ± .02

[a]Plasmids were transformed into strain RH305 ($a_{uncB205}$) (Chapter 2).

[b]Growth on succinate was scored as colony formation and designated as normal colonies (+++) or no colonies (-).

[c]Specific activity was measured at pH 8.0 and the values are the average of two assays obtained at two protein concentrations.

[d]DCCD sensitive activity is the ATPase activity lost after treatment with 50 μM DCCD for one hour at room temperature.

[e]The activity reported for strain 1100ΔBC (Shaefer et al., 1989) denotes membrane activity contributed by enzymes other than F_1F_O ATP synthase.

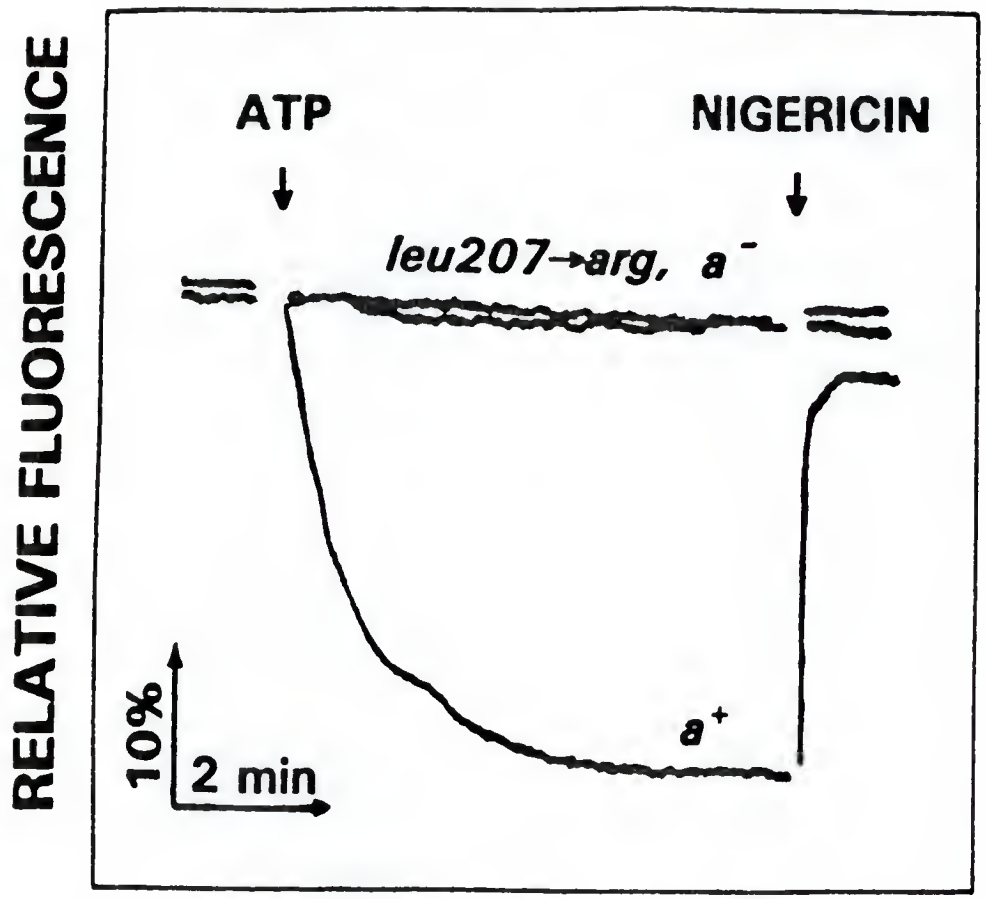

Figure 5-3. F_1F_0 ATP synthase mediated ATP-driven vesicle acidification for $a_{leu207\rightarrow arg}$. Vesicle acidification was followed by ACMA fluorescence quenching as described previously (Chapter 2). Arrows mark the addition of ATP (0.4 mM) and nigericin (0.05 μM). Traces: a^+, strain RH305 ($a_{uncB205}$) carrying plasmid pPH12 (a); a^-, strain RH305 ($a_{uncB205}$) carrying plasmid pPH11 (a_{del}); *leu207→arg*, strain RH305 ($a_{uncB205}$) carrying plasmid pUNCB4.70 ($a_{L207\rightarrow R}$).

displaced from the membrane-associated F_O portion by a mild, low ionic strength wash procedure. Functional F_O remaining in the F_1-depleted membrane vesicles derived from cells harboring plasmid pPH12 (*a*) acted as a passive protonophore collapsing an imposed proton gradient. Experiments with F_1-depleted inverted vesicles from cells with plasmid pUNCB4.70 ($a_{L207\rightarrow R}$) displayed no apparent passive proton conductance (Figure 5-4).

The effects of the $a_{L207\rightarrow R}$ mutation on F_1 activity were studied by determining the ATP hydrolysis activity in membrane vesicles. F_1 remains bound to inverted membrane vesicles when F_O is properly assembled. The membranes from cells carrying plasmid pUNCB4.70 ($a_{L207\rightarrow R}$) showed levels of membrane-associated ATPase activity equivalent to the negative control pPH11 (a_{del}), indicating that the mutation affects either assembly or stability of F_O (Table 5-1). DCCD inhibits F_1F_O ATP synthase by covalently modifying the proteolipid subunit (*c* subunit in *E. coli*) blocking proton translocation and inhibiting coupled ATP hydrolysis activity. The residual membrane-associated F_1 activity from cells carrying plasmid pUNCB4.70 ($a_{L207\rightarrow R}$) was uncoupled since DCCD-sensitive ATPase activity was far below that of the wild type control (Table 5-1). In summary, the $a_{L207\rightarrow R}$ mutation apparently caused a perturbation in the structure of F_O which disrupts proton translocation and its coupling to catalytic function in F_1F_O ATP synthase.

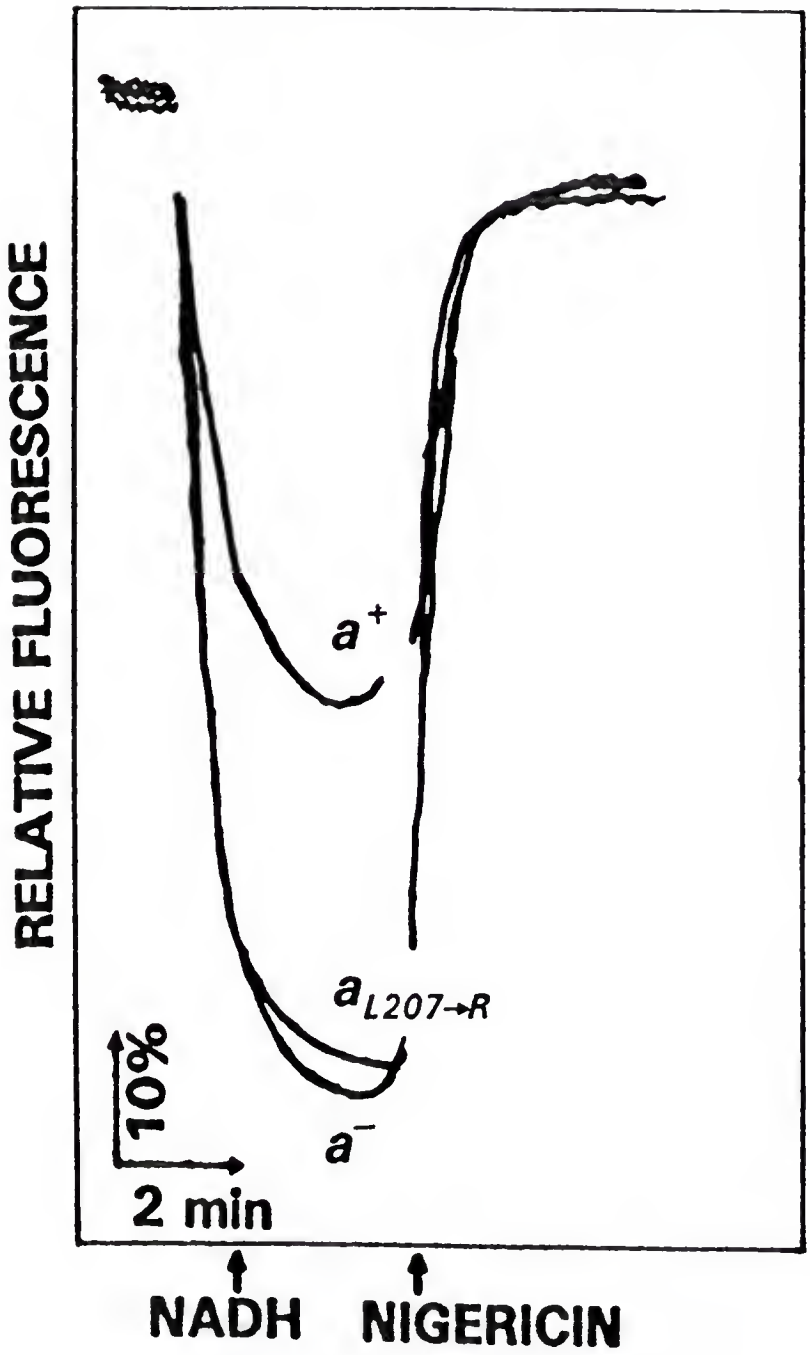

Figure 5-4. NADH driven ACMA fluorescence quenching of $a_{leu207\rightarrow arg}$ stripped vesicles. Arrows mark the addition of NADH (0.5 mM) and nigericin (0.05 μM). Traces: a^+, strain RH305 ($a_{uncB205}$) carrying plasmid pPH12 (a); a^-, strain RH305 ($a_{uncB205}$) carrying plasmid pPH11 (a_{del}); $a_{L207\rightarrow R}$, strain RH305 ($a_{uncB205}$) carrying plasmid pUNCB4.70 ($a_{L207\rightarrow R}$).

The $a_{L207\rightarrow P}$ Mutation

The recombinant plasmid pUNCB4.71 ($a_{L207\rightarrow P}$) was constructed via cassette site-directed mutagenesis in the same manner as plasmid pUNCB4.70 ($a_{L207\rightarrow R}$) (Chapter 2; Figure 5-2). Plasmid pUNCB4.71 ($a_{L207\rightarrow P}$) was transformed into strains PH105 (a_{del}) and RH305 ($a_{uncB205}$), and scored for growth on succinate minimal medium to test F_1F_0 ATP synthase function *in vivo*. The phenotype of plasmid pUNCB4.71 ($a_{L207\rightarrow P}$) depended on the strain in which it complemented. When plasmid pUNCB4.71 ($a_{L207\rightarrow P}$) was carried in strain PH105 (a_{del}), it demonstrated no growth on succinate minimal medium. However, when plasmid pUNCB4.71 ($a_{L207\rightarrow P}$) was carried in strain RH305 ($a_{uncB205}$), a partial phenotype of clearly smaller than wild-type colonies were observed (Table 5-2). The difference may have been due to the increased levels of the subunits in F_1F_0 ATP synthase found in strain RH305 ($a_{uncB205}$) over strain PH105 (a_{del}) (Chapter 3). Apparently, effects of the $a_{L207\rightarrow P}$ mutation were partially compensated for by increasing the levels of the other F_1F_0 ATP synthase subunits.

Biochemical analysis of the mutant plasmid pUNCB4.71 ($a_{L207\rightarrow P}$) in strain RH305 ($a_{uncB205}$) supported the conclusion of a partial phenotype. In contrast to plasmid pUNCB4.70 ($a_{L207\rightarrow R}$), plasmid pUNCB4.71 ($a_{L207\rightarrow P}$) carried in strain RH305 ($a_{uncB205}$) exhibited membrane bound F_1-ATPase activities significantly greater than the negative control plasmid

Table 5-2
Properties of the $a_{L207\rightarrow P}$ Mutation

Plasmid	Mutation	Growth on succinate[a] Strains PH105	RH305	ATPase specific activity[b] (μmol ATP/mg protein/min) Membrane bound	DCCD sensitive[c]
pPH12	a^+	+++	+++	1.40 ± .08	0.81 ± .06
pPH11	a^-	-	-	0.52 ± .35	0.06 ± .25
pUNCB4.71	$a_{L207\rightarrow P}$	-	+	1.13 ± .04	0.50 ± .06

[a]Growth on succinate was scored as colony formation and designated as wild-type colonies (+++), smaller than wild-type colonies (+) or no colonies (-).

[b]Specific activity was measured at pH 8.0 and the values are the average of two assays obtained at two protein concentrations. ATPase activity was assayed for the mutant plasmid transformed into strain RH305 ($a_{uncB205}$), and membrane vesicles prepared from these strains were washed one additional time in PSB as compared to Table 5-1 (Chapter 2).

[c]DCCD sensitive activity is the ATPase activity lost after treatment with 50 μM DCCD for one hour at room temperature.

pPH11 (a_{del}) carried in strain RH305 ($a_{uncB205}$) (Table 5-2). The DCCD sensitive activity for strain RH305 ($a_{uncB205}$)/plasmid pUNCB4.71 ($a_{L207\rightarrow P}$) was about 60% of the positive control strain RH305 ($a_{uncB205}$)/plasmid pPH12 (a) indicating lower amounts of coupled F_1F_0 ATP synthase on the membrane vesicles.

Membrane energization can be followed with the quenching of the fluorescent dye ACMA (Chapter 2). ATP-driven fluorescence quenching was observed with strain RH305 ($a_{uncB205}$)/plasmid pUNCB4.71 ($a_{L207\rightarrow P}$) (Figure 5-5) in contrast to strain RH305 ($a_{uncB205}$)/plasmid pUNCB4.70 ($a_{L207\rightarrow R}$) (Figure 5-3). Once again the activity of strain RH305 ($a_{uncB205}$)/plasmid pUNCB4.71 ($a_{L207\rightarrow P}$) was at an intermediate level compared to the wild type strain RH305 ($a_{uncB205}$)/plasmid pPH12 (a).

A functioning F_0 sector will partially collapse the proton-electrochemical gradient induced by the electron transport chain. Figure 5-6 shows that the wild-type strain RH305 ($a_{uncB205}$)/plasmid pPH12 (a) does partially neutralize ACMA quenching compared to the negative control strain RH305 ($a_{uncB205}$)/plasmid pPH11 (a_{del}). The surprising result is that mutant strain RH305 ($a_{uncB205}$)/plasmid pUNCB4.71 ($a_{L207\rightarrow P}$) does not significantly reduce NADH-driven ACMA quenching, and has an activity almost identical to the negative control strain RH305 ($a_{uncB205}$)/plasmid pPH11 (a_{del}). This is in contrast to the observations of the $a_{L207\rightarrow P}$ mutant with ATP-driven fluorescence quenching. A similar phenotype was seen with

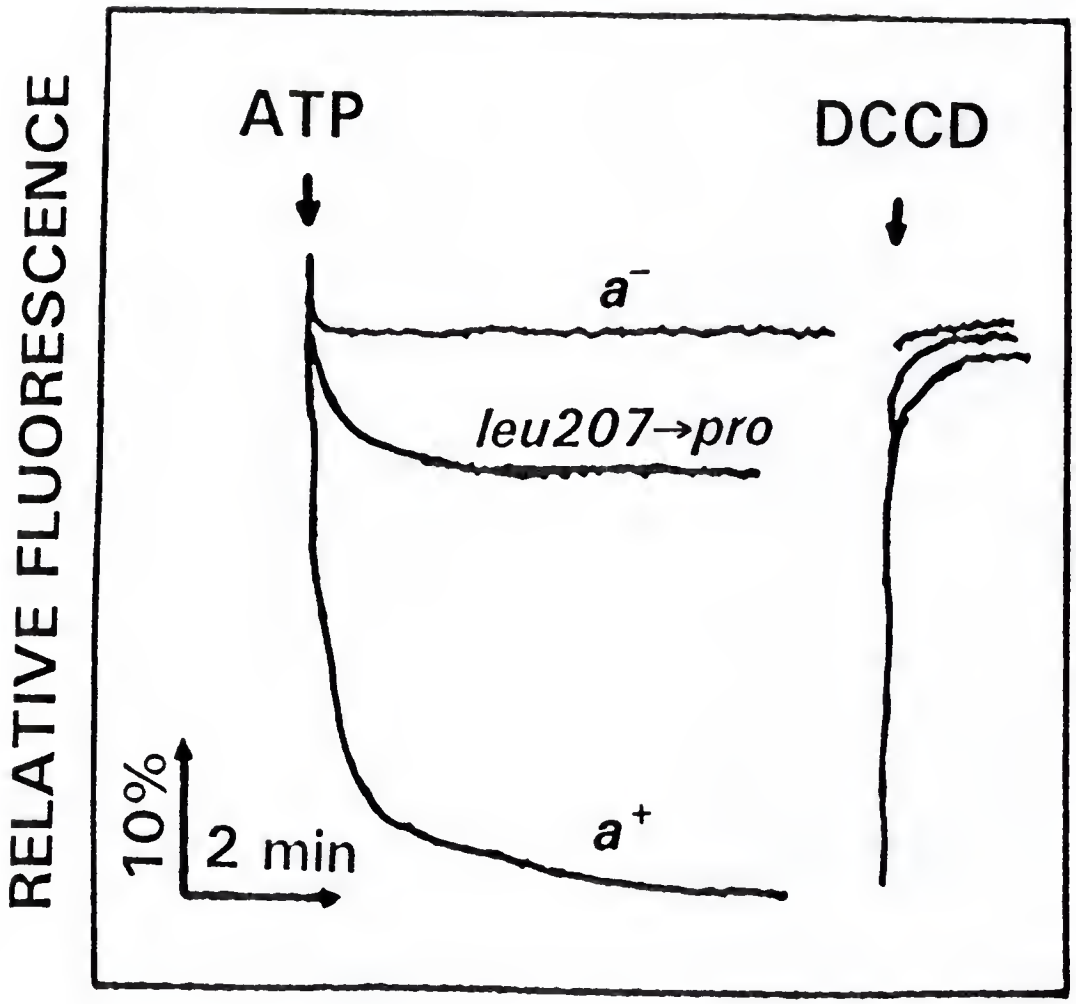

Figure 5-5. F_1F_0 ATP synthase mediated ATP-driven vesicle acidification for $a_{leu207\rightarrow pro}$. Vesicle acidification was followed by ACMA fluorescence quenching as described previously (Chapter 2). Membrane vesicles and assays were performed as described previously (Chapter 2). Arrows mark the addition of ATP (0.4 mM) and nigericin (0.05 μM). Traces: a^+, strain RH305 ($a_{uncB205}$) carrying plasmid pPH12 (a); a^-, strain RH305 ($a_{uncB205}$) carrying plasmid pPH11 (a_{del}); $a_{L207\rightarrow P}$, strain RH305 ($a_{uncB205}$) carrying plasmid pUNCB4.70 ($a_{L207\rightarrow P}$).

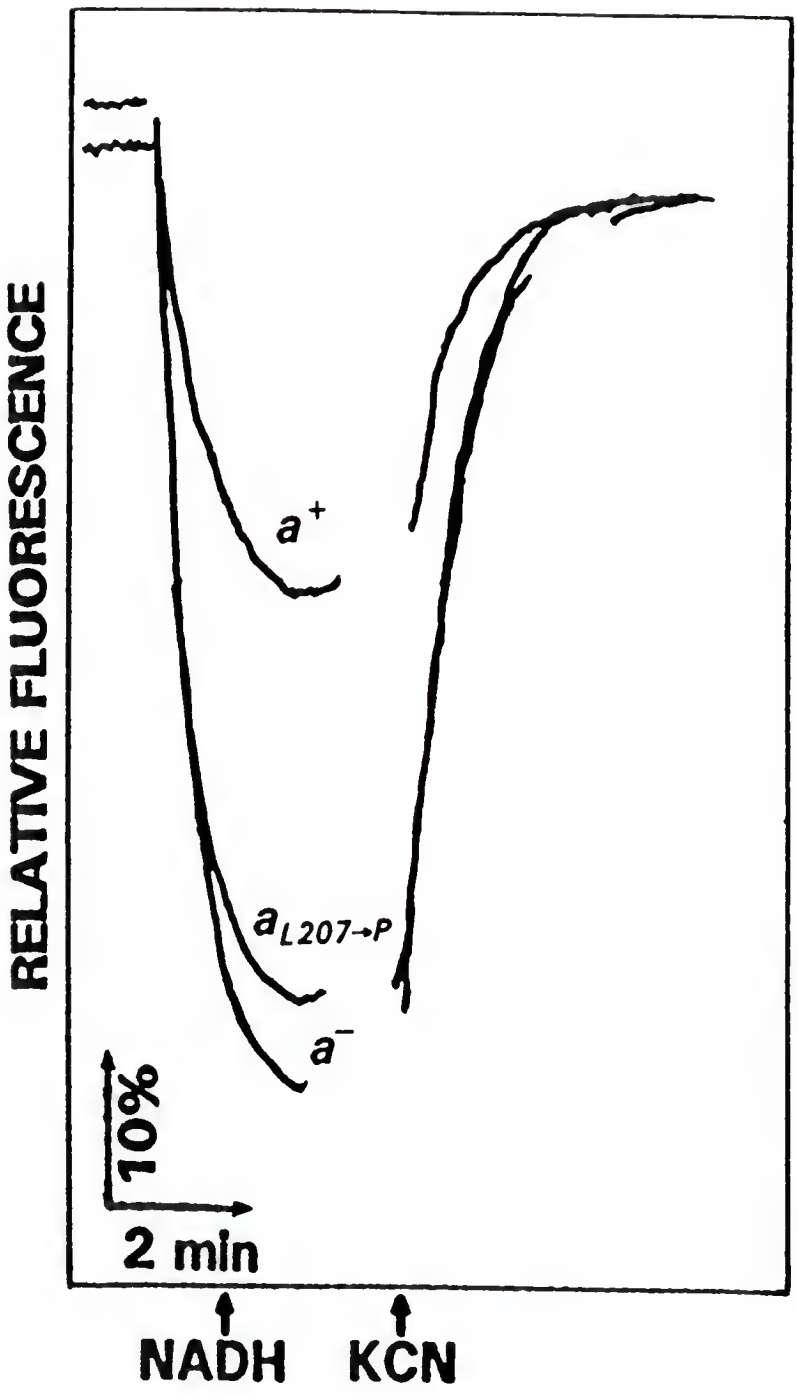

Figure 5-6. NADH driven ACMA fluorescence quenching of $a_{leu207 \rightarrow pro}$ stripped vesicles. Arrows mark the addition of NADH (0.5 mM) and KCN (0.5 mM). Traces: a^+, strain RH305 ($a_{uncB205}$) carrying plasmid pPH12 (a); a^-, strain RH305 ($a_{uncB205}$) carrying plasmid pPH11 (a_{del}); $a_{L207 \rightarrow P}$, strain RH305 ($a_{uncB205}$) carrying plasmid pUNCB4.71 ($a_{L207 \rightarrow P}$).

mutants in Chapter 4 and interpreted to indicate structural instability.

The loss of F_O-proton translocation activity was further investigated by Western analysis of the *b* subunit. Figure 5-7 shows no loss of the *b* subunit between expression from the mutant plasmid pUNCB4.71 ($a_{L207\rightarrow P}$) and expression from the control plasmids, whether the membrane vesicles were isolated with F_1 or without. The slightly higher levels seen in stripped membranes was due to the removal of membrane associated proteins , which increases the ratio of F_O subunits to the total membrane protein concentration. The Western analysis demonstrates that the F_O subunits (followed by the *b* subunit) are still present in the F_1 depleted membranes, indicating the loss of proton conductance in the mutant $a_{L207\rightarrow P}$ is due to a destabilization of the F_O complex with the loss of the F_1 sector.

In summary it appears that the $a_{L207\rightarrow P}$ mutation blocks proton translocation by destabilizing the F_O sector. It also appeared that the destabilization of the F_O sector may be compensated for by increasing the levels of the F_1 sector of F_1F_O ATP synthase. This was demonstrated by the ability of the ability of the mutant plasmid pUNCB4.71 ($a_{L207\rightarrow P}$) to complement strain RH305 ($a_{uncB205}$) on succinate minimal medium, but not strain PH105 (a_{del}) which has been shown to have lower levels of F_1F_O ATP synthase (Chapter 3). The amount of F_1 present is apparently affects the stability of the

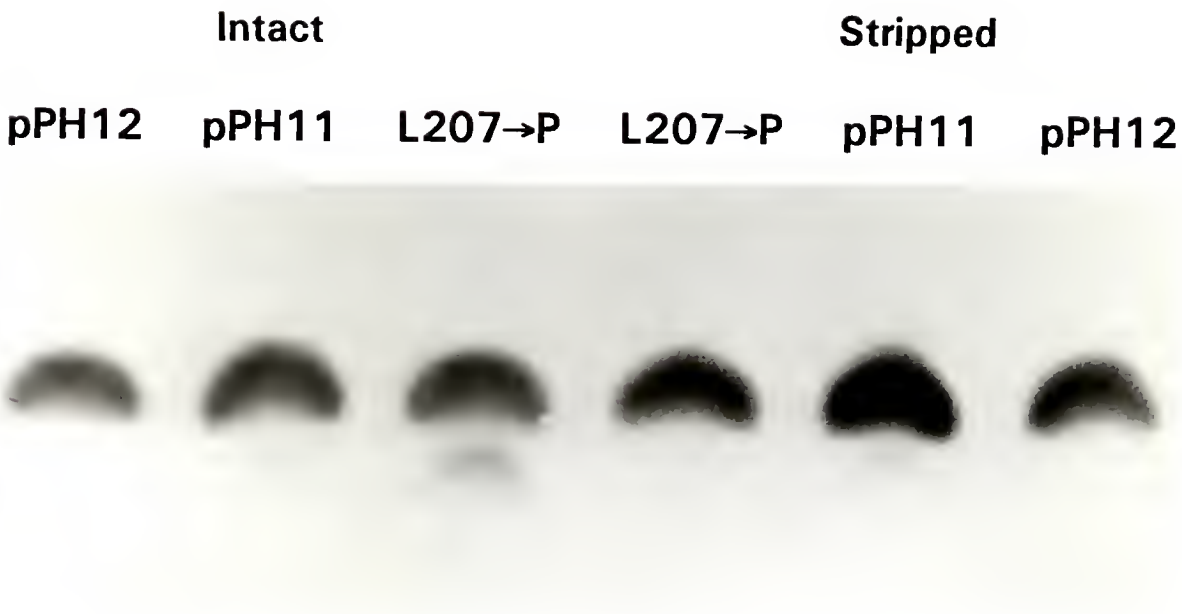

Figure 5-7. Western Analysis of $a_{L207\rightarrow P}$ comparing intact verses stripped vesicles. pPH12, strain RH305 ($a_{uncB205}$) carrying plasmid pPH12 (a); pPH11, strain RH305 ($a_{uncB205}$) carrying plasmid pPH11 (a_{del}); L207→P, strain RH305 ($a_{uncB205}$) carrying plasmid pUNCB4.71 ($a_{L207\rightarrow P}$). $a_{L207\rightarrow P}$ mutation. This is supported by NADH-driven fluorescence quenching, where the dissociation of the F_1 sector from the $a_{L207\rightarrow P}$ mutant F_O sector results in a loss of the ability to transport protons observed in ATP-driven fluorescence quenching.

Discussion

The results indicate that the $a_{L207\rightarrow R}$ mutation is sufficient to abolish detectable F_1F_0 ATP synthase function in *E. coli*. The biochemical basis for the defect is a failure in F_0-mediated proton translocation resulting from a structural perturbation in the enzyme complex. The most likely mechanism of the structural perturbation is a charge repulsion between the arginine substitution at a_{L207} and the wild-type arginine at amino acid position a_{210}. This potential charge repulsion probably results in a defect in the folding of the *a* subunit. The folding defect results in a failure to assemble F_1F_0 ATP synthase.

The structural and functional similarities between *E. coli* and mitochondrial F_1F_0 ATP synthases suggests that both share a common molecular mechanism, and that observations in the bacterial system are directly applicable to mutations occurring in the human enzyme. Therefore, the phenotype of the $a_{L207\rightarrow R}$ mutation observed here in *E. coli* implies that the human *ATPase* $6_{L156\rightarrow R}$ mutation linked to NARP and maternally inherited Leigh's syndrome also results in a similar defect in F_1F_0 ATP synthase leading to a failure of OXPHOS. The fact that Tatuch and Robinson (1993) were unable to see complete loss of F_1F_0 ATP synthase activity in the cell line they used demonstrates the limitations of a hybrid system that has copies of the wild-type enzyme present.

The $a_{L207\rightarrow P}$ mutation had a more subtle phenotype than exhibited by the $a_{L207\rightarrow R}$ mutation. The ability of the $a_{L207\rightarrow P}$ mutation to reduce F_1F_O ATP synthase function is apparently dependent on the concentration of F_1 in *E. coli*. The ability of increased levels of expression to compensate for mutations in F_O has been reported previously (McCormick *et al.*, 1993), and that F_1 plays a role in assembling F_O has been suggested previously (Cox *et al.*, 1984). The implications of this phenotype on human mitochondrial disease is discussed in Chapter 7. The phenotype observed in *E. coli* indicates that this alternate NARP mutation reduces the efficiency of F_1F_O ATP synthase without completely abolishing the enzymes activity.

Studies of the *E. coli* F_1F_O ATP synthase *a* subunit have indicated that many positions are sensitive to missense mutations (Cain & Simoni, 1986, 1988, 1989; Lightowlers *et al.*, 1987, 1988; Howitt *et al.*, 1988; Vik *et al.*, 1988, 1990, 1991; Eya *et al.*, 1988, 1991; Paule & Fillingame, 1989; see also Chapters 4 and 6). Mutations replacing the conserved amino acids in the *a* subunit with basic amino acids, such as occurs with the human *ATPase* $6_{L156\rightarrow R}$ mutation, frequently resulted in substantial losses of enzyme function (Cain & Simoni, 1988, 1989; Vik *et al.*, 1991; Chapter 4). Similar mutations undoubtedly occur in the human mitochondrial *ATPase 6* gene at positions other than a_{L156}, implying that a large number of point mutations in the conserved region of *ATPase 6* should be sufficient for significant losses in capacity for

synthesis of ATP. Recently, mutations in mtDNA have also been linked to degenerative diseases associated with aging (Wallace, 1992a). Given that the mutation rate is ten-to-twenty-fold higher in mtDNA as compared to the nuclear genome (Wallace, 1992b), missense mutations in the *ATPase 6* gene are likely to be among the most common mutations affecting human F_1F_0 ATP synthase.

Point mutations affecting the *ATPase 6* gene are likely to remain undiagnosed in the clinical setting making it difficult to assess the contributions of these defects to degenerative disease. NARP patients do not display the gross mitochondrial abnormalities or the lactate imbalances characteristic of mitochondrial genetic diseases associated with electron transport deficiencies (Holt *et al.*, 1990). Other *ATPase 6* gene mutations, whether inherited or arising through somatic mutation, will probably exhibit a similar pathology. Additionally, most point mutations in the *ATPase 6* gene can not be expected to change a restriction endonuclease recognition sequence, so RFLP analysis will not suffice as a definitive diagnostic approach.

CHAPTER 6
SECOND SITE SUPPRESSOR MUTATIONS

Introduction

The primary structures of chloroplast CF_OIV and alkaliphilic bacterial *a* subunits both display variance from the mitochondrial *ATPase-6* and *E. coli a* subunit at positions homologous to a_{G218}, a_{E219} and a_{H245}. This chapter details the construction of double mutations in the *E. coli uncB (a)* gene modeled after the chloroplast and *Bacillus firmus* F_1F_O ATP synthases. Both pairs of mutations are shown to be mutually suppressing mutations. The double mutants displayed growth characteristics near wild-type levels and substantial enzyme activity *in vitro*. In view of the different physiological environments that the enzymes occupy in nature and the variations in primary sequence at the three positions, the possibility exists that the model enzymes might have different properties with respect to proton translocation. The single mutations displayed phenotypes that indicated that these sites may be involved in the mechanism of coupling proton translocation to ATP catalysis.

Results

Construction of Mutants

The comparable positions occupied by a_{G218}, a_{E219} and a_{H245} in *E. coli* F_1F_0 ATP synthase displayed a possible example of co-variance during evolution (Figure 6-1). In order to model the possible functional relationship between these amino acids, site-directed mutagenesis of the *uncB (a)* gene was used to construct plasmids pUNCB5.43 ($a_{G218\rightarrow D,H245\rightarrow G}$) and pUNCB5.43 ($a_{G218\rightarrow K,H245\rightarrow G}$) reflecting the motifs found in the primary structures of all reported chloroplast CF_0IV subunits and the *B. firmus a* subunit, respectively. In addition, the three single mutation plasmids pUNCB5.40 ($a_{G218\rightarrow D}$), pUNCB5.40 ($a_{G218\rightarrow K}$) and pUNCB5.43 ($a_{H245\rightarrow G}$) were constructed to determine the effects of each of the individual mutations (Table 6-1). Chapter 2 details the mutagenesis techniques used.

Growth Characteristics of Mutants

The *uncB (a)* gene mutation plasmids and the control plasmids pPH12 (*a*) and pPH11 (a_{del}) were transformed into *uncB (a)* chromosomal mutation strain PH105 (a_{del}). Colony formation on non-fermentable carbon sources and growth yield in limiting glucose media were studied in strain PH105 (a_{del}) as measures of OXPHOS, *in vivo* (Table 6-2). Strain PH105(a_{del})/pUNCB5.41 ($a_{G218\rightarrow K}$) exhibited growth characteristics comparable to PH105(a_{del})/pPH11 (a_{del}) indicating that F_1F_0 ATP

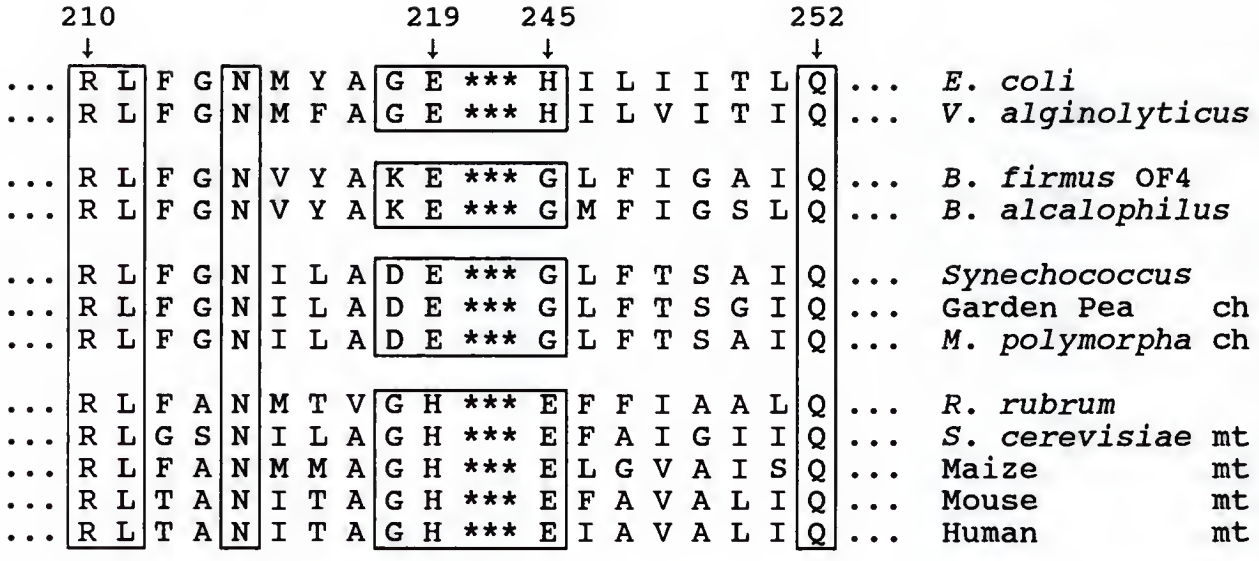
210
219
245
252
... R L F G N M Y A G E *** H I L I I T L Q ... E. coli
... R L F G N M F A G E *** H I L V I T I Q ... V. alginolyticus
... R L F G N V Y A K E *** G L F I G A I Q ... B. firmus OF4
... R L F G N V Y A K E *** G M F I G S L Q ... B. alcalophilus
... R L F G N I L A D E *** G L F T S A I Q ... Synechococcus
... R L F G N I L A D E *** G L F T S G I Q ... Garden Pea ch
... R L F G N I L A D E *** G L F T S A I Q ... M. polymorpha ch
... R L F A N M T V G H *** E F F I A A L Q ... R. rubrum
... R L G S N I L A G H *** E F A I G I I Q ... S. cerevisiae mt
... R L F A N M M A G H *** E L G V A I S Q ... Maize mt
... R L T A N I T A G H *** E F A V A L I Q ... Mouse mt
... R L T A N I T A G H *** E I A V A L I Q ... Human mt

Figure 6-1. Alignment of the sequence variations seen at a_{G218}, a_{E219}, and a_{H245}. Numbers above denote amino acid position in the a subunit of *E. coli*. The *** symbol represents a varying number of amino acids that separate the two positions aligned. For more details see Chapter 1, Figure 1-3.

Table 6-1
Mutations Generated in the *uncB* (*a*) Gene

Oligonucleotide /Primer[a]	Plasmid	Mutant codons	Mutation
151/149	pUNCB5.40	GAC	$a_{G218 \rightarrow D}$
	pUNCB5.41	AAG	$a_{G218 \rightarrow K}$
	pUNCB5.42	GGA	$a_{H245 \rightarrow G}$
150/135	pUNCB5.43	GAC/GGA	$a_{G218 \rightarrow D,H245 \rightarrow G}$
	pUNCB5.44	AAG/GGA	$a_{G218 \rightarrow K,H245 \rightarrow G}$

[a]Oligonucleotide cassette site-directed mutagenesis was used to construct plasmid pUNCB5.40 ($a_{G218 \rightarrow D}$) and plasmid pUNCB5.41 ($a_{G218 \rightarrow K}$) from plasmid pBDC26 ($a_{L207 \rightarrow W,E219 \rightarrow K}$) (Chapter 2; Figure 5-2). A mutagenic primer (150) was used with a non-mutagenic (135) primer to construct the plasmids pUNCB5.42 ($a_{H245 \rightarrow G}$), pUNCB5.43 ($a_{G218 \rightarrow D,H245 \rightarrow G}$), and pUNCB5.44($a_{G218 \rightarrow K,H245 \rightarrow G}$) by PCR directed mutagenesis (Chapter 2).

Table 6-2
Growth Properties of Mutant Strains

Plasmid	Mutation	Growth on succinate[a] 37°C	42°C	Anaerobic Growth[b]	Growth Yield[c]
pPH12	wild-type	+++	+++	+++	98 ± 3
pUNCB5.44	$a_{G218\rightarrow K,H245\rightarrow G}$	+++	+++	+++	93 ± 3
pUNCB5.43	$a_{G218\rightarrow D,H245\rightarrow G}$	+++	+++	+++	89 ± 3
pUNCB5.42	$a_{H245\rightarrow G}$	+	-	+++	74 ± 3
pUNCB5.40	$a_{G218\rightarrow D}$	±	-	+++	73 ± 3
pUNCB5.41	$a_{G218\rightarrow K}$	-	-	+++	65 ± 3
pPH11	a_{del}	-	-	±	64 ± 3

[a]Colony size after 48 hrs of incubation at the indicated temperatures on solid succinate (0.2% w/v) minimal medium A. Growth was scored as normal colonies (+++) comparable to the wild type control strain, smaller than normal colonies (+), barely visible colonies that didn't appear till after 48 hrs (±) and no visible colonies (-).

[b]Anaerobic growth at 37°C for 48 hrs on glucose minimal medium.

[c]Growth yield in 5mM glucose minimal medium A monitored turbidimetrically using a Klett-Summerson colorimeter.

synthase was defective. Plasmids pUNCB5.40 ($a_{G218\rightarrow D}$) and pUNCB5.42 ($a_{H245\rightarrow G}$) partially complemented PH105 (a_{del}) allowing development of small colonies on succinate medium plates and intermediate densities in limiting glucose medium. Clearly, all three mutations were sufficient to impair enzyme activity. In contrast, growth of PH105 (a_{del}) strains carrying either of the double mutation plasmids pUNCB5.43 ($a_{G218\rightarrow D,H245\rightarrow G}$) or pUNCB5.44 ($a_{G218\rightarrow K,H245\rightarrow G}$) were similar to the wild-type control strain indicating that both pairs of mutations allowed abundant F_1F_0 ATP synthase activity. Some *uncB (a)* mutations have shown temperature-sensitive phenotypes, so growth on succinate was also determined following incubation at 42°C (Chapter 4). Results of these experiments were essentially the same as growth at 37°C with the exception that plasmids pUNCB5.40 ($a_{G218\rightarrow D}$) and pUNCB5.42 ($a_{H245\rightarrow G}$) supported no apparent growth of strain PH105 (a_{del}).

The chloroplast F_1F_0 ATP synthase translocates protons from a very acidic environment (pH 5) in the lumen of the thylakoid membrane, and the *B. firmus* enzyme functions under conditions of extreme alkalinity (pH 10). Therefore, we considered the possibility that the different motifs in each enzyme contributed to the adaptations necessary for F_1F_0 ATP synthases to operate under widely varying pH conditions. Aerobic growth of *E. coli* at pH 6.0 results in ΔpH exhibiting its largest contribution relative to $\Delta\psi$ in the proton motive force ($\Delta\mu_H^+$). The smallest contribution of

ΔpH relative to $\Delta\mu_H^+$ can be obtained in the pH range 7.46-7.65 (Padan *et al.*, 1976, Felle *et al.*, 1980). Therefore, growth yields in limiting glucose minimal medium at pH 6.0 and pH 7.54 were determined for strains PH105 (a_{del})/pUNCB5.43 ($a_{G218\rightarrow D,H245\rightarrow G}$) and PH105 ($a_{del}$)/pUNCB5.44 ($a_{G218\rightarrow K,H245\rightarrow G}$). Both strains had growth properties similar to the control strain expressing a normal *uncB* (*a*) gene.

In the course of these experiments and routine monitoring of growth phenotypes of cultures used for biochemical analyses, it became clear that strains harboring plasmids pUNCB5.41 ($a_{G218\rightarrow K}$) and pUNCB5.40 ($a_{G218\rightarrow D}$) were prone to generate revertant strains with improved growth characteristics. In one case, membrane vesicles were prepared from a strain derived from an apparent reversion of PH105 (a_{del})/pUNCB5.40 ($a_{g218\rightarrow D}$). These membranes had biochemical properties virtually identical to membranes from PH105 (a_{del})/pUNCB5.43 ($a_{G218\rightarrow D,H245\rightarrow G}$) and distinct from positive control membranes (data not shown). Although the secondary mutation in the revertant strain has not been identified, we submit that the reversion frequency may be related to second-site suppression from substitutions at the three positions occupied by a_{G218}, a_{E219} and a_{H245}.

Effects on Assembly of F_1F_0 ATP Synthase

The amount of F_1 ATP hydrolysis activity associated with the membrane was studied as an preliminary indication of the amount of assembled F_1F_0 ATP synthase present in

cells. The *uncB (a)* mutation plasmids were transformed into RH305 ($a_{uncB205}$) and membrane vesicles prepared under conditions of low ionic strength in the presence of p-aminobenzamidine. This preparation allowed F_1 bound in the F_1F_0 ATP synthase complex to remain associated with the membrane vesicles, while non-specifically bound F_1 was stripped from the membrane vesicles (Chapter 2). Membranes derived from strains with double mutation plasmids possessed amounts of ATP hydrolysis activity comparable to RH305 ($a_{uncB205}$)/pPH12 (*a*) (Table 6-3). However, membranes from cells carrying either plasmid pUNCB5.42 ($a_{H245\rightarrow G}$) or plasmid pUNCB5.41 ($a_{G218\rightarrow K}$) displayed a 20% reduction in F_1 activity. Measuring the quantity of ATP hydrolysis activity was not a useful measure of F_1F_0 ATP synthase complexes for RH305 ($a_{uncB205}$)/pUNCB5.40 ($a_{G218\rightarrow D}$), because the substitution increased ATP hydrolysis activity (Table 6-3). The increased activity was insensitive to LDAO (0.4 %) activation (Lötscher *et al.*, 1984) of ATP hydrolysis suggesting that the amino acid substitution is activating ATPase activity by affecting the ϵ subunit (data not shown).

Since ATPase activity appeared to be altered for strain RH305 ($a_{uncB205}$)/pUNCB5.40 ($a_{G218\rightarrow D}$), the amount of F_0 *b* subunit was determined as an alternative measure of F_1F_0 ATP synthase complex present in the membrane vesicles. The *b* subunit is stabilized in intact F_1F_0 ATP synthase complexes, so the signal obtained using anti-*b* antibodies in immunoblot

Table 6-3
Biochemical Properties of Mutant Strains

Plasmid	Mutation	ATPase Specific Activity[a] Membrane Bound	ATPase Specific Activity[a] DCCD Sensitive[b]	ACMA Quenching[c] ATP	ACMA Quenching[c] NADH
pPH12	wild-type	1.40±.08	0.81±.06	37%	26%
pUNCB5.44	$a_{G218\rightarrow K,H245\rightarrow G}$	1.21±.03	0.63±.03	29%	28%
pUNCB5.43	$a_{G218\rightarrow D,H245\rightarrow G}$	1.35±.03	0.71±.03	16%	32%
pUNCB5.42	$a_{H245\rightarrow G}$	1.06±.01	0.50±.01	5%	38%
pUNCB5.40	$a_{G218\rightarrow D}$	2.42±.17	1.88±.13	10%	20%
pUNCB5.41	$a_{G218\rightarrow K}$	1.08±.12	0.48±.09	<1%	38%
pPH11	a_{del}	0.52±.35	0.06±.25	<1%	47%

[a]Specific activity = μmol ATP hydrolyzed/mg protein/min determined at pH 8.0. Values are the average of two assays done at two different protein concentrations.

[b]DCCD sensitive activity = specific activity lost after treatment with 50 μM DCCD for one hour at room temperature.

[c]ACMA quenching as measured from Figure 6-3. Values denote percentage of relative fluorescence. Membranes derived from strains carrying plasmid pUNCB5.40 ($a_{G218\rightarrow D}$) for ATP driven quenching and plasmid pUNCB5.41 ($a_{G218\rightarrow K}$) for NADH driven quenching were done in a separate experiment so are standardized to the membranes from strains carrying the wild-type plasmid pPH12 (*a*).

analyses was used to follow complex assembly (Figure 6-2). With the exception of a small reduction in signal observed in membranes derived from strains with plasmid pUNCB5.41 ($a_{G218\rightarrow K}$), the amount of *b* subunit was comparable in membranes from both mutants and wild-type controls. Plasmid pPH11, the negative control, also displays the same amount of *b* subunit present. The stabilization of the *b* subunit by the truncated *a* subunit from strain RH305 was observed earlier (Chapter 3). The background of strain RH305 limits the Western analysis of the F_1F_O ATP synthase complex via the *b* subunit. However, the observation that the *b* subunit is not increased compared to wild-type along with the fact that the increased activity of the $a_{G218\rightarrow D}$ mutant is DCCD sensitive, indicates that there is not an increased amount of enzyme complex present.

Both the levels of membrane-associated F_1 ATP hydrolysis activity and the amount of F_O *b* subunit in the membranes indicated that the *a* subunits with the $a_{G218\rightarrow D}$, $a_{G218\rightarrow K}$ and $a_{H245\rightarrow G}$ substitutions participate in assembly of F_1F_O ATP synthase. Therefore, the losses in enzyme function observed in growth studies of these mutants was not attributable to failure in enzyme assembly, but rather to the formation of inactive F_1F_O ATP synthase complexes. Membranes from strains with the double mutations appeared to be normal with respect to the number of F_1F_O ATP synthase complexes.

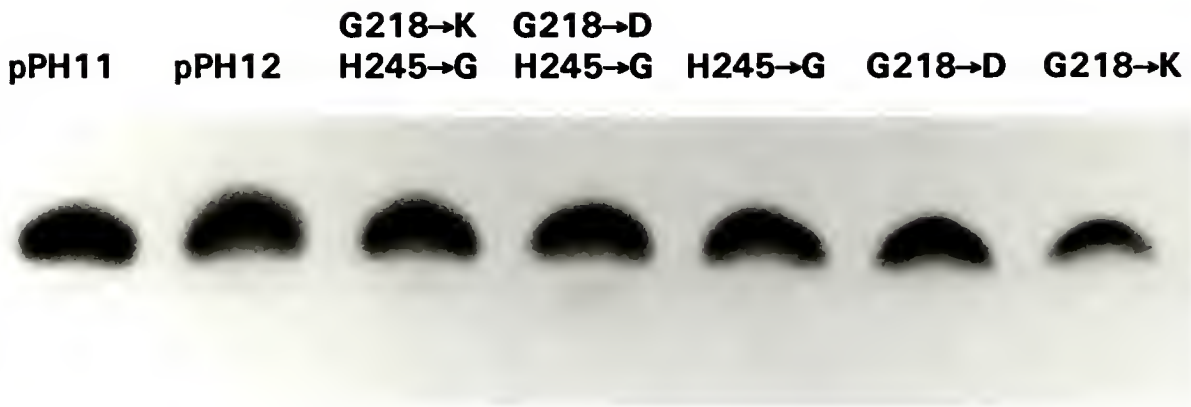

Figure 6-2. Western analysis of mutant strains. Stripped membranes prepared from mutant strains were used for immunoblotting with anti-*b* antibody. The *a* subunit mutation(s) are listed above each lane. pPH12 (*a*) denotes wild-type. pPH11 (a_{del}) denotes strain RH305 ($a_{uncB205}$) background.

Effects on Proton Translocation

The most likely causes for the losses of F_1F_O ATP synthase activity were defects in proton translocation. ATP-driven ACMA fluorescence quenching was used to assay F_1F_O ATP synthase-mediated proton pumping in membranes vesicles prepared from the *uncB* (a) mutants.

Membranes derived from strain RH305 ($a_{uncB205}$)/pUNCB5.41 ($a_{G218\rightarrow K}$) had no significant ATP-driven proton translocation (Figure 6-3). This indicated that the $a_{G218\rightarrow K}$ substitution was sufficient to virtually abolish active proton translocation. Limited proton pumping activity was detected in membranes from the cells with pUNCB5.43 ($a_{H245\rightarrow G}$) (Figure 6-3). Inclusion of both the $a_{G218\rightarrow K}$ and $a_{H245\rightarrow G}$ mutations in the *uncB* (*a*) gene resulted in a dramatic restoration of proton pumping activity. Membranes from strain RH305 ($a_{uncB205}$)/pUNCB5.44 ($a_{G218\rightarrow K,H245\rightarrow G}$) had more than 75% of the activity observed in the strain RH305 ($a_{uncB205}$)/pPH12 (*a*) membranes. Although the increase in activity was less, the membranes from strain RH305 ($a_{uncB205}$)/pUNCB5.44 ($a_{G218\rightarrow D,H245\rightarrow G}$) also showed convincing evidence of the phenotypic suppression resulting from the two amino acid substitutions (Figure 6-3). In all membrane preparations in which ATP-driven proton translocation observed, treatment of F_1F_O ATP synthase with DCCD under conditions which were expected to specifically modify the *c* subunit fully inhibited activity.

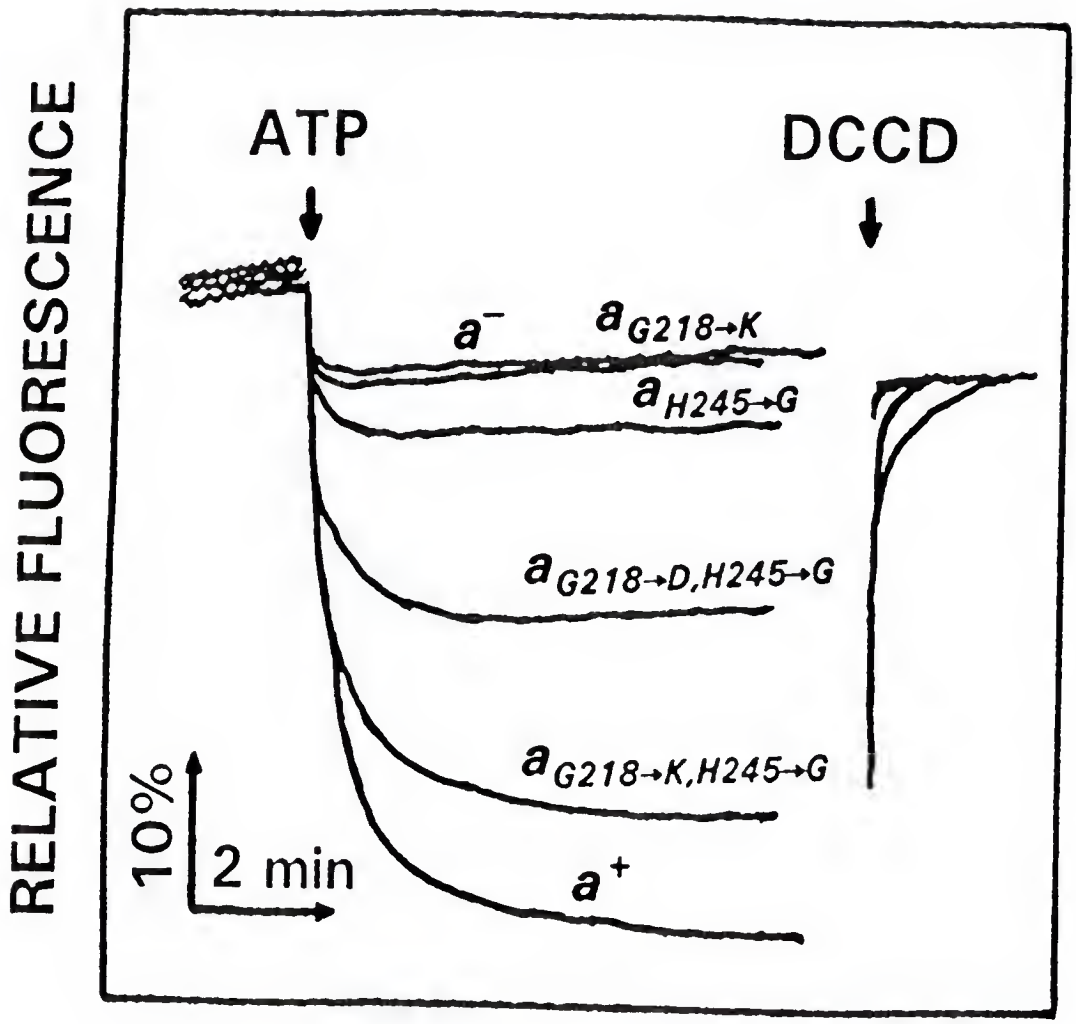

Figure 6-3. ATP driven energization of membrane vesicles determined by ACMA. ACMA was added to a final concentration of 1 μM, and membrane vesicles were at a concentration of 150 μg of protein/mls buffer [50 mM Tris-HCl and 10 mM $MgCl_2$, pH 7.5]. The reagents were added to final concentrations of: ATP 0.5 mM; DCCD 100 μM. The *a* subunit mutation is listed above the trace and carried by plasmid (see Table 6-1) in strain RH305 ($a_{uncB205}$).

Normally, F_O functions as a passive proton pore in the absence of F_1, and the capacity to collapse an imposed proton gradient was used to measure loss of proton translocation in mutant F_O. F_1 was stripped from membrane vesicles and NADH-driven ACMA fluorescence quenching followed to monitor passive proton translocation. The range of NADH-driven fluorescent quenching was established by assaying membranes from the strains carrying the control plasmids pPH11 (a_{del}) or pPH12 (*a*) (Table 6-3; Figure 6-4). Mutant plasmids pUNCB5.44 ($a_{G218\rightarrow K,H245\rightarrow G}$), pUNCB5.43 ($a_{G218\rightarrow D,H245\rightarrow G}$), and surprisingly, pUNCB5.40 ($a_{G218\rightarrow D}$) exhibited passive proton conductance at wild-type levels. The mutant plasmids pUNCB5.42 ($a_{H245\rightarrow G}$) and pUNCB5.41 ($a_{G218\rightarrow K}$) (not shown in figure) displayed NADH-driven fluorescence quenching at intermediate levels between the control values. The reduction in the efficiency of proton conductance exhibited by mutant plasmids pUNCB5.42 ($a_{H245\rightarrow G}$) and pUNCB5.41 ($a_{G218\rightarrow K}$) reflected the reductions in DCCD sensitive ATPase activity for these two mutant plasmids (Table 6-3).

In general, the data suggested that each of the single mutants were assembling F_O capable of at least limited proton conductance. This was true of cells with plasmid pUNCB5.41 ($a_{G218\rightarrow K}$) which exhibited neither ATP-driven proton translocation nor growth on succinate-based medium. The results from studies of the $a_{G218\rightarrow K}$ mutation was even more unusual for an *uncB* (*a*) gene mutation. Passive proton

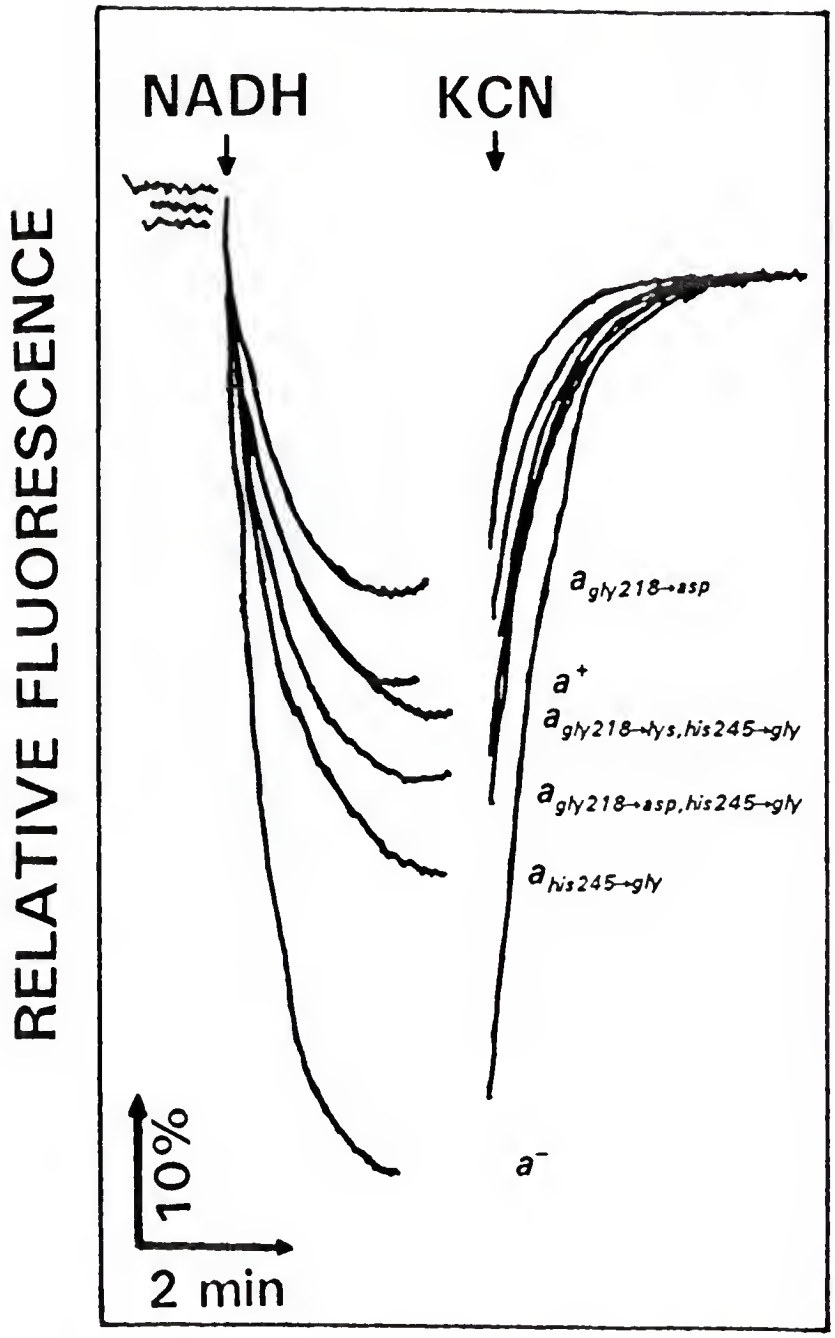

Figure 6-4. NADH driven energization of stripped membrane vesicles determined by ACMA. ACMA was added to a final concentration of 1 μM, and membrane vesicles were at a concentration of 50 μg of protein/mls buffer [50 mM Tris-HCl and 10 mM $MgCl_2$, pH 7.5]. Arrows mark the addition of reagents at the final concentrations of: NADH 0.1 mM; KCN 0.5 mM. The *a* subunit mutation is listed beside the trace and carried by plasmid (see Table 6-1) in strain RH305 ($a_{uncB205}$).

translocation in stripped membranes and high F_1 ATP hydrolysis in intact membrane vesicles suggested that the substitution resulted in a partial uncoupling of F_O and F_1 activities in the enzyme complex.

Effects of pH and ATP on Proton Pumping

ATP driven proton pumping was also assayed under differing pH conditions. The fluorescence properties of ACMA did not significantly change over the pH range used (data not shown). However, the ability of wild-type F_1F_O ATP synthase to actively transport protons decreased as the pH was raised from 7.25 to 8.5 (Figure 6-5). However, an increase in F_1F_O-ATPase activity was observed over this pH range (Cain & Simoni, 1989). The data suggested that raising the pH uncouples proton translocation from ATP hydrolysis.

Reducing the ATP concentration also reduced the amount of F_1F_O-mediated proton transport. It was observed that the initial slope of the ACMA fluorescence trace coorelated with the eventual fluorescence equilibrium reached under the varying ATP concentrations (Figure 6-6A). The initial slope of the fluoresence trace was designated the change in relative fluoresence per minute (ΔRF/min) and was plotted verses the ATP concentration that generated the fluorescence quenching. The $a_{G218\rightarrow K,H245\rightarrow G}$ and $a_{G218\rightarrow D,H245\rightarrow G}$ double mutants were assayed under varying ATP concentrations and compared to a wild-type *a* subunit (Figure 6-6B). While the double mutants

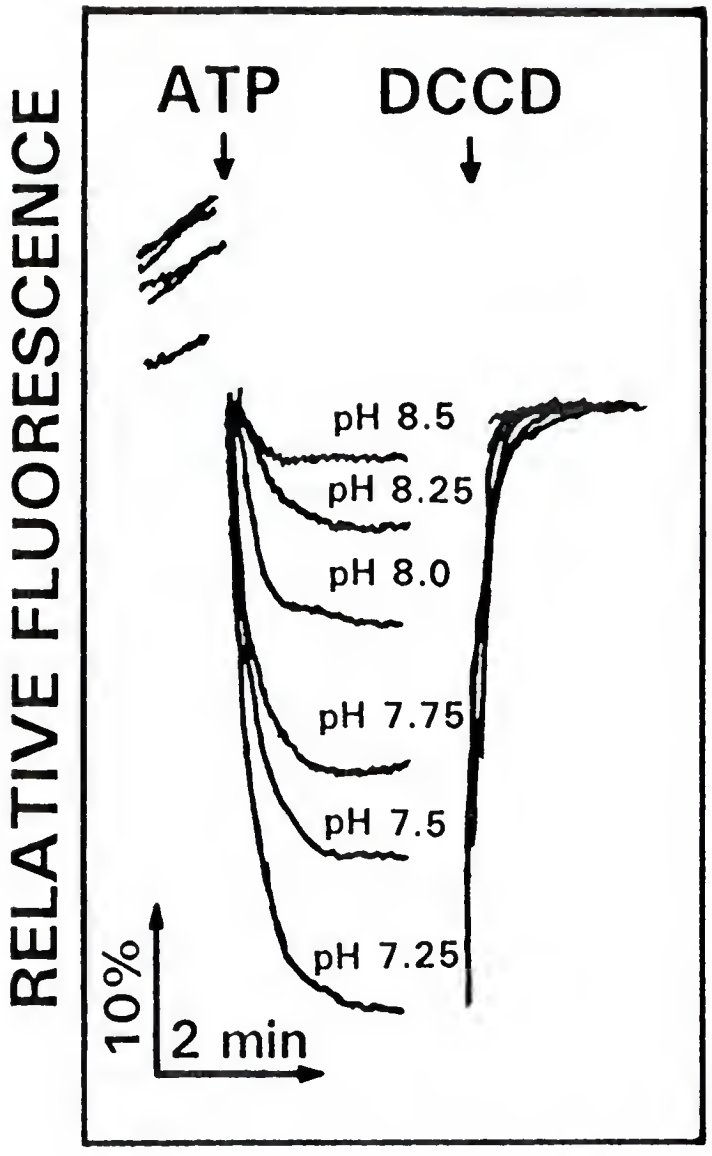

Figure 6-5. ATP driven energization of membrane vesicles under different pH conditions. ACMA was added to a final concentration of 1 μM, and membrane vesicles were at a concentration of 150 μg of protein/mls buffer [50 mM Tris-HCl and 10 mM $MgCl_2$] and the pH listed above the trace. The reagents were added to final concentrations of: ATP 30 μM; DCCD 100 μM. The membrane vesicles were prepared from strain RH305 ($a_{uncB205}$) carrying plasmid pPH12 (*a*) and considered to contain a wild-type F_1F_O ATP synthase.

A

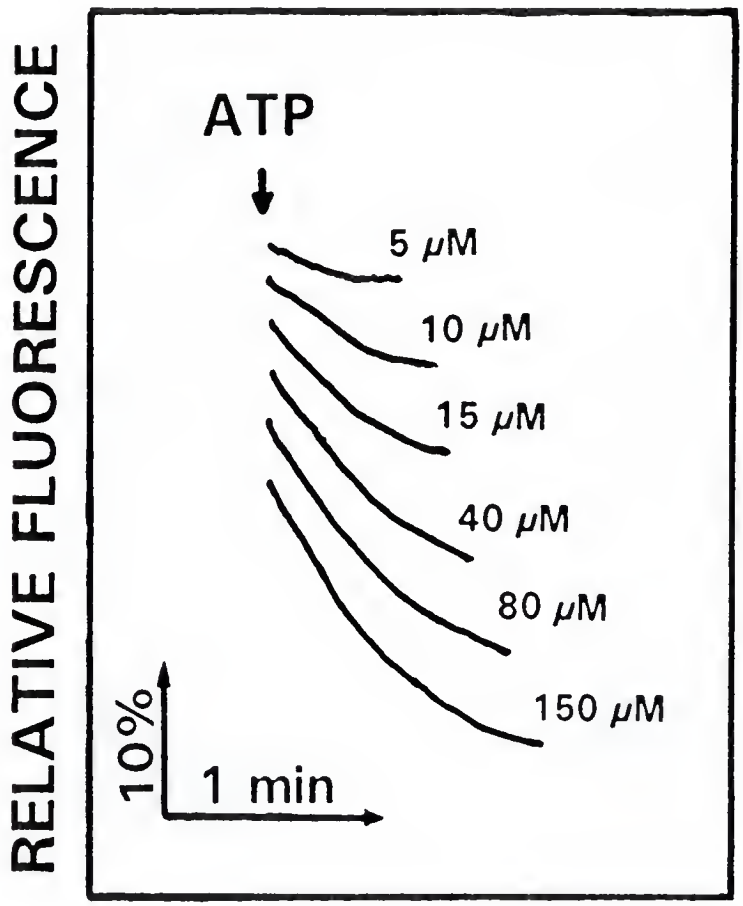

Figure 6-6. ATP driven energization of membrane vesicles under different ATP concentrations. ATP driven ACMA fluoresence quenching was assayed at 150 μg membrane protein/ml buffer [50 mM Tris-HCl and 10 mM $MgCl_2$, pH 7.2]. A. The initial slope of the fluoresence trace increased with an increase in ATP concentration and was used as an intial velocity measurement (Δ relative fluorescence/min). Traces are of the plasmid pPH12 (*a*) in strain RH305 ($a_{uncB205}$), wild-type control. B. Plot of the initial velocity verses ATP concentration. Key: 218G/245H denotes plasmid pPH12 (*a*) in strain RH305 ($a_{uncB205}$), 218K/245G denotes plasmid pUNCB5.44 ($a_{G218\rightarrow K,H245\rightarrow G}$) in strain RH305 ($a_{uncB205}$), 218D/245G denotes plasmid pUNCB5.43 ($a_{G218\rightarrow D,H245\rightarrow G}$) in strain RH305 ($a_{uncB205}$).

B

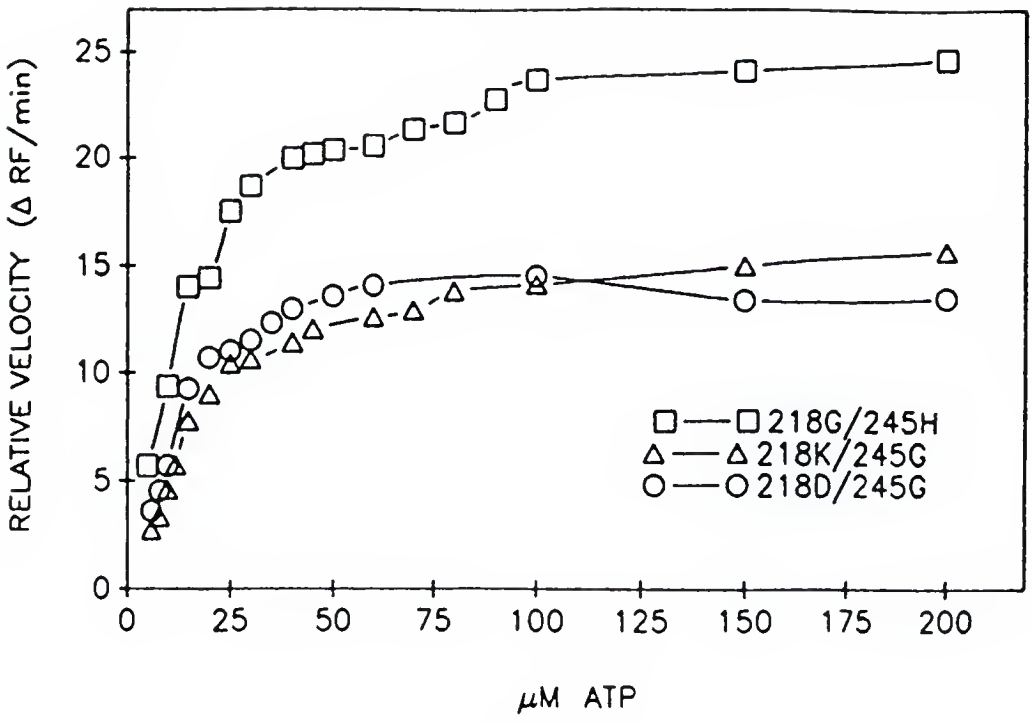

Figure 6-6--continued. ATP driven ACMA fluoresence quenching was assayed at 150 μg membrane protein/ml buffer [50 mM Tris-HCl and 10 mM $MgCl_2$, pH 7.2]. A. The initial slope of the fluoresence trace increased with an increase in ATP concentration and was used as an intial velocity measurement (Δ relative fluorescence/min). Traces are of the plasmid pPH12 (*a*) in strain RH305 ($a_{uncB205}$), wild-type control. B. Plot of the initial velocity verses ATP concentration. Key: 218G/245H denotes plasmid pPH12 (*a*) in strain RH305 ($a_{uncB205}$), 218K/245G denotes plasmid pUNCB5.44 ($a_{G218\rightarrow K,H245\rightarrow G}$) in strain RH305 ($a_{uncB205}$), 218D/245G denotes plasmid pUNCB5.43 ($a_{G218\rightarrow D,H245\rightarrow G}$) in strain RH305 ($a_{uncB205}$).

did not exhibit changes in relative fluoresence at as high a rate as the wild-type control, they displayed a similar dependence on ATP concentration (apparent Km = 12-17 μM). Additional kinetic analysis was not pursued for two reasons. First, the relative fluoresence verses time depended on the quality of the membrane vesicle preparation. However, regardless of the membrane preparation the same dependence on ATP concentration was observed. Second, the response of ACMA to changes in pH across the vesicle membrane was not linear (Rottenberg & Moreno-Sanchez, 1993). The limitations of the assay therefore prevented further analysis.

Discussion

The present work establishes that the effects of mutations altering a_{G218} are largely suppressed by the $a_{H245\rightarrow G}$ mutation. In a dramatic example of second-site suppression, the $a_{G218\rightarrow K}$ substitution inhibits F_1F_0 ATP synthase activity below detectable levels; the $a_{H245\rightarrow G}$ mutation restores most of the lost activity. *E. coli* carrying both mutations have sufficient F_1F_0 ATP synthase function for essentially normal growth. The $a_{H245\rightarrow G}$ mutation also suppresses the $a_{G218\rightarrow D}$ mutation. The $a_{H245\rightarrow G}$ mutation alone displays a partial phenotype.

Combined with the earlier study (Cain & Simoni, 1988) demonstrating mutual suppression of the $a_{E219\rightarrow H}$ and the $a_{H245\rightarrow E}$

mutations, the data support a model in which positions a_{G218}, a_{E219} and a_{H245} have a critical functional interaction in F_0. The fact that multiple second-site suppressors have now been constructed argues that the relationship between the three positions reflects a close structural interaction within the a subunit.

The data also suggest that these amino acid positions are involved in the coupling mechanism. The $a_{G218\rightarrow D}$ and $a_{G218\rightarrow K}$ mutants exhibit both F_0 mediated proton conductance and DCCD sensitive ATPase activity (Figure 6-4, Table 6-3), while apparently severely limiting ATP synthesis *in vivo* (Table 6-2). The $a_{G218\rightarrow K}$ mutant also exhibited an uncoupling phenotype *in vitro*, as shown in the ATP driven proton pumping assay (Figure 6-3). Additionally, the mutant $a_{G218\rightarrow D}$ demonstrated a profound affect on F_1 through a two fold increase in DCCD sensitive ATP hydrolysis. The double mutation $a_{G218\rightarrow D,H245\rightarrow G}$ does not exhibit this increase activity suggesting the histidine at position a_{245} forces the aspartic acid at position a_{218} into a conformation that effects F_1.

The mutant $a_{G218\rightarrow D}$ could affect F_1 through the coupling mechanism. One hypothesis is that the additional negative charge in the wrong position confers a conformational change on F_1. This conformational change could normally be transmitted by amino acid position a_{E219} during proton translocation. This hypothesis is supported by the $a_{E219\rightarrow Q}$ mutant reported by Lightowlers, *et al*. (1988) in which F_1-

ATPase activity was inhibited by about 50% when membrane bound. While changes of this magnitude were not reported by Cain and Simoni (1988, 1989) with the same mutations, they reported smaller change in the ATPase activity in the same direction as the larger changes reported here.

It is proposed that the $a_{G218 \rightarrow D}$ mutation causes a conformational change in F_1 that favors increased ATPase activity. This conformational change may be mediated by the ϵ subunit in F_1. This hypothesis is supported by the observation that LDAO does not increase ATPase activity in the $a_{G218 \rightarrow D}$ mutation. LDAO has been hypothesized to increase ATPase activity in F_1 by changing the conformation of the ϵ subunit (Lötscher *et al.*, 1984). The ϵ subunit is believed to undergo conformational changes, demonstrated by the effects of different ligands (ATP + Mg_2^+ verses ATP EDTA) on cross-linking and cyroelectron microscopy (Chapter 1).

One conclusion from the data is that position a_{G218}, a_{E219} and a_{H245} effect the coupling of proton translocation to ATP catalysis. This is demonstrated by the fact that all the above mutants allow passive proton translocation, even $a_{G218 \rightarrow K}$ which reduces active proton translocation beyond detectable levels. Also evident is an effect on F_1 ATP hydrolysis demonstrated by the $a_{G218 \rightarrow D}$ mutant. Interestingly, none of the mutants seem to affect the ability of DCCD to inhibit F_1-ATPase activity. This implies that the binding of DCCD

to the *c* subunit may affect bound F_1-ATPase activity by a different mechanism.

The relative velocity of ATP driven ACMA quenching was dependent on pH. This was not apparently due to an effect upon ACMA fluorescence, but rather an effect on F_1F_O-mediated proton pumping activity. Since the F_1 ATPase activity is known to increase with increasing pH, this effect is probably related to the coupling mechanism or the F_O sector (Chapter 1). DCCD sensitivity of the F_1 ATPase activity is retained at pH 9.1 so the loss of proton quenching is not due to a removal of F_1 from the membrane. DCCD sensitivity is usually considered a test for coupling, however, its mode of action probably differs from the effects of pH and the uncoupling *a* mutants.

Observations from this Chapter are incorporated into a proposed model of coupling proton transport to ATP catalysis in Chapter 7.

CHAPTER 7
CONCLUSIONS AND FUTURE DIRECTIONS

Overview of the *a* Subunit Missense Mutations

Since the original report by Cain & Simoni (1986) that missense mutations in the *a* subunit were sufficient for virtual abrogation of F_o-mediated proton translocation, at least ninety-five different missense mutations at thirty-one separate sites in the *a* subunit have been constructed by a number of independent investigators (Cain & Simoni, 1986, 1988, 1989; Eya *et al.*, 1988, 1991; Howitt *et al.*, 1988, 1993; Lightowlers *et al.*, 1987, 1988; Paule & Fillingame, 1989; Vik *et al.*, 1988, 1990, 1991; Chapter 4, 5, 6). With the present work all of the obviously conserved positions, as well as, the charged amino acids which are predicted to lie within the membrane bilayer have been studied. Although some minor controversies have appeared in the reported phenotypes, the combined data provide a substantial basis for considering the role of the *a* subunit in proton translocation. A compilation of *a* subunit single missense mutations is presented in Figure 7-1.

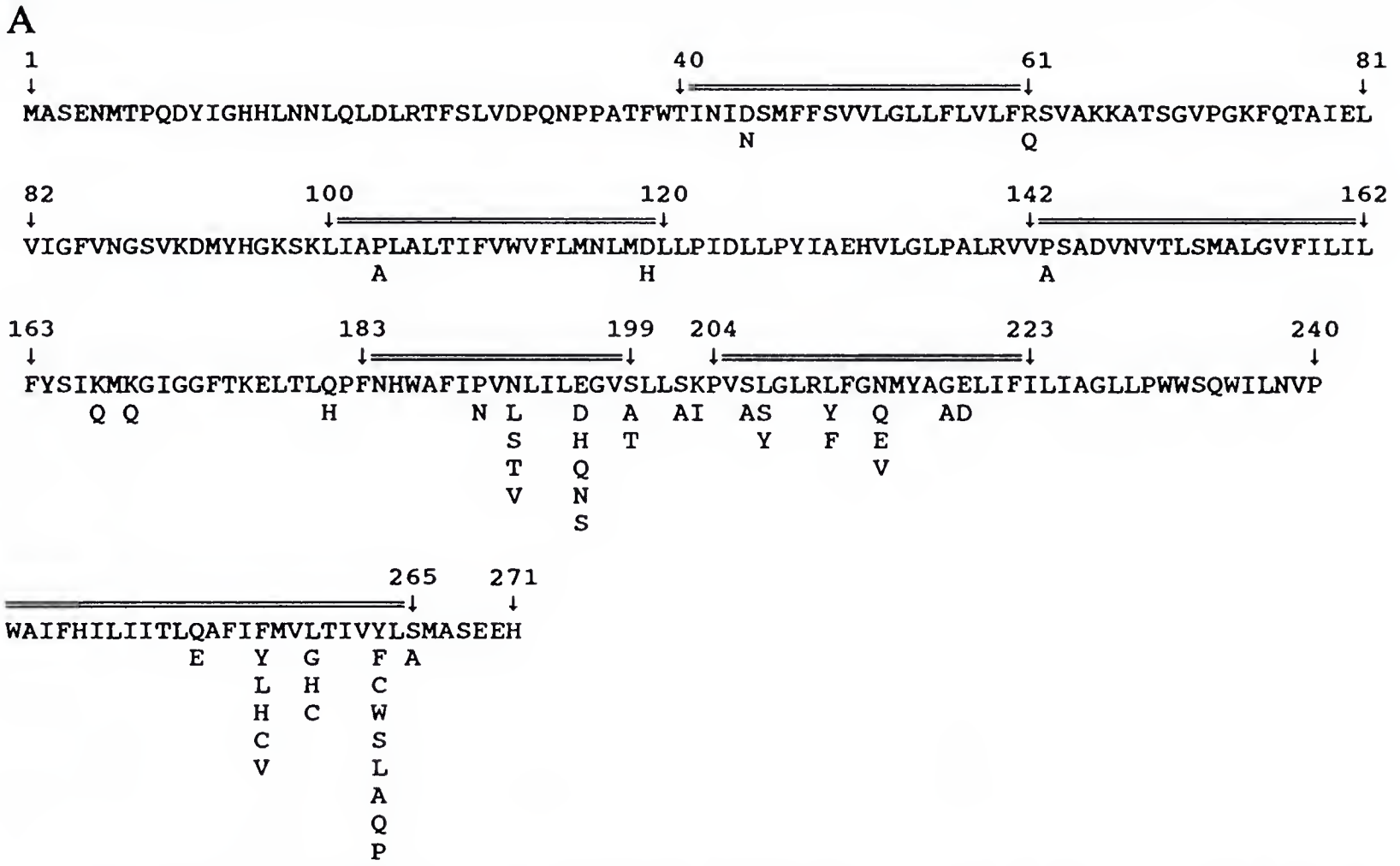

Figure 7-1. Compilation of missense mutations in the *a* subunit. Numbers denote amino acid position. Proposed membrane spanning regions are marked by bars. A. Mutations with minimal effect on F_1F_o ATP synthase function. B. Substitutions that significantly reduce enzyme function. Substitutions that abolish enzyme activity are highlighted.

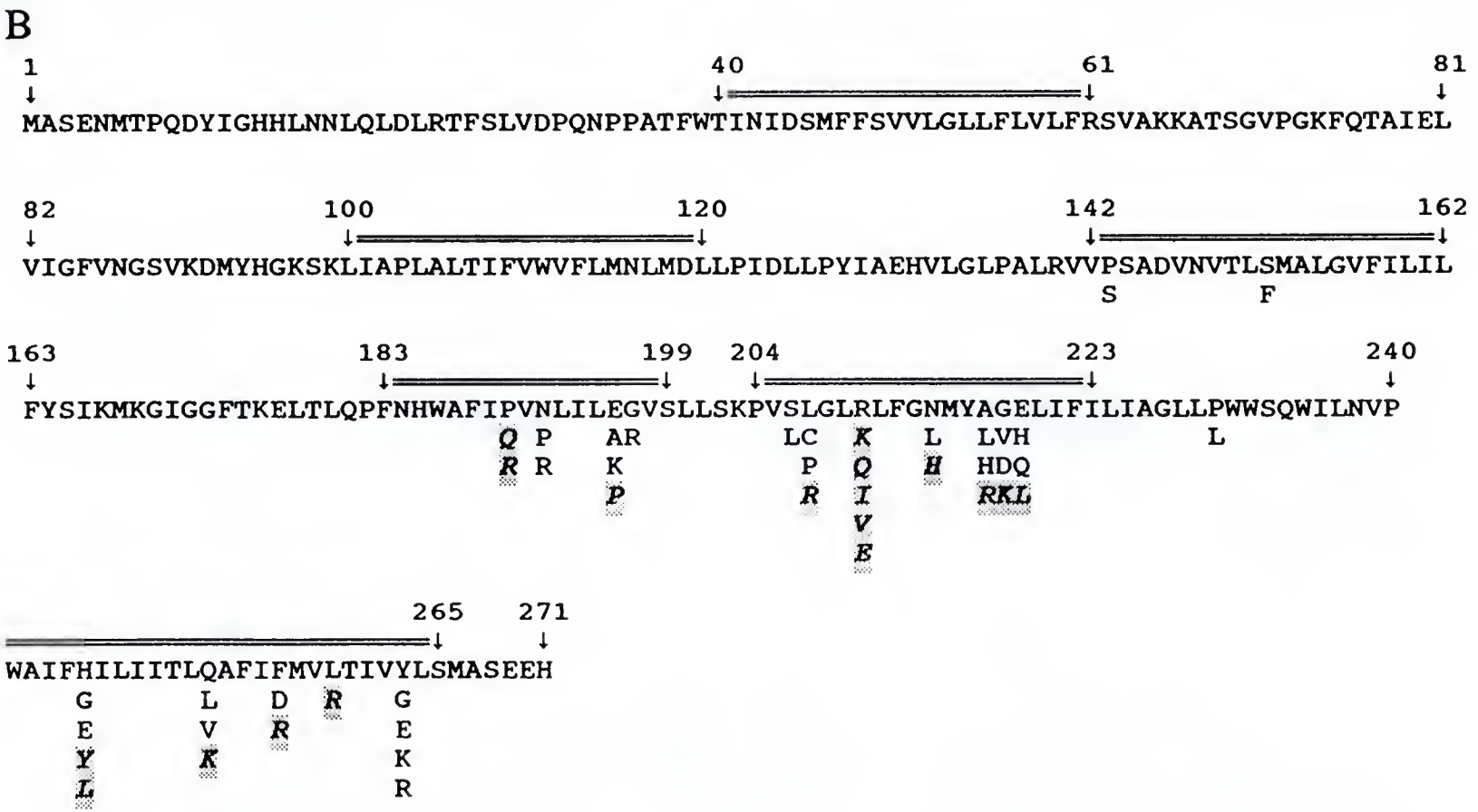

Figure 7-1--continued. Numbers denote amino acid position. Proposed membrane spanning regions are marked by bars. A. Substitutions with minimal effect on F_1F_o ATP synthase function. B. Substitutions that significantly reduce enzyme function. Substitutions that abolish enzyme activity are highlighted.

The mutagenesis approach has established that a_{R210} is apparently the only essential amino acid for ATP synthase proton translocation (Cain & Simoni, 1989, Eya *et al.*, 1991, Lightowlers *et al.*, 1987). All substitutions at position a_{R210} have resulted in loss of proton translocation. The conservation of a positive charge is not the reason arginine is required since $a_{R210\rightarrow K}$ mutant abolishes activity (Cain & Simoni, 1989; Eya *et al.*, 1991). It is probable that position a_{R210} interacts with other essential amino acids in the F_O sector. A very likely candidate is the amino acid c_{D61}. Both amino acids are predicted to be located near the center of the membrane lipid bilayer (Chapter 1; Fillingame, 1993). In support of this hypothesis third-site suppressors were isolated for the double mutant $c_{A24\rightarrow D,D61\rightarrow G}$, and the majority of the suppressor mutants were in *a* subunit amino acid with the potential to affect the positioning of amino acid a_{R210} (Fraga *et al.*, 1994). Positioning of amino acid c_{D61} is apparently important since the mutant $c_{D61\rightarrow E}$ exhibits a partial phenotype while the double mutant $c_{A24\rightarrow D,D61\rightarrow G}$ displays only slightly more activity (Miller *et al.*, 1990). If the amino acid a_{R210} is involved in an interaction with amino acid c_{D61}, then it seems reasonable that a change in the positioning of the a_{R210} amino acid could compensate for a change in the positioning of the c_{D61} amino acid. Many third site suppressor mutants were isolated at the ends of the proposed membrane spanning helix V, where they could affect

the positioning of amino acid a_{R210} by shifting the helix. The interaction between helix V of the *a* subunit and the *c* subunit is supported by the $a_{A217 \rightarrow R}$ mutant, which was shown to greatly decrease DCCD sensitivity (Cain & Simoni, 1989). Amino acid position a_{A217} may be in close proximity to amino acid c_{D61} based on predicted structures (Chapter 1; Fillingame, 1993). Amino acid position a_{Q252} is also hypothesized to be located in this region of the lipid bilayer (Chapter 1). The $a_{Q252 \rightarrow K}$ mutant exhibited no DCCD sensitive F_1-ATPase activity (Chapter 4), and other mutations at position a_{Q252} also reduced DCCD sensitivity (Eya *et al.*, 1991; Chapter 4). The apparent effects a_{Q252} mutants have on the binding of DCCD to amino acid c_{D61} indicate a close proximity as shown with the DCCD insensitive mutant $c_{A24 \rightarrow S}$ (Hoppe *et al.*, 1980; Fillingame *et al.*, 1991). A model with the last two membrane spanning regions of the *a* subunit interacting with the two membrane spanning regions of the *c* subunit is supported by the mutagenesis data (Cain & Simoni, 1989; Eya *et al.*, 1991; Chapter 4; Fraga *et al.*, 1994).

Mutations of the conserved amino acids in the last two membrane spanning regions of the *a* subunit support this conclusion. Indirect support for including only the last two proposed membrane spanning regions of the *a* subunit in this interaction is the limited effects of mutants outside of this region (Lightowlers *et al.*, 1987, 1988; Howitt *et*

al., 1988?, 1993; Eya *et al.*, 1988, 1991; Vik *et al.*, 1988, 1990; Paule & Fillingame, 1989). With the exception of amino acid position a_{R210}, all the conserved amino acids in this region can be substituted with at least one amino acid that allows partial activity, but many of the substitutions also abolish activity (Cain & Simoni, 1986, 1988, 1989; Lightowlers *et al.*, 1987, 1988; Howitt *et al.*, 1988?; Eya *et al.*, 1988, 1991; Vik *et al.*, 1991; Chapter 4, 5, 6). A general observation from the substitutions in this region is that changes to basic amino acids is not conducive to enzyme function (Cain & Simoni, 1989; Chapter 4, 5). Many of these mutants were shown to bind the F_1 sector, indicating assembly of the F_O sector (Cain & Simoni, 1989). One conclusion from this data is that the positive charges adversely affect interactions with protons. This is supported by the fact that negatively charged substitutions in this region do not result in as severe phenotypes (Cain & Simoni, 1989; Eya *et al.*, 1991; Chapter 4). Alternatively, basic amino acids may significantly alter the insertion of the *a* subunit into the membrane. However, while this is probably the case with substitutions such as the NARP mutant $a_{L207\rightarrow R}$ (Chapter 5), it does not explain the phenotype of the $a_{G218\rightarrow K}$ mutant (Chapter 6).

Even though amino acid positions a_{G218}, a_{E219} and a_{H245} are not highly conserved, mutations in these positions can have very detrimental effects on F_1F_O ATP synthase activity (Cain

& Simoni, 1988, Eya *et al.*, 1991, Lightowlers *et al.*, 1988; Chapter 6). It has been demonstrated that these amino acid positions probably interact (Cain & Simoni, 1988; Chapter 6). It is also evident that these amino acids can effect F_1-ATPase activity (Lightowlers *et al.*, 1987, 1988; Cain & Simoni, 1989; Chapter 6). Mutations in amino acid positions a_{R210}, a_{N214}, and a_{A217} have also been shown to affect F_0 bound F_1 ATPase activity (Lightowlers *et al.*, 1987; Cain & Simoni, 1989), though their phenotype may be an indirect effect on amino acid a_{E219} through effecting the membrane spanning helix V. This is supported by the observation that at amino acid position a_{R210} the substitution of a more bulky amino acid, like the $a_{R210\rightarrow K}$ mutant, increases coupled F_1 ATPase activity while substitutions of less bulky amino acids, the $a_{R210\rightarrow V}$ mutant, the $a_{R210\rightarrow E}$ mutant, and the $a_{R210\rightarrow Q}$ mutant decrease activity, and a substitution with an amino acid of similar bulk, the $a_{R210\rightarrow Q}$ mutant, does not affect ATPase activity (Lightowlers *et al.*, 1987; Cain & Simoni, 1989).

It is proposed that amino acid positions a_{G218}, a_{E219} and a_{H245} play a role in coupling proton translocation to ATP catalysis. An interpretation of the data is that the negative charge of amino acid a_{E219} interacts with the coupling mechanism in some way that effects the F_1-ATPase activity. In support of this hypothesis it has been observed that the $a_{E219\rightarrow Q}$ mutant reduces membrane bound F_1-ATPase activity by two fold (Lightowlers *et al.*, 1988),

while the $a_{G218\rightarrow D}$ mutant increases the membrane bound F_1-ATPase activity by two fold (Chapter 6). Membrane bound F_1-ATPase activity is apparently dependent on a negative charge in this region of the *a* subunit. Consequently a negative charge is present in one of the analogous amino acid positions (a_{219} or a_{245}) for all *a*-like subunits (Figure 1-3). The hypothesis is that a conformational change in the F_O sector is induced by the binding of a proton(s), which moves amino acid a_{E219} into a position where it can promote additional conformational changes that result in an effect on the F^1 ATP binding site. The $a_{G218\rightarrow D}$ mutant disrupts this process by being in, or forcing amino acid a_{E219} into, a position that favors the conformational change that increases F_1-ATPase activity (see below). In the $a_{G218\rightarrow D,H245\rightarrow G}$ double mutant the increased ATPase activity is lost, which is explained by the aspartic acid at position a_{218} occupying the space vacated by the substitution of glycine for histidine at position a_{245} and no longer inducing the conformational change. If membrane spanning region V of the *a* subunit is in an α-helical conformation then amino acid a_{E219} would face away from the proposed interaction between the *a* and *c* subunits (see above). A potential interaction amino acid a_{E219} might have is with amino acid b_{R36}. The amino acid b_{R36} is conserved in *b*-like subunits that are anchored in the membrane (McCormick, 1993). Amino acid b_{R36} is currently under investigation by Cain and colleagues.

However, a negative charge at the a_{219} or a_{245} positions is not absolutely essential (Cain & Simoni, 1988) so there must be an additional component to the coupling mechanism. The function of positions a_{218}, a_{219} and a_{245} in the coupling of proton transport to ATP synthesis is supported by the fact that all the mutations in this region not only assembled, but were capable of proton conductance. The $a_{G218\rightarrow K}$ mutant displayed a true uncoupled phenotype, where F_1 ATPase was bound to F_O and DCCD sensitive, passive proton conductance was evident, but active transport of protons was not be detected. Small amounts of ATP driven proton transport could not be ruled out since anaerobic growth was supported by the $a_{G218\rightarrow K}$ mutant, but this activity was not sufficient to allow growth of mutant strains on succinate.

Double mutants where activity has been restored, like $a_{E219\rightarrow H,H245\rightarrow E}$, $a_{G218\rightarrow D,H245\rightarrow G}$, and $a_{G218\rightarrow K,H245\rightarrow G}$ (Cain & Simoni, 1988; Chapter 6) have demonstrated specific amino acid interactions. Double mutations where activity is decreased are harder to interpret (Vik *et al.*, 1990; Howitt *et al.*, 1993). Cumulative structural alterations could influence stability and assembly, without directly interacting.

This is a likely interpretation for the reported hypothetical second site suppressor of the $a_{R210\rightarrow K}$ mutant, the $a_{G53\rightarrow D}$ mutant (Howitt & Cox, 1992). The $a_{G53\rightarrow D}$ suppressor mutation, was isolated in an *uncB* (*a*) gene also carrying the deleterious $a_{R210\rightarrow K}$ mutation. However, the suppressor

phenotype required a wild type copy of the *uncB* (*a*) gene in the genome. The phenotype of *a* subunits expressed from genomic copy of the *uncB* (*a*) gene was obscured by the plasmid derived expression of the $a_{R210\rightarrow K}$ mutant, because the $a_{R210\rightarrow K}$ mutant folds correctly and assembles in the F_O complex. Expression of the $a_{G53\rightarrow D,R210\rightarrow K}$ mutation potentially disrupted the folding of the mutant *a* subunit, allowing the wild-type a subunit expressed from the genomic *uncB* (*a*) gene to assemble in the F_O complex. This hypothesis is supported by the observation that the $a_{G53\rightarrow D,R210\rightarrow K}$ mutant did not complement a strain carrying a defective *a* subunit. Additionally, the single $a_{G53\rightarrow D}$ mutation was not constructed, so the affects of its expression were undetermined.

Modeling Mitochondrial Mutations

The modeling the of NARP mutations, *ATPase* $6_{L156\rightarrow R}$ and *ATPase* $6_{L156\rightarrow P}$, in the *a* subunit with the $a_{L207\rightarrow R}$ and $a_{L207\rightarrow P}$ mutants demonstrated the validity of the comparison of *E. coli* F_1F_O ATP synthase with other F_1F_O ATP synthases (Chapter 5). The bacterial system holds many advantages over the alternative cell culture lines. Heteroplasmy arising from mitotic segregation of the mtDNA occurs in cell lines as well as the somatic cells of whole organism (Ashley *et al.*, 1989). Sub-populations of cells carrying less of the mtDNA mutation will have a selective advantage over the rest of

the population. This is a problem because cell lines require some functional activity to survive since they can not survive solely by fermentation. This background of wild-type activity will mask the effects of the mutants. This has been observed to be the case with the *ATPase* $6_{L156\rightarrow R}$ mutation, where even with a high percentage of mutant mtDNA, the cells still exhibit at least 50% of the wild-type F_1F_O ATP synthase function (Tatuch & Robinson, 1993; Eric Schon personal communication).

The *E. coli* model system does not have a background or heteroplasmy problem. This makes the bacterial system superior for determining the biochemical effects of mutations in the *a*-like *ATPase 6* gene. While the cell line analysis of mitochondrial ATP synthase activities reported reduced activity for the NARP mutation, analysis of the comparable mutation in the a subunit determined the mutant destablized the F_O sector, abolishing the proton transport and *in vivo* ATP synthesis.

Analysis of a second mitochondrial mutation at the same nucleotide position revealed a different phenotype. The resulting mutant $a_{L207\rightarrow P}$ (*ATPase* $6_{L156\rightarrow P}$ in humans) was found to inhibit F_1F_O ATP synthase function in a manner dependent on the amount of F_1 subunits present (Chapter 5). This observation reveals a potential human phenotype that might depend on additional mutations in F_1 subunits. Since the F_1 subunits are encoded in the nucleus, a mixed genetic

inheritance would prevail. Classical Mendelian genetics with only maternal inheritance would be difficult to distinguish from an X-linked gene without a sufficiently large pedigree. Clinically the *ATPase* $6_{L156\rightarrow P}$ mutation may exhibit heteroplasmy due to somatic mutation as well as mtDNA segregation. The possibility of complementing the *ATPase* $6_{L156\rightarrow P}$ mutant with increased expression of F_1 subunits appears to be a potential treatment. One method to accomplish this would be with gene therapy. However, since all the F_1 subunits have not been cloned this may not be a possibility for some time to come.

The first isolated missense mutations (NARP 8993) in the *ATPase 6* (*a*) subunit, although defective in activity, are not in the more functionally important amino acid positions. Implications from study of the *a* subunit in *E. coli* ATP synthase is that a multitude of mutations in the conserved region could result in loss of ATP synthase activity in human mitochondria, as well as, bacteria. Therefore, many mutations may exist in the human *ATPase 6* (*a*) subunit that effect ATP synthesis, but have not been detected because they can not be followed by RFLP analysis.

The unique clinical phenotype of the NARP mutation seen in some of the cases, including lack of mitochondrial abnormalities and no lactate imbalances, will probably make diagnosis of other *ATPase 6* subunit mutations difficult. Additionally, many partial phenotypes have been observed in

the study of the *a* subunit. The same mutations occurring in the *ATPase 6* subunit in human mitochondria may not clinically manifest till later in a patients life, even with high ratios of mutant mtDNA to wild type. However, partial phenotypes may still effect muscle performance and neurologic activity. With the high rate of mtDNA mutation (Wallace, 1992a, b) it is probable that many mutations in the *ATPase 6* subunit (*a* subunit) of the human ATP synthase exist. It is probable also that many of these mutations may have minor effects that will lead to degenerative diseases later in the carriers life. Clinically the manifestations of these partial phenotypes may be hard to detect but just as devastating when the energy output of a tissue drops below its energy requirements.

Coupling Proton Transport to ATP Catalysis

The Ion(s) Binding-Site

The mutagenesis of the *a* subunit supports a model with the last two membrane spanning regions of the *a* subunit and the two membrane spanning regions of the *c* subunit forming a proton(s) binding site. Most likely the proton is in the form of a H_3O^+ ion, which is chemically similar to a hydrated Na^+ ion, and explains the almost identical function of *P. modestum* F_1F_0 ATP synthase to other F_1F_0 ATP synthases (see Chapter 1). Multiple proton binding sites are

indicated by work in *P. modestum* where three hydrated Na^+ ion binding sites were reported (Kluge & Dimroth, 1993). The existence of three binding sites is also supported by the $3H^+$/ATP stoichiometry reported for *E. coli* (Kashket, 1982, 1983). Fillingame (1993) has proposed three proton binding sites located on three different *c* subunits, in which amino acid c_{D61} constitutes the majority of the binding. However, evidence indicates that only one c_{D61} amino acid needs to bind to DCCD in order to inhibit F_1 ATPase activity, while apparently all the *c* subunits will react with DCCD (Hermolin & Fillingame, 1989). Another potential position for multiple proton binding sites is along the interface of the *a* and *c* subunits. If this was the case then mutations in this region might be expected to alter the $3H^+$/ATP ratio. However, evidence supports an additional role for the *a* subunit besides the binding and translocation of protons.

Regardless of the number of binding sites, the binding of an ion(s) is likely to result in a conformational change within the F_O sector. Such a conformational change would be a candidate for the mechanism by which the transport of protons supplies the energy for ATP synthesis. As mentioned above the conformational change would induce a secondary interaction facilitated by the negative charge at a_{E219}. The facilitation of the second interaction would be position

dependent, explaining the mechanism by which *a* subunit mutants affect F_1 ATPase activity (see above).

The conformational change in the F_o sector is likely to be from a conformation in which the ion(s) binding-site is accessible on the periplasmic side of the membrane to a conformation in which the binding-site is accessible from the cytoplasmic side of the membrane. Alterations in the conformation may also alter the affinity of the ion(s) binding-site as well.

The Coupling Connection

The conformational change in the F_o sector has to be transferred to the F_1 sector. Since this energy is most likely transferred through a stalk structure (Chapter 1) then two subunits are probably required. The *b* subunit is proposed to transmit a conformational change to the F_1 sector (see above), most likely through some type of movement. Due to the proposed structure of the *b* subunit as an extended coiled-coil, other methods of the transfer of energy are difficult to justify (McCormick, 1993). However, a conformational movement of the *b* subunit alone would only accomplish the movement of the whole F_1 sector. If the *b* subunit moved in relation to the F_1 sector it could then induce a conformational change in the F_1 sector. The δ subunit is a good candidate to hold the F_1 sector in place so that the movement of the *b* subunit can induce conformational changes. The δ subunit has been predicted to

fold into a coiled-coil similar to the *b* subunit (McCormick, 1993), and is required for the binding of the F_1 sector to the F_O sector (Bragg *et al.*, 1973; Sternweis & Smith, 1977). Mutations in the δ subunit have resulted either in reducing F_1 binding to the F_O sector (Senior 1990), or in reducing F_1 ATPase sensitivity to DCCD binding in the F_O sector (Hazard & Senior, 1994). However, a direct role is indicated for the *b* subunit because the $b_{A79\rightarrow K}$ mutant alters the coupling mechanism (McCormick *et al.*, 1993). For the δ subunit to serve as an anchor in relation to the *b* subunit it must bind the F_O sector through a subunit other than *b*. The *c* subunit demonstrates the ability to effect the binding of F_1 (Fillingame, 1993), so may play this role through binding the δ subunit. The δ and *b* subunit double connection is also supported by the apparent double pathway of affecting F_1 ATPase activity, through the a_{E219} mutants and DCCD binding to the F_O sector. It is proposed here that the actions of DCCD inhibition on F_1 ATPase is mediated through the δ subunit and via its connection to F_O, and that the increase in F_1 activity due to raising the pH to 9.1 is mediated through the uncoupling of ATPase activity to proton transport. Proposed mechanisms for this uncoupling can be the titration of the pKa of a functional group involved in coupling or perhaps the titration of the pKa of the proton binding site(s) involved in transport.

The *b* subunit probably interacts with the γ or ϵ subunits or maybe a complex of both (Cox *et al.*, 1993). The γ subunit has also been reported to alter the coupling mechanism (Shin *et al.*, 1992), so it is probably involved in the coupling mechanism. The β subunit has also been reported to cross-link with *b* subunit (Aris & Simoni, 1983), indicating it may be involved, though maybe only indirectly. Since a conformational change has already been characterized for both the γ and ϵ subunit (Chapter 1), it seems likely that the mechanism of coupling involves these subunits.

The Catalytic-Site

The ϵ subunit has been shown to inhibit F_1 ATPase activity in a manner that can be reversed with LDAO (Chapter 1). The fact that the $a_{G218\rightarrow D}$ mutant increases the ATPase activity in an LDAO insensitive manner indicates that this mutant is effecting the F_1 ATPase activity through the ϵ subunit (Chapter 6). The characterized conformational change of the ϵ subunit can also be used in F_1F_O ATP synthases carrying the $a_{G218\rightarrow D}$ mutant to see if it effects the ϵ subunit. The conformational change in ϵ was found to be sensitive to phosphate concentration (Mendel-Hartvig & Capaldi, 1991b). Interestingly, one of the steps of ATP synthesis that requires energy is the binding of phosphate to the active site (Senior, 1990).

A proposed mechanism during ATP synthesis starts with ADP binding in the active site. At this step the ϵ subunit

is in the conformation that is sensitive to trypsin proteolysis. A conformational change is next induced in the ϵ subunit that allows the binding of P_i and results in a decrease in sensitivity to trypsin proteolysis. The change in conformation is driven by conformational changes in F_o for the intact F_1F_o ATP synthase, or can be induced by the addition of P_i in the F_1-ATPase. Once ADP and P^i are bound together in an active site, the formation of ATP occurs almost spontaneously. The release of ATP from the active site is rate limiting after the addition of P_i and is probably accelerated by the binding of ADP to another catalytic site (Chapter 1).

During ATP hydrolysis ATP would bind at an active site and spontaneously form ADP and P_i. The conformation of the ϵ subunit would be that of insensitive to trypsin cleavage. The release of P_i from the active site would drive the conformational change of the ϵ to that of being sensitive to trypsin cleavage. If the F_1 sector is coupled to the F_o sector then the ϵ subunit conformational change would induce a conformational change in F_o. The binding of ATP at a second catalytic site would then facilitate the release of ADP.

Combined Mechanism

In summary the proposed mechanism of ATP syntheses is as follows. The binding of a proton(s) at the interface of the *a* and *c* subunits induces a conformational change in the

F_o sector. The conformational change may alter the accessibility of the proton(s) binding-site to the two membrane facings, or the affinty of the binding-site for protons. Additionally, the F_o conformational change potenially results in an interaction between the *a* and *b* subunit resulting in a conformational movement of the *b* subunit in relation to the δ subunit. The movement of the *b* subunit induces a conformational change in one of the nucleotide binding sites located in the F_1 sector. The conformational change is probably mediated through the γ and ϵ subunits. The F_1 sector conformational change would alter the affinity of the nucleotide binding site for P_i, allowing P_i to bind in the catalytic-site with ADP. ATP is formed spontaneously and then released in a manner that is accelerated via binding of ADP at a second catalytic-site. The binding of new ADP or release of ATP may induce a conformational in the F_o sector that results in the loss of the proton(s) from the binding-site(s) in F_o. The membrane potential is also very likely to play an important role in the removal of the proton(s) from the binding-site(s). The release of the proton(s) may also induce the release of ATP from the catalytic-site. The binding of a new proton(s) from the periplasmic side of the membrane would then restart the cycle.

The above hypothesis can be tested through the use of the *a* subunit mutants $a_{E219\rightarrow Q}$ and $a_{G219\rightarrow D}$. The $a_{E219\rightarrow Q}$ mutant may

inhibit F_1-ATPase activity by favoring a conformation that results in an increase in the affinity for P_i at catalytic-site. The $a_{G219\rightarrow D}$ mutant may increases F_1-ATPase by favoring a conformation that results in a reduction in the affinity for P_i at the catalytic-site. Since the affinity for P_i at the catalytic-site is mediated through the conformational state of the ϵ subunit, then the mutants should favor one of the conformations of the ϵ subunits. One mechanism by which this can be followed is with the sensitivity of the ϵ subunit to trypsin. Therefore, the $a_{E219\rightarrow Q}$ mutant should favor a conformation of the ϵ subunit which is relatively insensitive to trypsin cleavage compared to the conformation of the ϵ subunit induced by the $a_{G219\rightarrow D}$ mutant.

REFERENCES

Abrahams, J. P., Lutter, R., Todd, R., J., van Raaij, M. J., Leslie, A. G. W., & Walker, J. E. (1993) *EMBO Journal 12*, 1775-1780.

Aggeler, R. & Capaldi, R. A. (1992) *J. Biol. Chem. 267*, 21344-21359.

Aggeler, R., Chicas-Cruz, K., Cai, S-X.,Keana, J. F. W., & Capaldi, R. A. (1992) *Biochemistry 31*, 2956-2961.

Aggeler, R., Mendel-Hartvig, J., & Capaldi, R. A. (1990) *Biochemistry 29*, 10387-10393.

Aggeler, R., Zhang, Y., & Capaldi, R. A. (1987) *Biochemistry 26*, 7107-7113.

Akey, C. W., Crepeau, R. H., Dunn, S. D., McCarty, R. E., & Edelstein, S. J. (1983) *EMBO J. 2*, 1409-1415.

Al-Shawi, M. K., Parsonage, D., & Senior, A. E. (1990) *J. Biol. Chem. 265*, 4402-4410.

Al-Shawi, M. K., & Senior, A. E. (1988) *J. Biol. Chem. 263*, 19640-19648.

Altendorf, K., Steffens, K., Schneider, E., & Schmid, R. (1987) in *Membrane receptors, dynamics, and energetics* (K. W. A. Wirtz, Ed) pp 221-235, Plenum Publishing Corp. New York.

Amann, R., Ludwig, W., Laubinger, W., Dimroth, P. & Schleifer, K. H. (1988) *FEMS Microbiol. Lett. 56*, 253-260.

Amersham Corp. (1990) *Oligonucleotide-directed in vitro Mutagenesis System Version 2 Manual*. Amersham Corp., Arlington Heights, IL.

Amzel, L. M., McKinney, M., Narayanan, P., & Pedersen, P. L. (1982) *Proc. Natl. Acad. Sci. U. S. A. 79*, 5852-5856.

Anderson S., Bankier, A. T., Barrell, B. G., de Bruijin, M. H. L., Coulson, A. R., Drouin, J., Eperon, I. C., Nierlich, D. P., Roe, B. A., Sanger, F., Schreier, P. H., Smith, A. J. H., Staden, R., & Young, I. G. (1981) *Nature 290*, 457-465.

Anderson S., de Bruijin, M. H. L., Coulson, A. R., Eperon, I. C., Sanger, F., & Young, I. G. (1981) *J. Mol. Biol. 156*, 683-717.

Angov, E., Ng, T. C. N., & Brusilow, W. S. A. (1991) *J. Bacteriol. 173*, 407-411.

Aris, J. P., Klionsky, D. J., & Simoni, R. D. (1985) *J. Biol. Chem. 260*, 11207-11215.

Aris, J. P., & Simoni, R. D. (1983) *J. Biol. Chem. 258*, 14599-14609.

Ashley, M. V., Laipis, P. J. and Hauswirth, W. W. (1989) *Nucleic Acids Res. 17*, 7325-7331.

Bianchet, M., Ysern, X., Hullihen, J., Pedersen, P., & Amzel, L. M. (1991) *J. Biol. Chem. 266*, 21197-21201.

Bibb, M. J., Van Etten, R. A., Wright, C. T., Walberg, M. W., & Clayton, D. A. (1981) *Cell 26*, 167-180.

Birdsell, D. C., and Cota-Robles, E. H. 1967. *J. Bacteriology 93*, 427-437.

Birnboim, H. C., & Doly, J. (1979) *Nucleic Acids Res. 7*, 1513-1523.

Bjorbaek, C., Foersom, V., & Michelsen, O. (1990) *FEBS Lett. 260*, 31-34.

Bland, M. M., Levings III, C. S., & Matzinger, D. F. (1987) *Curr. Genet. 12*, 475-481.

Boekema, J. Berden, J. A., & van Heel, M. G. (1986) *Biochim. Biophys. Acta 851*, 353-360.

Boyer, P. D. (1975) *FEBS Lett. 58*, 1-6.

Boyer, P. D. (1987) *Biochemistry 26*, 8503-8507.

Boyer, P. D. (1989) *FASEB J. 3*, 2164-2178.

Boyer, P. D. (1993) *Biochim. Biophys. Acta 1140*, 215-250.

Bragg, P. D., Davies, P. L., & Hou, C. (1973) *Arch. Biochem. Biophys. 159*, 664-670.

Bragg, P. D., & Hou, C. (1975) *Arch. Biochem. Biophys. 167*, 311-321.

Bragg, P. D., & Hou, C. (1986) *Biochim. Biophys. Acta 851*, 385-394.

Brown, L. D., Dennehy, M. E., & Rawlings, D. E. (1991) unpublished, Genbank accesssion number M81087.

Brown, M. D., Voljavec, A. S., Lott. M. T., Torroni, A., Yang, C., & Wallace, D. C. (1992) *Genetics 130*, 163-173.

Brusilow, W. S. A., Gunsalus, R. P., Hardeman, E. C., Decker, K. P., & Simoni, R. D. (1981) *J. Biol. Chem. 256*, 3141-3144.

Brusilow, W. S. A., Klionsky, D. J., & Simoni, R. D. (1982) *J. Bacteriol. 151*, 1363-1371.

Brusilow, W. S. A., Scarpetta, M. A., Hawthorne, C. A., & Clark, W. P. (1989) *J. Biol. Chem. 264*, 1528-1533.

Cain, B. D., & Simoni, R. D. (1986) *J. Biol. Chem. 261*, 10043-10050.

Cain, B. D., & Simoni, R. D. (1988) *J. Biol. Chem. 263*, 6606-6612.

Cain, B. D., & Simoni, R. D. (1989) *J. Biol. Chem. 264*, 3292-3300.

Capaldi, R. A., Aggeler, R., Gogol, E. P., & Wilkens, S. (1992) *J. Bioenerg. Biomembr. 24*, 435-439.

Chernyak, B. C., & Kozlov, I. A. (1979) *FEBS Lett. 104*, 215-219.

Ciafaloni, E., Santorelli, F. M., Shanske, S., Deonna, T., Roulet, E., Janzer, C., Pescia, G., & DiMauro, S. (1993) *J. Pediatr. 122*, 419-422.

Cox, G. B., Downie, J. A., Langman, L., Senior, A. E., Ash, G., Fayle, D. R. H., & Gibson, F. (1981) *J. Bacteriol. 148*, 30-42.

Cox, G. B., Fimmel, A. L., Gibson, F., & Hatch, L. (1986) *Biochim. Biophys. Acta 849*, 62-69.

Cox, G. B., & Gibson, F. (1987) *Curr. Top. Bioenerg. 15*, 163-175.

Cox, G. B., Gibson, F., & McCann, L. (1973) *Biochem. J. 134*, 1015-1021.

Cox, G. B., Jans, D. A., Fimmel, A. L., Gibson, F., and Hatch, L. (1984) *Biochim. Biophys. Acta 768*, 201-208.

Cozens, A. L., & Walker, J. E. (1987) *J. Mol. Biol. 194*, 359-383.

Cozens, A. L., Walker, J. E., Phillips, A. L., Huttly, A. K., & Gray, J. C. (1986) *EMBO J. 5*, 217-222.

Cross, R. L. (1988) *J. Bioenerg. Biomembr. 20*, 395-405.

Cross, R. L., Grubmeyer, C., & Penefsky, H. S. (1982) *J. Biol. Chem 257*, 12101-12105.

Cunningham, D., & Cross, R. L. (1988) *J. Biol Chem. 263*, 18850-18856.

Decker, K. P., Brusilow, W. S. A., Gunsalus, R. P., & Simoni, R. D. (1982) *J. Bacteriol. 152*, 815-821.

Deckers-Hebestreit, G. & Altendorf, K. (1986) *Eur. J. Biochem. 161,* 225-231.

Deckers-Hebestreit, G., & Altendorf, K. (1992a) *J. Biol. Chem. 267*, 12370-12374.

Deckers-Hebestreit, G., & Altendorf, K. (1992b) *J. Exp. Biol. 172*, 451-459.

Deckers-Hebestreit, G., Simoni, R. D., & Altendorf, K. (1992) *J. Biol. Chem. 267*, 12364-12369.

Deisenhofer, J., & Michel, H. (1989) *Science 245*, 1463-1473

de Vries, D. D.1, van Engelen, B. G. M., Gabreëls, F. J. M., Ruitenbeek, W., & van Oost, B. A. (1993) *Ann. Neurol. 34*, 410-412.

Dewey, R. E., Levings III, C. S., & Timothy, D. H. (1985) *Plant Physiol. 79*, 914-919.

Dimroth, P. (1987) *Microbiol. Rev. 51*, 320-340

Dimroth, P. (1992) *Biochim. Biophys. Acta 1101*, 236-239.

Dmitriev, O., Deckers-Hebestreit, G., & Altendorf, K. (1993) *J. Biol. Chem. 267*, 14776-14780.

Downie, J. A., Cox, G. B., Langman, L., Ash, G., Becker, M., & Gibson, F. (1981) *J. Bacteriol. 145*, 200-210.

Downie, J. A., Gibson, F., & Cox, G. B. (1979) *Annu. Rev. Biochem. 48*, 103-131.

Du, Z., & Boyer, P. D. (1989) *Biochemistry 28*, 873-879.

Duncan, T. M., Parsonage, D., & Senior, A. E. (1986) *FEBS Lett. 208*, 1-6.

Duncan, T., M., & Senior, A. E. (1985) *J. Biol. Chem. 260*, 4901-4907.

Dunn, S. D. (1992) *J. Biol. Chem. 267*, 7630-7636.

Dunn, S. D., & Heppel, L. A. (1981) *Arch. Biochem. Biophys. 210*, 421-436.

Dunn, S. D., Heppel, L. A., & Fullmer, C. S. (1980) *J. Biol. Chem. 255*, 6891-6896.

Dunn, S. D., Zadorozny, V. D., Tozer, R. G., Orr, L. E. (1987) *Biochemistry 26*, 4488-4493.

Esser, U., Krumholz, L. R., & Simoni, R. D.(1990) *Nucleic Acids Res. 18*, 5887.

Eya, S., Maeda, M., & Futai, M. (1991) *Arch. Biochem. Biophys. 284*, 71-77.

Eya, S., Maeda, M., Tomochika, K., Kanemasa, Y. & Futai, M. (1989) *J. Bacteriol. 171*, 6853-6858.

Eya, S., Noumi, T., Maeda, M., & Futai, M. (1988) *J. Biol. Chem. 263*, 10056-10062.

Falk, G, & Walker, J. E. (1988) *Biochem. J. 254*, 109-122.

Felle, H., Porter, J. S., Slayman, C. L., & Kaback, H. R. (1980) *Biochemistry 19*, 3585-3590.

Fillingame, R. H. (1980) *Annu. Rev. Biochem. 49*, 1079-1113.

Fillingame, R. H. (1990a) in *The Bacteria: A Treatise on Structure and Function* (Sokatch, J. R., & Ornston, L. N., Eds) Vol 12, pp 345-391, Academic Press, San Diego.

Fillingame, R. H. (1990b) Molecular mechanics of ATP synthesis by F_1F_o-type H^+-transporting ATP synthases. The Bacteria, Vol. XII, Bacterial Energetics (T. A. Krulwich, ed.), pp. 345-391, Academic Press, New York.

Fillingame, R. H. (1992a) *Biochim. Biophys. Acta 1101*, 240-243.

Fillingame, R. H. (1992b) *J. Bioenerg. Biomemb. 24*, 485-491.

Fillingame, R. H., Girvin, M. E., Fraga, D., & Zhang, Y. (1993) *Ann. N. Y. Acad. Sci. 671*, 323-334.

Fillingame, R. H., Oldenburg, M., & Fraga, D. (1991) *J. Biol. Chem. 266*, 20934-20939.

Fillingame, R. H., Peters, L. K., White, L. K., Mosher, M. E., & Paule, C. R. (1984) *J. Bacteriol. 158*, 1078-1083.

Fillingame, R. H., Porter, B., Hermolin, J., & White, L. K. (1986) *J. Bacteriol. 165*, 244-251.

Foster, D. L., & Fillingame, R. H. (1979) *J. Biol. Chem. 254*, 8230-8236.

Foster, D. L., & Fillingame, R. H. (1982) *J. Biol. Chem. 257*, 2009-2015.

Fraga, D., & Fillingame, R. H. (1989) *J. Biol. Chem. 264*, 6797-6803.

Fraga, D., & Fillingame, R. H. (1991) *J. Bacteriol. 173*, 2639-2643.

Friedl, P., Friedl, C., & Schairer, H. U. (1979) *Eur. J. Biochem.* 100, 175-180.

Futai, M., & Kanazawa, H. (1983) *Microbiol. Rev. 47*, 285-312.

Futai, M., Noumi, T., & Maeda, M. (1989) *Annu. Rev. Biochem. 58*, 111-136.

Futai, M., Sternweis, P. C., & Heppel, L. A. (1974) *Proc. Natl. Acad. Sci. USA 71*, 2725-2929.

Garger, S. J., Griffith, O. M., & Grill, L. K. (1983) *Biochem. Biophys. Res. Comm. 117*, 835-842.

Garoff, H., & Ansorge, W. (1981) *Anal. Biochem. 115*, 450-457.

Gibson, F., Downie, J. A., Cox, G. B., & Radik, J. (1978) *J. Bacteriol. 134*, 728-736.

Girvin, M. E., & Fillingame, R. H. (1991) *J. Cell Biol., Suppl. 15-G*, 61 (abstract).

Gogol, E. P., Aggeler, R., Lücken, U., Bork, T., & Capaldi, R. A. (1989a) *Biochemistry 28*, 4709-4716.

Gogol, E. P., Aggeler, R., Sagermann, M., & Capaldi, R. A. (1989b) *Biochemistry 28*, 4717-4724.

Gogol, E. P., Johnston, E., Aggeler, R., & Capaldi, R. A. (1990) *Proc. Natl. Acad. Sci. USA*, 9585-9589.

Gogol, E. P., Lücken, U., & Capaldi, R. A. (1987) *FEBS Lett. 219*, 274-278.

Grisi, E., Brown, T. A., Waring, R. B., Scazzocchio, C. & Davies, R. W. (1982) *Nucleic Acids Res. 10*, 3531-3539.

Grosskopf, R., & Feldmann, H. (1981) *Curr. Genet. 4*, 151-158.

Grubmeyer, C., & Penefsky, H. S. (1981) *J. Biol. Chem. 256*, 3728-3734.

Gunsalus, R. P., Brusilow, W. S. A., & Simoni, R. D. (1982) *Proc. Natl. Acad. Sci. USA 79*, 320-324.

Gyllensten, U., Wharton, D., Josefsson, A. & Wilson, A. C. (1991) *Nature 352*, 255-257.

Hamilton, C. M., Aldea, M., Washburn, B. K., Babitzke, P., & Kushner, S. R. (1989) *J. Bacteriol. 171*, 4617-4622.

Hartzog, P. E., & Cain, B. D. (1993a) *J. Bacteriol. 175*, 1337-1343.

Hartzog, P. E., & Cain, B. D. (1993b) *J. Biol. Chem. 268*, 12250-12252.

Hatefi, Y., & Matsuno-Yagi, A. (1992) in *Adenine Nucleotides in Cellular Energy Transfer and Signal Transduction*. (Papa, S., Azzi, A., & Tager, J., Eds.) pp 33-46, Birhauser Verlag, Basel, Switzerland.

Hazard, A. L., & Senior, A. E. (1994) *J. Biol. Chem. 269*, 427-432.

Heinonen, J. K., & Lahti, R. J. (1981) *Anal. Biochem. 113*, 313-317.

Hennig, J. & Herrmann, R. G. (1986) *Mol. Gen. Genet. 203*, 117-128.

Hermolin, J., & Fillingame, R. H. (1989) *J. Biol. Chem. 264*, 3896-3903.

Hermolin, J., Gallant, J., & Fillingame, R. H. (1983) *J. Biol. Chem. 258*, 14550-14555.

Holt, I. J., Harding, A. E., Petty, R. K. H., & Morgan-Hughes, J. A. (1990) *Am. J. Hum. Genet. 46*, 428-433.

Hoppe, J., Brunner, J., & Jorgensen, B. B. (1984a) *Biochemistry 23*, 5610-5616.

Hoppe, J., Friedl, P., Schairer, H. U., Sebald, W., von Meyenburg, K., & Jorgensen, B. B. (1983) *EMBO J. 2*, 105-110.

Hoppe, J., & Sebald, W. (1984b) *Biochim. Biophys. Acta 768*, 1-27.

Hoppe, J., & Sebald, W. (1986) *Biochimie 68*, 427-434.

Houstek, J., Kopecky, J., Zanotti, F., Guerrieri, F., Capozza, G., & Papa, S. (1988) *Eur. J. Biochem. 173*, 1-8.

Howell, N., Kubacka, I., Xu, M., & McCullough, D. A. (1991) *Am. J. Hum. Genet. 48*, 935-942.

Howitt, S. M., & Cox, G. B. (1992) *Proc. Natl. Acad. Sci. USA 89*, 9799-9803.

Howitt, S. M., Gibson, F., & Cox, G. B. (1988) *Biochim. Biophys. Acta 936*, 74-80.

Hudson, G. S., Mason, J. G., Holton, T. A., Koller, B., Cox, G. B., Whitfeld, P. R., & Bottomley, W. (1987) *J. Mol. Biol. 196*, 283-298.

Humbert, R., Brusilow, W. S. A., Gunsalus, R. P., Klionsky, D. J., & Simoni, R. D. (1983) *J. Bacteriol. 153*, 416-422.

Huoponen, K., Vilkki, J., Aula, P., Nikoskelainen, E. K. & Savontaus, M. L. (1991) *Am. J. Hum. Genet. 48*, 1147-1153.

Innis, M. A., & Gelfand, D. H. (1990) in *PCR protocols: A Guide to Methods and Applications* (Innis, M. A., Gelfand, D. H., Sninsky, J. J., & White, T. J., Eds.), pp 3-12, Academic Press, San Diego, CA.

Ishii, N., Yoshimura, H., Nagayama, K., Kagawa, Y., & Yoshida, M. (1993) *J. Biochem. 113*, 245-250.

Ivey, D. M., & Krulwich, T. A. (1991) *Mol. Gen. Genet. 229*, 292-300.

Ivey, D. M., & Krulwich, T. A. (1992) *Res. Microbiol. 143*, 467-470.

Iwamoto, A., Miki, J., Maeda, M., & Futai, M. (1990) *J. Biol. Chem. 265*, 5043-5048.

Jacobs, H. T., Elliott, D. J., Math, V. B., & Farquharson, A. (1988) *J. Mol. Biol. 202*, 185-217.

Jans, D. A., Fimmel, A. L., Hatch, L., Gibson, F., & Cox, G. B. (1984) *Biochem. J. 221*, 43-51.

Jans, D. A., Hatch, L., Fimmel, A. L., Gibson, F., & Cox, G. B. (1985) *J. Bacteriol. 162*, 420-426.

Jounouchi, M., Takayama, M., Chaiprasert, P., Noumi, T., Moriyama, Y., Maeda, M., & Futai, M. (1992) *Arch. Biochem. Biophys. 292*, 376-381.

Kaim, G., Ludwig, W., Dimroth, P., & Schleifer, K. H. (1992) *Eur. J. Biochem. 207*, 463-470.

Kandpal, R. P., Stempel, K. E., & Boyer, P. D. (1987) *Biochemistry 26*, 1512-1517.

Klionsky, D. J., Brusilow, W. S. A., & Simoni, R. D. (1983) *J. Biol. Chem. 258*, 10136-10143.

Klionsky, D. J., Brusilow, W. S. A., & Simoni, R. D. (1984) *J. Bacteriol. 160*, 1055-1060.

Klionsky, D. J., & Simoni, R. D. (1985) *J. Biol. Chem. 260*, 11200-11206.

Klionsky, D. J., Skalnik, D. G., & Simoni, R. D. (1986) *J. Biol. Chem. 261*, 8096-8099.

Kluge, C., & Dimroth, P. (1992) *Biochemistry 31*, 12665-12672.

Kluge, C., & Dimroth, P. (1993) *J. Biol. Chem. 268*, 14557-14560.

Kluge, C., & Dimroth, P. (1993) *Biochemistry 31*, 10378-10386.

Krumholz, L. R., Esser, U., & Simoni, R. D. (1989) *Nucleic Acids Res. 17*, 7993-7994.

Kumamoto, C. A., & Simoni, R. D. (1986) *J. Biol. Chem. 261*, 10037-10042.

Kumamoto, C. A., & Simoni, R. D. (1987) *J. Biol. Chem. 262*, 3060-3064.

Laget, P. P., & Smith, J. B. (1979) *Arch. Biochem. Biophys. 197*, 83-89.

Lagoni, O. R., von Meyenburg, K., & Michelsen, O. (1993) *J. Bacteriol. 175*, 5791-5797.

Laubinger, W., Deckers-Hebestreit, G., Altendorf, K., & Dimroth, P. (1990) *Biochemistry 29*, 5458-5463.

Laubinger, W. & Dimroth, P. (1989) *Biochemistry 28*, 7194-7198.

Lewis, M. J., Chang, J. A., & Simoni, R. D. (1990) *J. Biol. Chem. 265*, 10541-10550.

Lewis, M. J., & Simoni, R. D. (1992) *J. Biol. Chem. 267*, 3482-3489.

Lightowlers, R. N., Howitt, S. M., Hatch, L., Gibson, F., & Cox, G. B. (1987) *Biochim. Biophys. Acta 894*, 399-406.

Lightowlers, R. N., Howitt, S. M., Hatch, L., Gibson, F., & Cox, G. B. (1988) *Biochim. Biophys. Acta 933*, 241-248.

Lill, H., Burkovski, A., Altendorf, K., Junge, W., & Engelbrecht, S. (1993) *Biochim. Biophys. Acta 1144*, 278-284.

Lücken, U., Gogol, E. P., & Capaldi, R. A. (1990) *Biochemistry 29*, 5339-5343.

Ludwig, W., Kaim, G., Laubinger, W., Hoppe, J., & Schleifer, K. H. (1990) *Eur. J. Biochem. 193*, 395-399.

Ludwig, B., Prochaska, L., & Capaldi, R. A. (1980) *Biochemistry 19*, 1516-1523.

Lunardi, J., Dupuis, A., Garin, J., Issartel, J.-P., Michel, L., Chabre, M., & Vignais, P. V. (1988) *Proc. Natl. Acad. Sci. USA 85*, 8958-8962.

Lutter, R., Abrahams, J. P., van Raaij, M. J., Todd, R. J., Lundqvist, T., Buchanan, S. K., Leslie, A. G., & Walker, J. E. (1993) *J. Mol. Biol. 229*, 787-790.

Maggio, M. B., Pagan, J., Parsonage, D., Hatch, L., & Senior, A. E. (1988) *J. Biol. Chem. 262*, 8981-8984.

Maggio, M. B., Parsonage, D., & Senior, A. E. (1988) *J. Biol. Chem. 263*, 4619-4623.

Markwell, M. A. K., Haas, S. M., Bieber, L. L., & Tolbert, N. E. (1978) *Anal. Biochem. 87*, 206-210.

Matsuno-Yagi, A., & Hatefi, Y. (1985) *J. Biol. Chem. 260*, 14424-14427.

Matsuno-Yagi, A., & Hatefi, Y. (1988) *Biochemistry 27*, 335-340.

Matsuno-Yagi, A., & Hatefi, Y. (1993a) *J. Biol. Chem. 268*, 1539-1545.

Matsuno-Yagi, A., & Hatefi, Y. (1993b) *J. Biol. Chem. 268*, 6168-6173.

Matsuno-Yagi, A., Yagi, T., & Hatefi, Y. (1985) *Proc. Natl. Acad. Sci. USA 82*, 7550-7554.

McCarthy, J. E. G., Schairer, H. U., & Sebald, W. (1985) *EMBO J. 4*, 519-526.

McCormick, K. A. (1993) PhD dissertation, University of Florida, Gainesville, FL.

McCormick, K. A., & Cain, B. D. (1991a) *FASEB J. 5*, A1192.

McCormick, K. A., & Cain, B. D. (1991b) *J. Bacteriol. 173*, 7240-7248.

McCormick, K. A., Deckers-Hebestreit, G., Altendorf, K., & Cain, B. D. (1993) *J. Biol. Chem. 268*, 24683-24691.

Mendel-Hartvig, J., & Capaldi, R. A. (1991a) *Biochim. Biophys. Acta 1060*, 115-124.

Mendel-Hartvig, J., & Capaldi, R. A. (1991b) *Biochemistry 30*, 1278-1284.

Mendel-Hartvig, J., & Capaldi, R. A. (1991c) *Biochemistry 30*, 10987-10991.

Miller, J. H. (1972) *Experiments in Molecular Genetics*, pp 431-435, Cold Spring Harbor Laboratory, Cold Spring Harbor, NY.

Miller, M. J., Fraga, D., Paule, C. R., & Fillingame, R. H. (1989) *J. Biol. Chem. 264*, 305-311.

Miller, M. J., Oldenburg, M., & Fillingame, R. H. (1990) *Proc. Natl. Acad. Sci. USA 87*, 4990-4904.

Mitchell, P. (1961) *Nature 191*, 144-148.

Mitchell, P. (1979) *Science 206*, 1148-1159.

Mitchell, P., & Moyle, J. (1974) *Biochem. Soc. Spec. Publ. 4*, 91-111.

Montecucco, C., Dabbeni-Sala, F., Friedl, P., & Galante, Y. M. (1983) *Eur. J. Biochem. 132*, 189-194.

Monticello, R. A., Angov, E. & Brusilow, W. S. A. (1992) *J. Bacteriol. 174*, 3370-3376.

Moriyama, Y., Iwamoto, A., Hanada, H., Maeda, M., & Futai, M. (1991) *J. Biol. Chem 266*, 22141-22146.

Mosher, M. E., White, L. K., Hermolin, J., & Fillingame, R. H. (1985) *J. Biol. Chem. 260*, 4807-4814.

Munn, A. L., Whitfeld, P. R., Bottomley, W., Hudson, G. S., Jans, D. A., Gibson, F., and Cox, G. B. (1991) *Biochim. Biophys. Acta 1060*, 82-88.

Nalin, C. M., Snyder, B., & McCarty, R. E. (1985) *Biochemistry 24*, 2318-2324.

Negrin, R. S., Foster, D. L., & Fillingame, R. H. (1980) *J. Biol. Chem. 255*, 5643-5648.

Ohta, S., Yohda, M., Ishizuka, M., Hirata, H., Hamaoto, T., Otawara-Hamamoto, Y., Matsuda, K., & Kagawa, Y. (1988) *Biochim. Biophys. Acta 933*, 141-155.

Padan, E., Zilberstein, D., & Rottenberg, H. (1976) *Eur. J. Biochem. 63*, 533-541.

Papa, S., Guerrieri, F., Zanotti, F., Capozza, G., Fiermonte, M., Cocco, T., Altendorf, K., and Deckers-Hebestreit, G. (1992) *Ann. N. Y. Acad. Sci. 671*, 345-358.

Pati, S., & Brusilow, W. S. A. (1989) *J. Biol. Chem. 264*, 2640-2644.

Pati, S., Brusilow, W. S. A., Deckers-Hebestreit, G., & Altendorf, K. (1991) *Biochemistry 30*, 4710-4714.

Paule, C. R. & Fillingame, R. H. (1989) *Arch. Biochem. Biophys. 274*, 270-284.

Penefsky, H. S. (1985) *J. Biol. Chem. 260*, 13735-13741.

Penefsky, H. S. (1988) *J. Biol. Chem. 263*, 6020-6022.

Penefsky, H. S., & Cross, R. L. (1991) *Advances Enzymol. 64*, 173-214.

Perkin Elmer Cetus (1992) *AmpliTaq® Cycle Sequencing Kit*, Norwalk, CT.

Perlin, D. S., Cox, D. N., & Senior (1983) *J. Biol. Chem. 258*, 9793-9800.

Perlin, D. S., Latchney, L. R., & Senior, A. E. (1985) *Biochim. Biophys. Acta 807*, 238-244.

Perlin, D. S., Latchney, L. R., Wise, J. G., & Senior, A. E. (1984) *Biochemistry 23*, 4998-5003.

Perlin, D. S., & Senior, A. E. (1985) *Arch. Biochem. Biophys. 236*, 603-611.

Porter, A. C. G., Brusilow, W. S. A., & Simoni, R. D. (1983) *J. Bacteriol. 155*, 1271-1278.

Porter, A. C. G., Kumamoto, C., Aldape, K., & Simoni, R. D. (1985) *J. Biol. Chem. 260*, 8182-8187.

Promega (1987) *K/RT Sequencing Systems Technical Manual*, Madison, WI.

Protein Identification Resource (1992) release 31, National Biomedical Research Foundation, Washington, DC.

Racker, E, & Stoeckenius, W. (1974) *J. Biol. Chem. 249*, 662-663.

Rao, R., Pagan, J., & Senior, A. E. (1988) *J. Biol. Chem. 263*, 15957-15963.

Ridgwell, K., Roberts, S. J., Tanner, M. J. A., & Anstee, D. J. (1983) *Biochem. J. 213*, 267-269.

Roberts, S. J., Tanner, M. J. A., & Denton, R. M. (1982) *Biochem. J. 205*, 139-145.

Roe, B. A., Din-Pow, M., Wilson, R. K., & Wong, J. F. H. (1985) *J. Biol. Chem. 260*, 9759-9774.

Rottenberg, H., & Moreno-Sanchez, R. (1993) *Biochim. Biophys. Acta 1183*, 161-170.

Ryrie, I. J., & Jagendorf, D. T. (1972) *J. Biol. Chem. 247*, 4453-4459.

Sambrook, J., Fritsch, E. F., & Maniatis, T. (1989) *Molecular Cloning: a Laboratory Manual*, 2nd ed., Cold Spring Harbor Laboratory, Cold Spring, NY.

Schaefer, E. M., Hartz, D., Gold, L., & Simoni, R. D. (1989) *J. Bacteriol. 171*, 3901-3908.

Schägger, H., & von Jagow, G. (1987) *Anal. Biochem. 166*, 368-379.

Schneider, E., & Alterdorf, K (1984) *Proc. Natl. Acad. Sci. USA 81*, 7279-7283.

Schneider, E., & Altendorf, K. (1985) *EMBO J. 4*, pp. 515-518.

Schneider, E., & Altendorf, K. (1987) *Microbiol. Rev. 51*, 477-497.

Schneppe, B., Deckers-Hebestreit, G., McCarthy, J. E. G., & Altendorf, K. (1991) *J. Biol. Chem. 266*, 21090-21098.

Schnizer, R. A. (1993) PhD dissertation, University of Florida, Gainesville, FL.

Sebald, W., & Hoppe, J. (1981) *Curr. Top. Bioenerg. 12*, 1-64.

Senior, A. E. (1983) *Biochim. Biophys. Acta 726*, 81-95.

Senior, A. E. (1988) *Physiol. Rev. 68*, 177-231.

Senior, A. E. (1990) *Annu. Rev. Biophys. Biophys. Chem. 19*, 7-41.

Senior, A. E., Langman, L., Cox, G. B., Gibson, F. (1983) *Biochem. J. 210*, 395-403.

Shin, K., Nakamoto, R. K., Maeda, M., & Futai, M. (1992) *J. Biol. Chem. 267*, 20835-20839.

Shoffner, J. M., & Wallace, D. C. (1990) *Adv. Hum. Genet. 19*, 267-330.

Shoffner, J. M., Fernhoff, P. M., Krawiecki, N. S., Caplan, D. B., Holt, P. J., Koontz, D. A., Takei, Y., Newman, N. J., Ortiz, R. G., Polak, M., Ballinger, S. W., Lott, M. T., & Wallace, D. C. (1992) *Neurology 42*, 2168-2174.

Singh, G., Lott, M. T., & Wallace, D. C. (1989) *N. Engl. J. Med. 320*, 1300-1305.

Stack, A. E., & Cain, B. D. (1994) *J. Bacteriol. 174*, 540-542.

Steffens, K., Schneider, E., Deckers-Hebestreit, G., & Altendorf, K. (1987) *J. Biol. Chem. 264*, 5866-5869.

Sternweis, P. C. (1978) *J. Biol. Chem. 253*, 3123-3128.

Sternweis, P. C., & Smith, J. B. (1977) *Biochemistry 16*, 4020-4025.

Sternweis,P. C., & Smith, J. B. (1980) *Biochemistry 19*, 526-531.

Stone, D. K., Crider, B. P., & Xie, X. S. (1990) *Kidney Int. 38*, 649-653.

Stratagene (1989) *pBS Vectors Instruction Manual*, Stratagene, La Jolla, CA.

Stroop, S. D., & Boyer, P. D. (1985) *Biochemistry 24*, 2304-2310.

Südhof, T. C., Fried, V. A., Stone, D. K., Johnston, P. A., & Xie, X. S. (1989) *Proc. Natl. Acad. Sci. USA 86*, 6067-6071.

Takeyama, M., Noumi, T., Maeda, M., & Futai, M. (1988) *J. Biol. Chem. 263*, 16106-16112.

Tamarappoo, B. K., Handlogten, M. E., Laine, R. O., Serrano, M. A., Dugan, J., & Kilberg, M. S. (1992) *J. Biol. Chem. 267*, 2370-2374.

Tartof, K., & Hobbs, C. A. (1987) *Bethesda Res. Lab. Focus 9*, 12.

Tatuch, Y., Christodoulou, J., Feigenbaum, A., Clarke, J., T., R., Wherret, J., Smith, C., Rudd, N., Petrova-Benedict, R., & Robinson, B. H. (1992) *Am. J. Hum. Genet. 50*, 852-858.

Tatuch, Y. & Robinson, B. H. (1993) *Biochem. Biophys. Re. Commun. 192*, 124-128.

Tiedge, H., Lunsdorf, H., Schafer, G., & Schairer, H. U. (1985) *Proc. Natl. Acad. Sci. USA 82*, 7874-7878.

Torok, K., & Joshi, S. (1985) *Eur. J. Biochem. 153*, 155-159.

Towbin, H., Staehelin, T., & Gordon, J. (1979) *Proc. Natl. Acad. Sci. 76*, 4350-4354.

Tozer, R. G., & Dunn, S. (1986) *Eur. J. Biochem. 161*, 513-518.

Tozer, R. G., & Dunn, S. D. (1987) *J. Biol. Chem. 262*, 10706-10711.

Tsuprun, V. L., Mesyanzhinova, I. V., Koxlow, I. A., & Orlova, E. V. (1984) *FEBS Lett. 167*, 285-290.

United States Biochemical Corp. (1987) *Step-by-Step Protocols for DNA Sequencing with Sequenase*, 3rd Ed., Cleveland, OH.

Velours, J., Durrens, P., Aigle, M., & Guerin, B. (1988) *Eur. J. Biochem. 170*, 637-642.

Vik, S. B., & Dao, N. N. (1992) *Biochim. Biophys. Acta 1140*, 199-207.

Vik, S. B., Cain, B. D., Chun, K. T., & Simoni, R. D. (1988) *J. Biol. Chem. 263*, 6599-6605.

Vik, S. B., Lee, D., Curtis, C. E., & Nguyen, L. T. (1990) *Arch. Biochem. Biophys. 282*, 125-131.

Vik, S. B., Lee, D., & Marshall, P. A. (1991) *J. Bacteriol. 173*, 4544-4548.

Vik, S. B., & Simoni, R. D. (1987) *J. Biol. Chem. 262*, 8340-8346.

von Meyenburg, K., Jorgensen, B. B., Nielsen, J., Hansen, F. G., & Michelsen, O. (1982) *Tokai J. Exp. Clin. Med 7* (Suppl.), 23-31.

Walker, J. E., Lutter, R., Dupuis, A., and Runswick, M. J. (1991) *Biochemistry 30*, 5369-5378.

Walker, J. E., Runswick, M. J., and Poulter, L. (1987) *J. Mol. Biol. 197*, 89-100.

Walker, J. E., Saraste, M., & Gay, N. J. (1982) *Nature* (London) *298*, 867-869.

Walker, J. E., Saraste, M., & Gay, N. J. (1984) *Biochim. Biophys. Acta 768*, 164-200.

Wallace, D. C. (1992a) *Science 256*, 628-632.

Wallace, D. C. (1992b) *Annu. Rev. Biochem. 61*, 1175-1212.

Webb, M. R., Grubmeyer, C., Penefsky, H. S., Trentham, D. R. (1980) *J. Biol. Chem. 255*, 11637-11639.

Westhoff, P., Alt, J., Nelson, N., & Herrmann, R. G. (1985) *Mol. Gen. Genet. 199*, 290-299.

Westhoff, P., Nelson, N., Bünemann, H., & Herrmann, R. G. (1991) *Curr. Genet. 4*, 109-120.

Wilkens, S., & Capaldi, R. A. (1992) *Arch. Biochem. Biophys. 299*, 105-109.

Wise, J. G., Latchney, L. R., Ferguson, A. M., & Senior, A. E. (1984) *Biochemistry 23*, 1426-1432.

Wise, J. G., Latchney, L. R., & Senior, A. E. (1981) *J. Biol.Chem. 256*, 10383-10389.

Wise, J. G., & Senior, A. E. (1985) *Biochemistry 24*, 6949-6954.

Woese, C. R., Kandler, O., & Wheelis, H. L. (1990) *Proc. Natl. Acad. Sci. USA 87*, 4576-4579.

Yoshida, M. (1983) *Biochem. Biophys. Res. Commun. 114*, 907-912.

Yoshida, Y., Wakabayashi, S., Matsubara, H., Hashimoto, T., Tagawa, K. (1984) *FEBS Lett. 170*, 135-138.

Yoshinaga, H., Ogino, T., Ohtahara, S., Sakuta, R., Nonaka, I., & Horai, S. (1993) *J. Child Neurol. 8*, 129-133.

Zhou, J. M., & Boyer, P. D. (1993) *J. Biol.Chem. 268*, 1531-1538.

Zhou, N. E., Zhu, B. Y., Kay, C. M., Hodges, R. S. (1992) *Biopolymers 32*, 419-426.

BIOGRAPHICAL SKETCH

Phillip Edwin Hartzog was born August 4, 1964, in Bryson City, NC, to Mildred and Everette Hartzog. He grew up in Yadkinville, NC, with his two younger sisters, Amy and Lisa. Between his sophomore and junior years in high school Phillip attended the North Carolina Governor's School East, a summer school program for talented students. There he learned the value of knowledge as opposed to education. Phillip attended North Carolina State University from the fall of 1982 to the fall of 1986, where he earned a Bachelor of Science in both chemistry and biochemistry. After a brief period working as an analytical chemist, Phillip left Raleigh, NC, and moved to Gainesville, FL, in the summer of 1988. There he attended the University of Florida as a graduate student in the Department of Biochemistry and Molecular Biology. Phillip's graduate career has been spent working with Dr. Brian Cain, where he produced the work described in this dissertation. Upon completing the requirements for his Ph.D., Phillip is moving back to North Carolina, where he plans to continue his scientific career in the Botany Department of Duke University. There Phillip will be working with Dr. Bruce Kohorn studying how proteins cross biological membranes.

I certify that I have read this study and that in my opinion it conforms to acceptable standards of scholarly presentation and is fully adequate, in scope and quality, as a dissertation for the degree of Doctor of Philosophy.

Brian D. Cain, Chair
Assistant Professor of
Biochemistry and
Molecular Biology

I certify that I have read this study and that in my opinion it conforms to acceptable standards of scholarly presentation and is fully adequate, in scope and quality, as a dissertation for the degree of Doctor of Philosophy.

Michael S. Kilberg
Professor of Biochemistry
and Molecular Biology

I certify that I have read this study and that in my opinion it conforms to acceptable standards of scholarly presentation and is fully adequate, in scope and quality, as a dissertation for the degree of Doctor of Philosophy.

Charles M. Allen
Professor of Biochemistry
and Molecular Biology

I certify that I have read this study and that in my opinion it conforms to acceptable standards of scholarly presentation and is fully adequate, in scope and quality, as a dissertation for the degree of Doctor of Philosophy.

Sheldon M. Schuster
Professor of Biochemistry
and Molecular Biology

I certify that I have read this study and that in my opinion it conforms to acceptable standards of scholarly presentation and is fully adequate, in scope and quality, as a dissertation for the degree of Doctor of Philosophy.

Paul A. Hargrave
Professor of
Ophthalmology

I certify that I have read this study and that in my opinion it conforms to acceptable standards of scholarly presentation and is fully adequate, in scope and quality, as a dissertation for the degree of Doctor of Philosophy.

Lonnie O. Ingram
Professor of Microbiology
and Cell Science

This dissertation was submitted to the Graduate Faculty of the College of Medicine and to the Graduate School and was accepted as partial fulfillment of the requirements for the degree of Doctor of Philosophy.

April 1994

Dean, College of Medicine

Dean, Graduate School

UNIVERSITY OF FLORIDA
3 1262 08556 9886